



UNIVERSITÀ DEGLI STUDI DI PARMA

DIPARTIMENTO DI SCIENZE BIOMEDICHE,
BIOTECNOLOGICHE E TRASLAZIONALI

Dottorato di ricerca in Medicina Molecolare
Ciclo XXIX

Expression study of XTP1 and SDP35 RhoGAPs in high-grade soft tissue sarcomas: correlation with prognosis

Coordinatore:

Chiar.mo Prof. Luciano Polonelli

Tutor Interno:

Chiar.mo Prof. Roberto Perris

Tutor Esterno Istituto Ortopedico Rizzoli:

Dott.ssa Maria Serena Benassi

Dottorando
Serena Pollino

..to my family and to Fabrizio...

*Nothing in life is to be feared, it is
only to be understood.
Now is the time to understand more,
so that we may fear less.*

[Marie Curie]

TABLE OF CONTENTS

1 - INTRODUCTION.....	7
1.1 - Soft Tissue Sarcoma.....	7
1.1.1 - Liposarcoma	9
1.1.2 - Fibrosarcoma	12
1.1.3 - Leiomyosarcoma	13
1.1.4 - Undifferentiated Pleomorphic Sarcoma	15
1.1.5 - Grading and staging of Soft tissue sarcomas.....	17
1.2 - STS biomarkers.....	19
1.2.1 - IGFBP7.....	21
1.2.2 - miRNA and STS.....	22
1.2.3 - miR-152.....	23
1.2.4 - MET, a miR-152 target.....	24
1.3 - Rho GTPase and RhoGAPs	25
1.3.1 - Human RhoGAP domain-containing proteins.....	27
1.3.2 - XTP1/DEPDC1B.....	28
1.3.3 - SDP35 / DEPDC1A.....	30
2 - AIM OF THE STUDY.....	33
3 - MATERIALS AND METHODS	34
3.1 - Phase 1.....	34
3.1.1 - Tumour specimens and clinical records	34
3.1.2 - Cell lines	37
3.1.3 - Primary cell cultures	38
3.1.4 - RNA extraction.....	38
3.1.5 - Reverse transcription and Real Time PCR of miR-152	39
3.1.6 - Reverse transcription and Real Time PCR of XTP1/DEPDC1B, SDP35/DEPDC1A, MET	40
3.1.7 - Immunohistochemistry (IHC) on TMA.....	41
3.1.8 - Protein extraction and Western blot	42
3.1.9 - Statistical analysis	43
3.1.10 - Monoclonal antibody (mAb)	44
3.2 - Phase 2: <i>In vitro</i> studies	44
3.2.1 - Cell count.....	44
3.2.2 - Transfection of miR-152 precursor molecules	44

3.2.3 - SDP35/DEPDC1A siRNA transfection.....	45
3.2.4 - Annexin test to determine apoptotic cells.....	45
3.2.5 - Wound Healing Assay	46
3.2.6 - Cell immunolabelling	46
3.2.7 - Cell pellets for Real time PCR and Western blot	46
4 - RESULTS	48
4.1 - Tumour samples and analysis of patients	48
4.1.1 - Population study	48
4.1.2 - Identification of MET as a putative STS-related miR-152 target and miR-152 role cell behaviour.....	50
4.1.3 - Immunohistochemical analysis on TMA of other potential biomarkers associated with STS metastatic progression	51
4.1.4 - XTP1/DEPDC1B and SDP35/DEPDC1A gene expression in human STS specimens	55
4.1.5 - Western blot analysis.....	58
4.1.6 - mAbs against both RhoGAPs in STS lesions.....	59
4.2 - <i>in vitro</i> studies	60
4.2.1 - mRNA and protein levels of RhoGAPs in STS primary cell cultures.....	60
4.2.2 - XTP1/DEPDC1B and SDP35/DEPDC1A expression in STS cell lines	62
4.2.3 - Western blot analysis of protein expression.....	62
4.2.4 - XTP1/DEPDC1B and SDP35/DEPDC1A mRNA in STS cell lines.....	63
4.2.5 - Analysis of cell proliferation, migration and apoptotic rate in basal condition	64
4.2.6 - Knockdown of SDP35/DEPDC1A in SW872 cell line	65
5 - DISCUSSION	67
6 - BIBLIOGRAPHY	71
7 - PUBLICATIONS	78
8 - ACKNOWLEDGMENTS	79

ABSTRACT

Aim Soft tissue sarcomas (STS) are rare tumours with uncertain histogenesis, difficulties in establishing correct diagnosis and no, or very few reliable prognostic markers. Similarly, biological factors that predict their aggressiveness and clinical evolution remain largely undefined. Prognosis of metastatic STS patients is strongly unfavourable and in need of new therapeutic strategies. To overcome some of these limitations, we investigated the expression patterns of two poorly studied unique signal transduction molecules belonging to the RhoGAP family, previously discovered to be misexpressed in STS. We also studied the relative expression levels of miR-152, previously found altered in STS, known to control MET expression, another vital factor in sarcomatogenesis.

Methods and Results By RT-PCR, miR-152 resulted down-regulated in 59 primary STS samples compared to healthy controls. miR-152 transfection in SKLMS-1 cells led to reduced expression of its target, the oncogene MET, transient decrease in cell growth and increased apoptosis. Immunohistochemistry revealed that MET, along with the growth factor IGFBP7 were more expressed in metastatic than in metastasis-free STS patients. We then evaluated *SDP35/DEPDC1A* and *XTP1/DEPDC1B* transcriptional levels in 86 primary STS and in 22 paired lung metastasis by RT qPCR. We detected a poor-to-absent transcript expression in 17 tumour surgical margin tissue samples used as healthy controls.

In contrast, STS specimens had abundant levels of both mRNAs which increased in metastases compared to paired primary tumours. Immunohistochemistry revealed that both RhoGAPs varied in intensity and distribution. *XTP1/DEPDC1B* was diffusely distributed in the cytoplasm, whereas *SDP35/DEPDC1A* displayed a predominant nuclear, and occasionally cytoplasmic, localization suggesting that it may undergo cytoplasmic-nuclear shuttling. In metastatic samples both proteins appeared more expressed than in paired primary lesions with a predominant nuclear localization. By immunoblotting a stronger *SDP35/DEPDC1A* expression was seen in metastatic lesions compared to primary tumours. Correlation analyses stressed that patients with more abundant *XTP1/DEPDC1B* and *SDP35/DEPDC1A* transcripts in primary lesions had a higher probability of incurring in metastatic disease, suggesting that RhoGAPs up-regulation was related to an increased metastatic capability. By multivariate analyses, over-abundance of *SDP35/DEPDC1A* transcript, age over 60 years and no post-surgery radiation therapy were strong independent risk factors. In a panel of STS cell lines and proprietary STS cells isolated from metastatic lesions both *XTP1/DEPDC1B* and *SDP35/DEPDC1A* were up-regulated in highly

replicating cells and correlated with rounding morphology. To study the precise role of RhoGAPs in the control of STS cell behaviour a RNAi-based knocked-down approach was adopted. These experiments indicated that abrogation of *SDP35/DEPDC1A* expression affected both cell proliferation and migration, suggesting that RhoGAP could be involved in the control of cytoskeletal dynamics and in cell shape changes needed in fundamental cellular events.

Conclusions Our data suggest that the observed MET overexpression may be associated with miR-152 down-regulation, causing a decrease in cell proliferation. Increased expression of MET and other biomarkers putatively involved in STS progression seem to significantly impact upon clinical behaviour. Notably, altered expression of RhoGAPs *SDP35/DEPDC1A* and *XPT1/DEPDC1B* strongly correlated with progression to a metastatic condition and these observations identified *SDP35/DEPDC1A* as a novel biomarker of poor prognosis. Preliminary studies on isolated STS cells suggest that increased *SDP35/DEPDC1A* and *XPT1/DEPDC1B* expression and their cytoplasmic-nuclear shuttling, may contribute to a more aggressive phenotype by promoting cell shape changes associated with cancer cell proliferation and movement.

SOMMARIO

Scopo I sarcomi delle parti molli (SPM) sono tumori rari che presentano istogenesi incerta e difficoltà nell'effettuare una corretta diagnosi. A oggi non esistono marcatori in grado di predire la loro aggressività ed evoluzione clinica. I pazienti metastatici affetti da SPM hanno prognosi sfavorevole e vi è la necessità di individuare nuovi biomarcatori da utilizzare anche per la pianificazione di nuovi protocolli terapeutici. A tale fine, in questo studio retrospettivo condotto su una serie di tessuti tumorali di SPM ad alto grado di malignità si è correlata l'espressione dell'oncogene MET, target del microRNA miR-152, precedentemente trovato sotto-espresso in SPM, della proteina IGFBP7 che appartiene al pathway del fattore di crescita IGF, e di due molecole di trasduzione del segnale appartenenti alla famiglia RhoGAP, *SDP35/DEPDC1A* e *XTP1/DEPDC1B*, con il decorso clinico della malattia in termini di progressione metastatica.

Metodi e risultati L'analisi di RT-PCR ha confermato la sotto-espressione di miR-152 in 59 tumori primitivi di SPM rispetto ai controlli sani, mentre l'analisi immunohistochimica su una ampia casistica di 131 campioni tumorali mostrava uniforme e forte espressione della proteina target MET. Tale over-espressione era particolarmente evidente in pazienti che svilupparono metastasi durante il follow-up. L'induzione di espressione di miR-152 in cellule di leiomiomasarcoma (SKLMS-1) riduceva l'espressione di MET, associata a riduzione di crescita cellulare e ad aumento di cellule apoptotiche, confermando così il ruolo di MET come target di miR-152. Anche la proteina 7 che lega il fattore di crescita IGF, IGFBP7, e la RhoGAP *SDP35/DEPDC1A* erano più espresse nei pazienti metastatici rispetto ai non metastatici consolidando il loro ruolo prognostico. In particolare, l'immunocolorazione ha mostrato una variazione nell'intensità e nella distribuzione delle due RhoGAPs : *XTP1/DEPDC1B* aveva una distribuzione citoplasmatica mentre *SDP35/DEPDC1A* una localizzazione prevalentemente nucleare. L'espressione di *SDP35/DEPDC1A* e *XTP1/DEPDC1B* è stata studiata anche a livello trascrizionale in 86 SPM primitivi, 22 metastasi polmonari e 17 tessuti adiacenti sani. Questi ultimi presentavano minima o assente espressione dei trascritti mentre i tessuti neoplastici avevano alti livelli di mRNA che erano significativamente più elevati nelle metastasi rispetto ai tumori primitivi. Inoltre, l'analisi statistica ha rivelato che i pazienti con alti livelli di trascritti nelle lesioni primitive avevano una maggiore probabilità di sviluppare metastasi, suggerendo che tale up-regolazione sia correlata con la progressione tumorale. Dall'analisi multivariata è emerso che l'over-espressione genica di *SDP35/DEPDC1A*, l'età superiore ai 60 anni e assenza di radioterapia post-operatoria sono fattori indipendenti di rischio metastatico. Studi preliminari in vitro

mostrarono che linee cellulari e culture primarie di STS mantenevano un'alta espressione di RhoGAP mentre il silenziamento di *SDP35/DEPDC1A* riduceva sia la proliferazione che la migrazione suggerendo un suo coinvolgimento nel controllo della dinamica del citoscheletro e dei cambiamenti morfologici importanti per le funzioni cellulari.

Conclusioni I nostri dati su una serie di SPM confermano il ruolo prognostico di MET e IGFBP7 e indicano *SDP35/DEPDC1A* come marcatore prognostico indipendente correlato ad un alto rischio di metastasi. Quest'ultimo dato è supportato da studi preliminari su cellule isolate da STS che suggeriscono che l'aumentata espressione di *SDP35/DEPDC1A* e *XTP1/DEPDC1B* e il loro transito nucleo-citoplasma possono contribuire ad un fenotipo più aggressivo promuovendo cambiamenti nella morfologia cellulare associati alla proliferazione e movimento delle cellule tumorali.

1 - INTRODUCTION

1.1 - Soft Tissue Sarcoma

Soft Tissue Sarcomas (STS) are a heterogeneous group of rare connective tissue tumours, representing 1% of all malignant tumours with more than 50 histological subtype [1-3]. They more frequently arise from extremities, trunk wall and retroperitoneum and the malignancy increase with the age (Fig.1). The most common include pleomorphic sarcoma, liposarcoma, and leiomyosarcoma (Fig.2). At time of diagnosis the 10–25% of patients shows metastatic disease to mostly in lung, bone and liver. Lymph node metastases are generally rare (3%) with the exception of synovial sarcoma, rhabdomyosarcoma and epitheloid sarcoma for which lymph node involvement has been observed in 10–20% of cases [2,3].

Over the past three decades, some advances in diagnostic and treatment methods have contributed to improve disease-free and overall survival rates in patients with STS [4]. Complete surgical removal of tumours in association with radiation and chemotherapy has brought an increase in the 5-year disease-free survival of patients with localized high-grade STS, while clinical outcome of metastatic patients at diagnosis, or following adjuvant therapy, remains strongly unfavourable (i.e. 5-year disease-free survival: 20%-40%). A better understanding of the cellular and molecular mechanisms underlying pre- and post-surgery metastasis formation and the development of chemo-resistance of these tumours are fundamental to improve prognosis and unveil novel parameters predicting therapeutic response. The majority of STS present multiple genomic diversity [5] and although consensus is emerging that the selection of treatment should be histology-driven, the identification of new clinical and biological markers will contribute to identify high risk patients who need more intensive treatments [6]. Although histological grading remains the most important prognostic factor [7] the implementation of immunohistochemistry, cytogenetics and molecular genetic analysis have improved clinical management and prognosis of STS [8].

World Health Organization (WHO) [2] updated tumour classification on the bases of currently phenotypic, cytogenetic, and molecular data and propagated new reproducible diagnostic criteria.

Cytogenetic analyses have allowed the detection of fusion transcripts useful for differential diagnosis of histologically peculiar cases and the association between specific fusion transcripts and cell cycle regulators has assessed the possibility that fusion transcripts could be novel molecular targets in specific histotypes. However, the majority of sarcomas lacks defined genetic alterations and shows significant diversity even among tumours with the

same diagnosis. The karyotypes of these tumours present numerous chromosomal gains, losses and amplifications leading to a strong genomic instability [5] (Tab.1A and 1B).

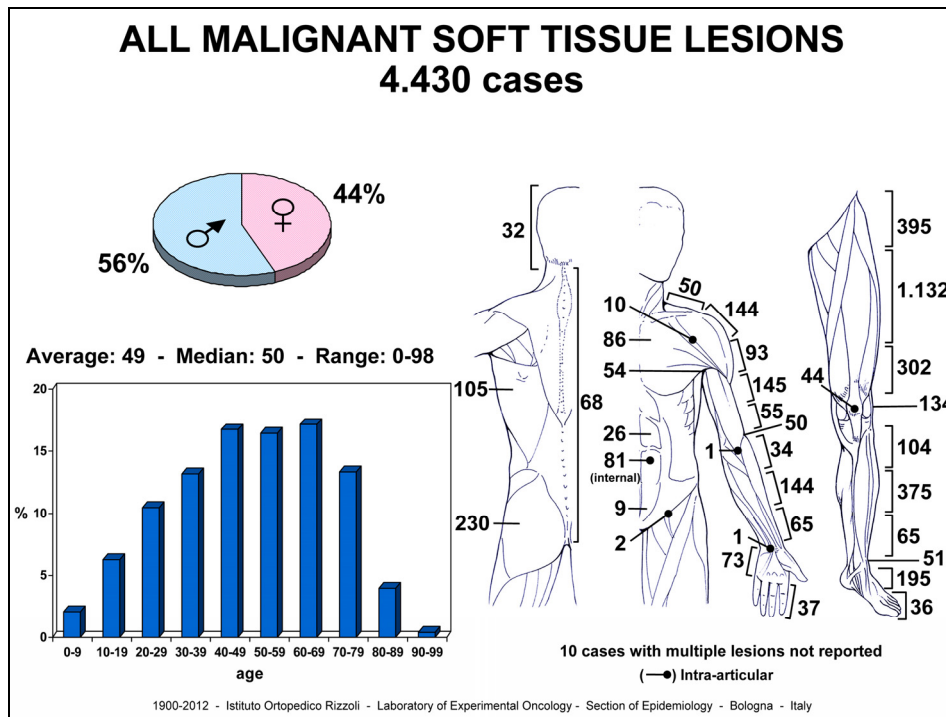


Figure 1 - Total cases of malignant Soft tissue sarcoma referred to the Rizzoli Orthopaedic Institute between 1900 and 2012 (*Atlas of musculoskeletal tumors and tumorlike lesions, 2014*).

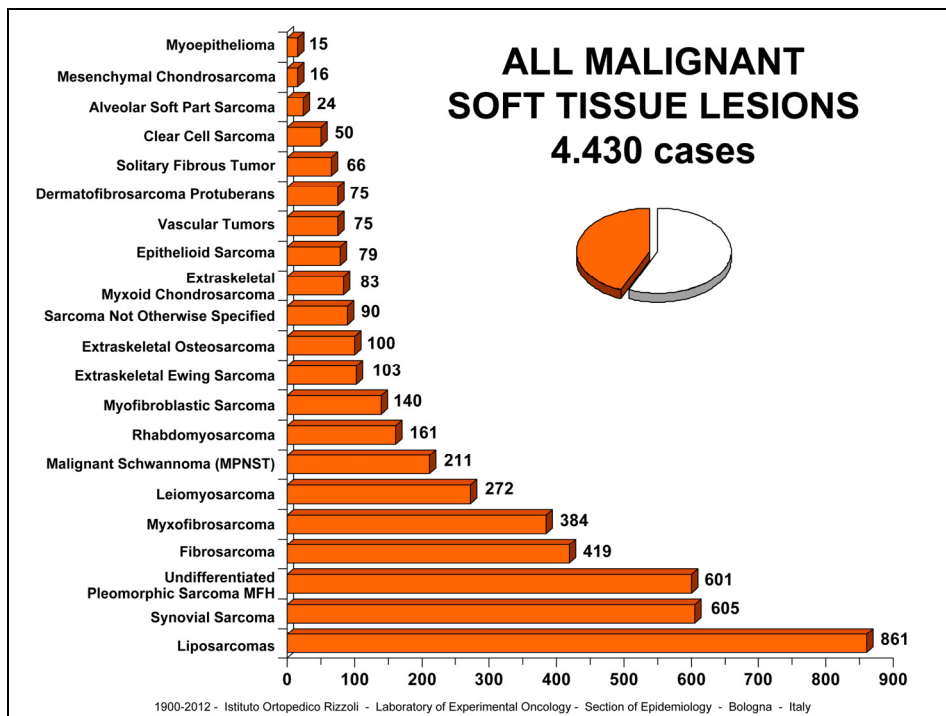


Figure 2 - Most common malignant Soft tissue sarcoma subtypes referred to the Rizzoli Orthopaedic Institute between 1900 and 2012 (*Atlas of musculoskeletal tumors and tumorlike lesions, 2014*).

Table 1A Histologic classification (WHO)	Table 1B Soft-tissue sarcomas with defined genetic translocations	
<ul style="list-style-type: none"> • Adipose tumors • Fibroblastic/Myofibroblastic tumors • Fibrohistiocytic tumors • Smooth muscle tumors • Peri-angiocytic tumors (perivascular) • Striated muscle tumors • Vascular tumors • Cartilaginous and osseous tumors • GIST (Gastro Intestinal Stromal tumors) • Nerve sheath tumors • Tumors with uncertain differentiation • Unclassified and undifferentiated sarcomas 	<ul style="list-style-type: none"> • Ewing sarcoma • Synovial sarcoma • Alveolar rhabdomyosarcoma • Myxoid liposarcoma • Myxoid chondrosarcoma • Clear-cell sarcoma • Fibromyxoid sarcoma • Desmoplastic tumor with small round cells • Infantile fibrosarcoma • Alveolar sarcoma of soft tissue • Inflammatory myofibroblastic tumor • Angiomatoid histiocytobroma 	<ul style="list-style-type: none"> t(11;22); t(21;22) t(X;18) t(2;13); t(1;13) t(12;16); t(12;22) t(9;22) t(12;22) t(7;16); t(11;16) t(11;22) t(12;15) t(X;17) t(2;19); t(1;2) t(12;16); t(12;22)

Table 1A and 1B – WHO histological classification (*Honoré C. et al. Journal of Visceral Surgery 2015*)

1.1.1 - Liposarcoma

Liposarcomas (LS) constitute a heterogeneous group of distinctive lesions that arise from fat cells in deep soft tissue, most commonly in patients older than 40 years (Fig.3). According to WHO [2], LS is subclassified into 4 categories including well differentiated liposarcoma/atypical lipomatous tumour (WDL/ALT), dedifferentiated liposarcoma (DDL), myxoid/round cell liposarcoma (MLS/RCLS), and pleomorphic liposarcoma (PLS). Different studies demonstrated amplification of the 12q13-15 chromosomal region in WDL and DDL [9], translocation of chromosome 12 in M/RCLS [10] and a complex karyotype in PLS [11].

Considering the histological characterization, up to 25% of liposarcomas are misclassified and this complicates the accurate diagnosis and treatment response. Previous biological studies identified biomarkers for LS diagnosis and prognosis considering the strong tendency of this tumour to develop local recurrence and metastasis [10,12,13].

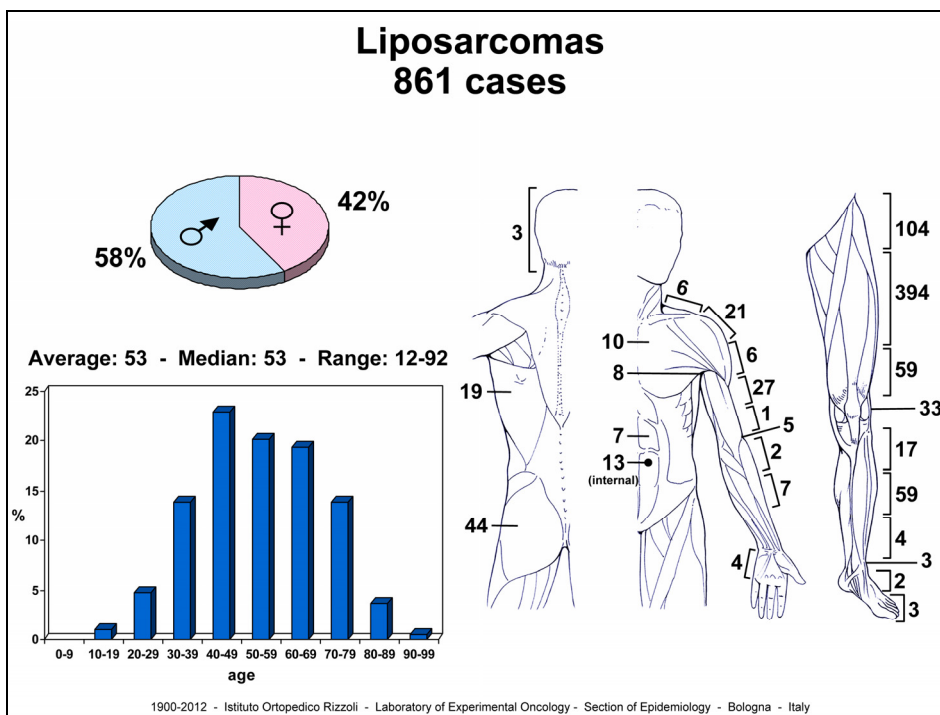


Figure 3 - Total cases of Liposarcoma referred to the Rizzoli Orthopaedic Institute between 1900 and 2012 (*Atlas of musculoskeletal tumors and tumorlike lesions, 2014*)

Well-differentiated Liposarcoma/Atypical Lipomatous Tumour (WDL/ALT) are considered synonyms by WHO and represent 40% of LS. With the term ALT are indicated those neoplasms situated in the accessible soft tissue both superficially and deeply. WDL is used for tumours localized in the retroperitoneum and mediastinum, which give the more aggressive behaviour [10,13]. WDL/ALT are low-grade non-metastatic malignant tumours [3,14]. Local recurrence occurs in 10% of cases [3]. A tissue section of this tumour is shown in figure 4.

Dedifferentiated liposarcoma (DDLs) is a rare high-grade tumour that typically occurs in the sixth decade of age [10,15]. It is localized more commonly in the abdominal cavity. The subcutaneous localizations are extremely rare [2]. The DDLs manifest a more aggressive behaviour than the WDL/ALT, with a risk of distant metastasis of 15%-20% and a 5-year disease-overall survival of 44% against the 93% of WDL/ALT. By immunohistochemistry, overexpression of MDM2 and CDK4 is consistently observed in both components [13,10,16]. A tissue section of this tumour is shown in figure 4.

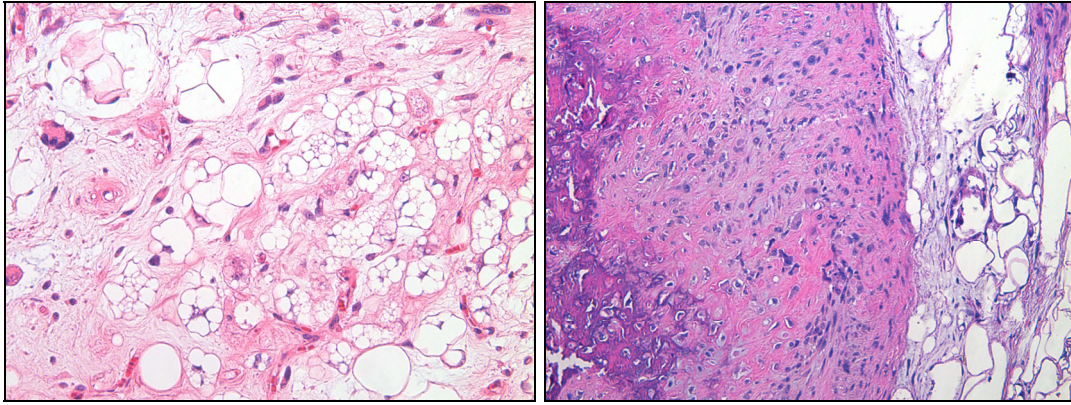


Figure 4 - Well differentiated liposarcoma (left) and Dedifferentiated liposarcoma (right) (*Atlas of musculoskeletal tumors and tumorlike lesions, 2014*)

Myxoid/Round cells Liposarcoma (MLS/RCLS) is the second most common subtype of LS accounting for approximately one-third of cases. It occurs most frequently in the limbs (30-35%) and generally appears in the adults. Histological grade is defined as having greater than 5% round cell component and this is predictor of worse outcome. The extent of hypercellularity predicts the risk of metastatic spread (up to 60% when round cell component represents more than 25% of the tumour volume). Five-year survival is less of 18%-21%.

Mixoid liposarcoma is composed of uniform, small, hyperchromic, from round to ovoid cells with variable lipoblastic differentiation (Fig.5). It is characterized by t(12;16) (q13;p11) or t(12;22) (q13;p12) translocation resulting in FUS-CHOP or EWS-CHOP fusion transcripts respectively [10,13].

Pleomorphic Liposarcoma (PLS) is a high-grade malignant lesion with an incidence of approximately 5% of cases, most frequently localized at the extremities. It consists predominantly of undifferentiated pleomorphic spindle cell sarcoma, with variable numbers of pleomorphic lipoblasts with vacuolated cytoplasm and arranged singly or in small groups but may also occurs in the retroperitoneum and trunk, including the skin. Similar to the pleomorphic high-grade sarcomas, PLS has a complex karyotypes with a strong genomic instability [10,13]. A tissue section of this tumour is shown in figure 5.

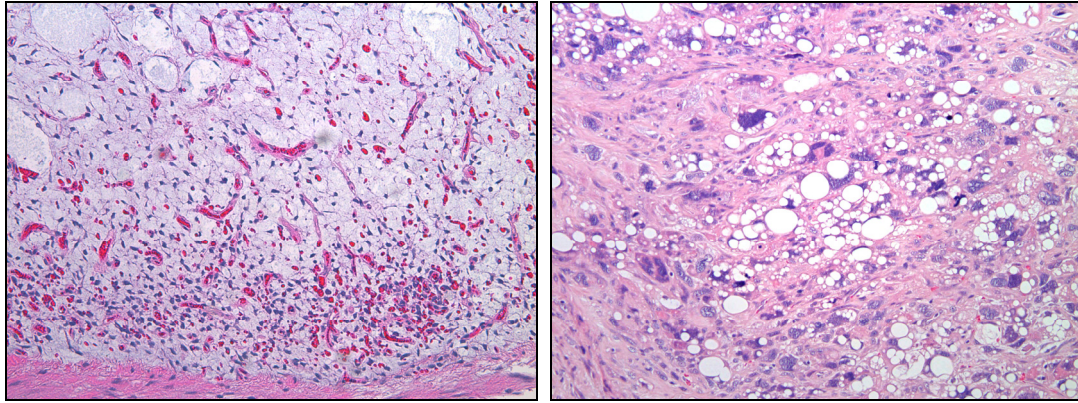


Figure 5 - Myxoid liposarcoma (left) and Pleomorphic liposarcoma (right) (*Atlas of musculoskeletal tumors and tumorlike lesions, 2014*)

1.1.2 - Fibrosarcoma

Fibrosarcoma (FS) is a low to high-grade STS that accounts for <1% of adult STS. The most frequent localizations are trunk and extremities (Fig.6) [17,18]. FS lacks any line of differentiation other than fibroblastic.

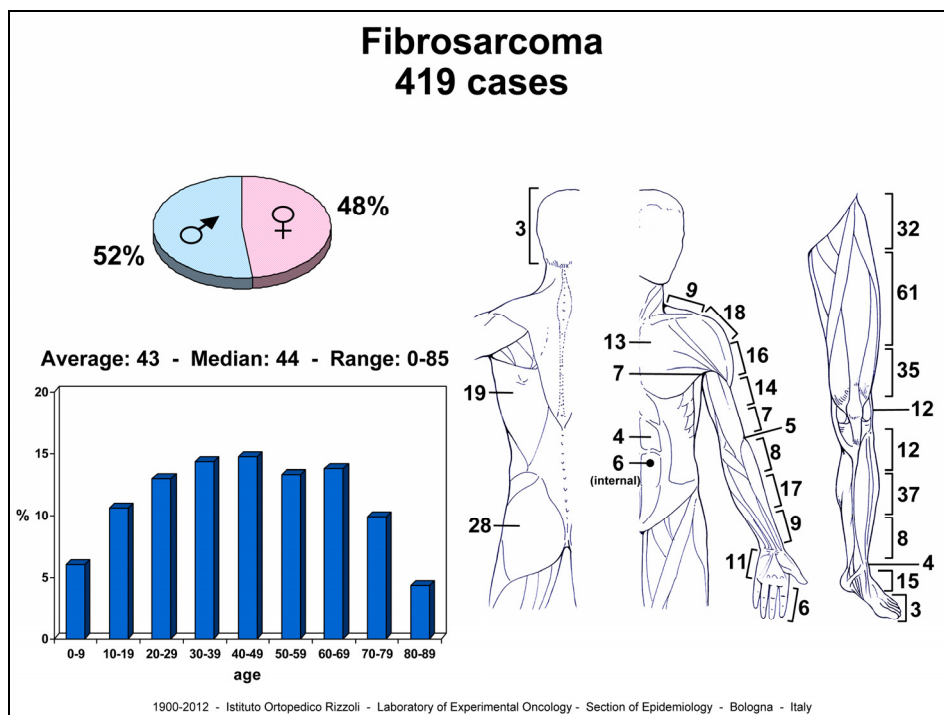


Figure 6 - Total cases of Fibrosarcoma referred to the Rizzoli Orthopaedic Institute between 1900 and 2012 (*Atlas of musculoskeletal tumors and tumorlike lesions, 2014*)

The tumour is composed by spindle cells and collagen fibres. The course of disease is slow and the grading is based on differentiation, polymorphism, anaplasia (Fig.7) [10,18]. This disease shows multiple chromosome rearrangements, immunohistochemistry analysis reveals a constant positivity for vimentin, and may be positive to pan muscle actin and smooth muscle actin but presently no target therapy is planned lacking specific biomarkers. The recurrence rates for adult fibrosarcoma range from 12% to 80% and 10- years survival rate is 60% for low-grade and 30% for high-grade FS. Furthermore, it is resistant to radiotherapy while adjuvant chemotherapy is favourable for a better prognosis [10,17,18].

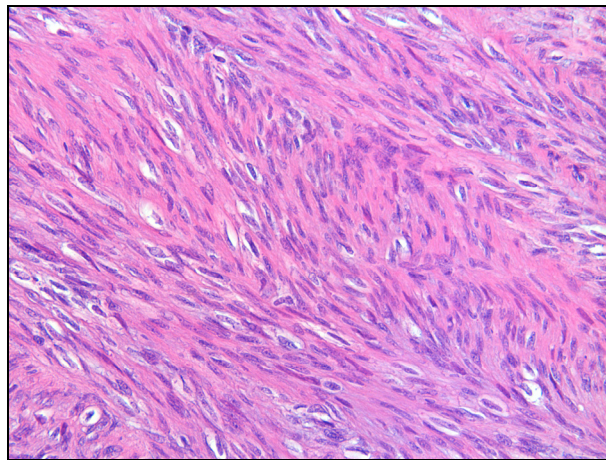


Figure 7 - Fibrosarcoma (*Atlas of musculoskeletal tumors and tumorlike lesions, 2014*)

1.1.3 - Leiomyosarcoma

Leiomyosarcoma (LMS) is a malignant tumour representing 7% of adult STS (Fig.8). It is composed of spindle cells and show a different degree of smooth muscle differentiation, which is inversely proportional to tumour grade (Fig.9). It grows slowly and it is resistant to radiotherapy and chemotherapy. LMS is classified into different types depending on the body site in which are located:

1. retroperitoneal;
2. cutaneous;
3. vascular;

The type 1 is highly aggressive and may cause death also by local extension. It has a 5-year overall survival from 0 to 29%. The cutaneous subtype has a good prognosis but manifests a frequent local recurrence (50%) while metastases are infrequent. The vascular subtype has a

poor prognosis, 50% of patients have metastases as well as tumours of the small veins seem to have a better prognosis. The first and the third lesions are encountered more frequently in women; no gender predilection is present for second type. [10,19,20]. All these variants are histologically similar and differ in the mode of growth and for biological and clinical characteristics [21].

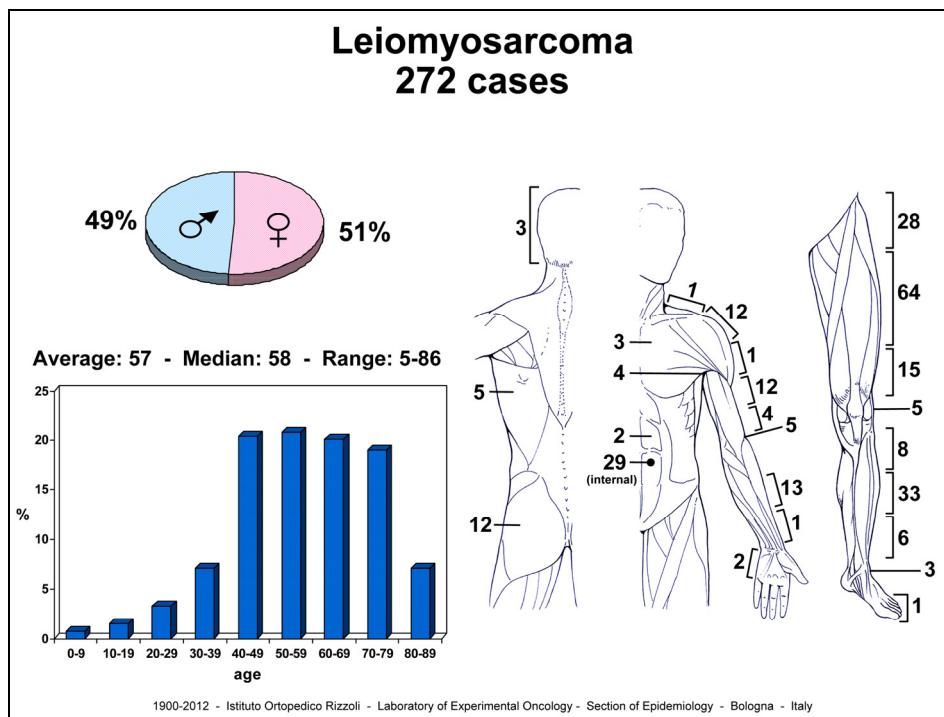


Figure 8 - Total cases of Leiomyosarcoma referred to the Rizzoli Orthopaedic Institute between 1900 and 2012 (*Atlas of musculoskeletal tumors and tumorlike lesions, 2014*)

Depending on the degree of differentiation, the proportion of spindle and pleomorphic cells present in LMS is variable. In well-differentiated lesions the spindle cells are arranged in longitudinal sharply demarcated bundles intersected at right angles with fibrillar or eosinophilic cytoplasm. The high-grade tumours are characterized by nuclear atypia associated with the presence of irregular cells which show rhabdoid appearance and abnormal mitosis. Furthermore areas of myxoid change, epithelioid morphology, fibrosis, hemorrhage, or necrosis can be present. Immunohistochemistry allows differential diagnosis with gastrointestinal stromal tumour and Schwann cells tumour. Muscle differentiation markers include pan-muscle actin, vimentin, desmin, Calponin, h-caldesmon and heavy chain myosin which give all a positive staining, while a negative expression is found for myogenin, S100 (marker of the Schwann cells neoplasms), c-kit and CD34 (marker of the gastrointestinal stromal tumours) [10,19,20].

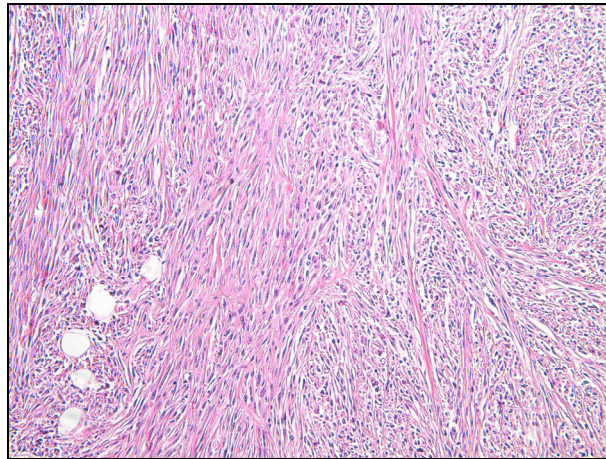


Figure 9 - Leiomyosarcoma (*Atlas of musculoskeletal tumors and tumorlike lesions, 2014*)

Genetically, LMS usually shows complex karyotype abnormalities different from each other and is characterized by numerous non-recurrent and non-specific aberrations that result from a high degree of genetic instability. Loss and acquisition of chromosomal material is associated with a poor prognosis in terms of metastasis-free and overall survival. Gain of function is frequently seen on the chromosomes 1, 5, 6, 8, 15, 16, 17, 19, 20, 22, X, loss of function on the chromosomes 1p, 2, 3, 4, 6q, 8, 9, 10p, 11p, 12q, 11q, 13, 16, 17p, 18, 19, 22q while amplifications involve the chromosomes 1, 5, 8, 12, 13, 17, 19, 20. Wide surgical excision is often in combination with radiation or conventional chemotherapy. Today there are not yet specific targeted treatment against LMS because the pathophysiology still remains poorly understood [10,19,20].

1.1.4 - Undifferentiated Pleomorphic Sarcoma

According to the definition of criteria, Undifferentiated Pleomorphic Sarcoma (UPS) presents a diffuse pleomorphism in the absence of specific line of differentiation and accounts for up to 20% of all STS. UPS is a high-grade malignant cancer, more frequent in adult-elderly life, [22,23] (Fig.10).

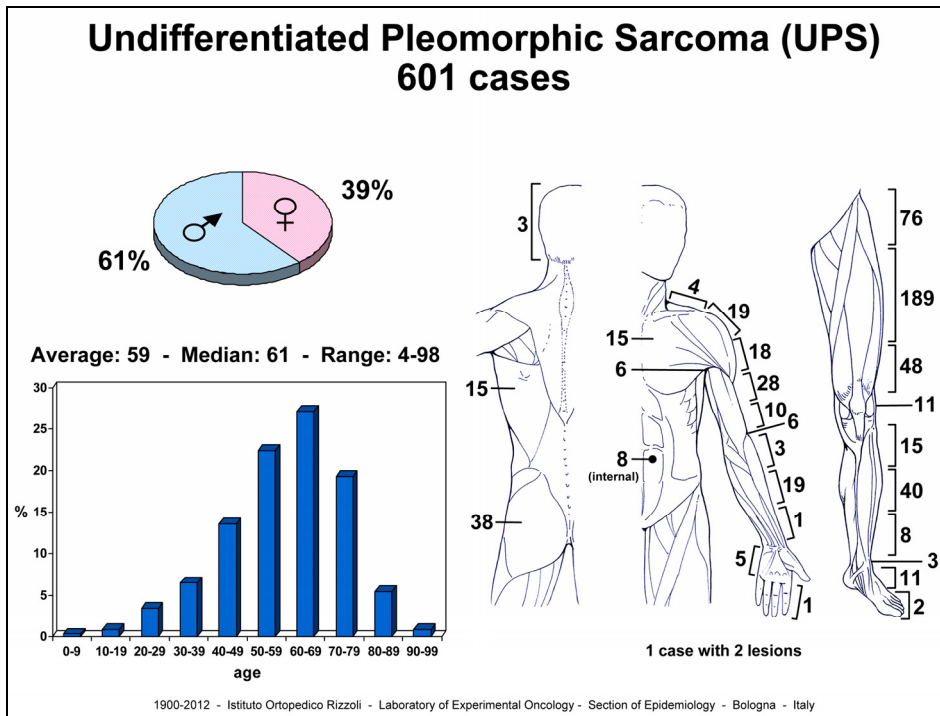


Figure 10 - Total cases of Undifferentiated pleomorphic sarcoma referred to the Rizzoli Orthopaedic Institute between 1900 and 2012 (*Atlas of musculoskeletal tumors and tumorlike lesions, 2014*)

The old term "malignant fibrous histiocytoma" is obsolete because it presents a differentiation fibroblastic rather than histiocytic [24]. The cellular origin is still a matter of debate. Matushansky et al. [25], demonstrated that mesenchymal stem cells would be involved in the development of UPS through the inactivation of the Wnt pathway mediated by DKK1, a mediator of cell proliferation, which results to be overexpressed in these types of tumours.

UPS is localized more frequently in the lower and upper extremity and the males seem to have an incidence of greater occurrence [10,22,23].

Microscopically, UPS has a variable morphologic pattern (storiform pleomorphic; myxoid; giant cell; inflammatory; angiomatoid). Storiform pleomorphic subtype contains fusiform and pleomorphic cells inserted inside a collagen matrix. Cell atypia, irregular mitosis, hyperchromatic large nuclei, and granular eosinophilic cytoplasm are associated to an aggressive highly malignant phenotype (Fig.11).

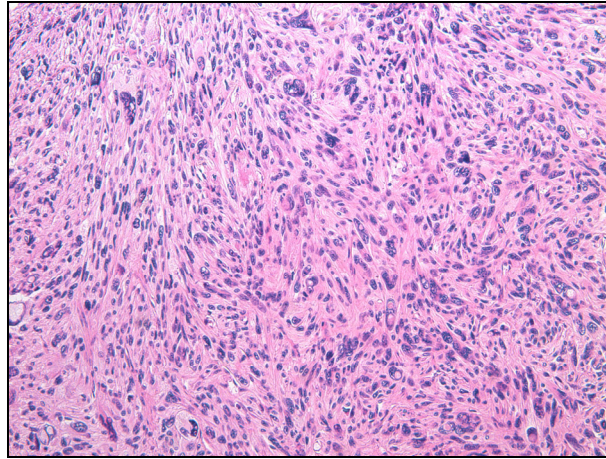


Figure 11 - Undifferentiated pleomorphic sarcoma
(*Atlas of musculoskeletal tumors and tumorlike lesions, 2014*)

UPS with numerous giant cells is a lesion formerly referred to as the giant cell subtype or malignant giant cell tumour of soft parts [10,22].

UPS and other pleomorphic sarcomas share many of chromosomal aberrations observed in leiomyosarcoma. The loss of chromosome 13(13q14) is frequent and lead to oncosuppressor gene RB deletion [19]. Radiotherapy is effective in 50% of cases and very aggressive tumours respond in a limited way to chemotherapy. 5-years overall survival is 30-50% [10] .

1.1.5 - Grading and staging of Soft tissue sarcomas

Histological grading represents the most important prognostic factor for STS and it is based on histological parameters [7,26,27] . The concept of histological grade was introduced by Broders in 1920 and it is distinguished from staging; the first parameter considers the intrinsic quality of the primary tumour only, while the staging also takes into account tumour extent. In 1977, Russell et al. [28] proposed the first coherent clinicopathological classification in which the patients were divided into four stages with a different prognosis and introduced a histological grading applicable to all adult STS. At present, two systems are the most commonly used, the National Cancer Institute (NCI) grading and the French Federation of Cancer Centers Sarcoma Group (FNCLCC) grading [1,27,29,30]. Both are 3 grade systems. The NCI system is based on six histological parameters: histological type, mitoses, necrosis, pleomorphism, cellularity and intercellular matrix. The French Sarcoma Group designs a system considering seven histological parameters: tumour differentiation, cellularity, nuclear atypia, presence of malignant giant cells, mitotic count, extent of tumour necrosis and presence of vascular emboli, all included in multivariate analyses [27]. The

latter identified three independent prognostic factors: tumour differentiation, mitotic index and extent of necrosis. These grading systems have been subject to numerous criticisms however histological grade remains a key parameter that allows us to indicate the probability of distant metastases, tumour mortality and overall survival in the 90% of all STS. At present, the diagnosis of primary STS is made by core needle biopsies that are also used for establishing treatment strategies. The purpose of a grading system is to separate tumours of good prognosis (grade 1) from those of poor prognosis (grade 3). Furthermore, the grading can be used to select patients to which it is possible to administer an adjuvant chemotherapy: patients with a grade 1 should not receive this treatment since it confers no clinical benefit while patients with a grade 3 sarcoma are good candidates for receiving adjuvant chemotherapy due to the high probability of distant metastases [27,30]. The histological grade can be considered as a morphological translation of molecular events that determine tumour aggressiveness, and, therefore, it should be continuously updated with the purpose of obtaining a definitive system based on molecular parameters. Since several years biologists and pathologists of the French Sarcoma Group have been studying the molecular analyses of adult sarcomas with complex genomic. The aim of these studies was to identify the genes and pathways related to the chromosomal complexity and to understand if there was a link between chromosomal complexity and prognosis. With this work it has been possible to generate the CINSARC (Complexity INdex in SARComas) expression profile signature offering a much superior prognostic value than histological grading. Molecular markers might be promising for refining our ability to establish early prognosis and to predict response to therapy. Among the most relevant criteria to determine the prognostic ability of a molecule is to demonstrate its specific association to outcome, its accuracy and reproducibility in an independent group of patients, and finally the independency of its prognostic value from other standard factors in a multivariate analysis. Considering these criteria, at present unfortunately, only few molecular markers could be recognized as prognostic in sarcomas [30].

Concerning the **staging** there are two staging system adopted for benign and malignant primary tumours of bone and soft tissue: one established in 1980 by Dr. William Enneking and the other one by AJCC/International Union Against Cancer.

Enneking's staging system is based on grade (G0 = benign, G1 = low-grade malignant and G2 = high-grade malignant); tumour extension (T0=intracapsular, T1=confined within anatomical compartment, T2= extracompartment); presence or absence of metastasis (M0=no mets, M1= mets).

[31,32]. The Enneking system is the most suitable for sarcomas that arise from the extremities, but does not include anatomic planes and compartments as the type, the size and depth of the tumour so, for this reason, oncologists prefer, for soft tissue sarcomas in contrast to bone sarcomas, the American Joint Committee System (AJCS) (Tab.2) [32]. This is applicable to each site and follows a TGNM system.

Tumour size (T1 = size < 5cm; T2 = size ≥ to 5cm; T3 = involvement of bones, vessels and nerves). The limit of 5 cm allowed further to categorize them as superficial or deep.

Histopathologic grade (G1 = low grade and well differentiated; G2 = moderately well differentiated; G3 = high-grade and poorly differentiated).

Nodes involvement (N0 = not metastases to regional lymph nodes; N1 = metastatic involvement of lymphonode).

Metastasis (M0 = no distant metastasis; M1 = distant metastases) [1,31-38].

STAGE	GRADE	SITE	LYMPH NODE METASTASES	DISTANT METASTASES	DEFINITION
IA	G1	T1	N0	M0	Low grade without metastases
IB	G1	T2	N0	M0	
IIA	G2	T1	N0	M0	Moderate grade without metastases
IIB	G2	T2	N0	M0	
IIIA	G3	T1	N0	M0	High grade without metastases Any tumours with lymph node metastases
IIIB	G3	T2	N0	M0	
IIIC	G1-3	T1-2	N1	M0	
IVA	G1-3	T3	N0-1	M0	Tumour involving bone, vessels, nerve with or without lymph node metastases
IVB	G1-3	T1-3	N0-1	M1	Any tumours with distant metastases

Table 2 - American Joint Committee system (*Atlas of musculoskeletal tumors and tumorlike lesions, 2014*)

1.2 - STS biomarkers

Clinical research conducted and developed in recent decades represents a revolution in the understanding of the pathogenesis of cancer. Now we possess abundant knowledge about the molecular mechanisms underlying the onset of cancer, but despite this, little progress has been made in understanding the etiology to prevent the disease and treat it. For this reason, clinical research applied to the study of neoplastic disease it is proposed, among many goals,

even to identify tumour biomarkers that can be used for a quicker and more accurate diagnosis.

A biomarker is a molecular, anatomical, physiological or biochemical indicator that can be used to measure the progression of a disease or response to a therapeutic treatment. It must be easily measurable and objectively assessed. The ideal biomarker must be minimal or not detectable in normal tissue so that the comparison between healthy and disease sampling allows to estimate the differences useful for early diagnosis. In addition, the expression or concentration changes of biomarkers detectable in tissues and fluids should reflect the progression of disease and/or treatment response [39-42]. Finally, the markers should be obtained in the least invasive way possible for the patients [43,44].

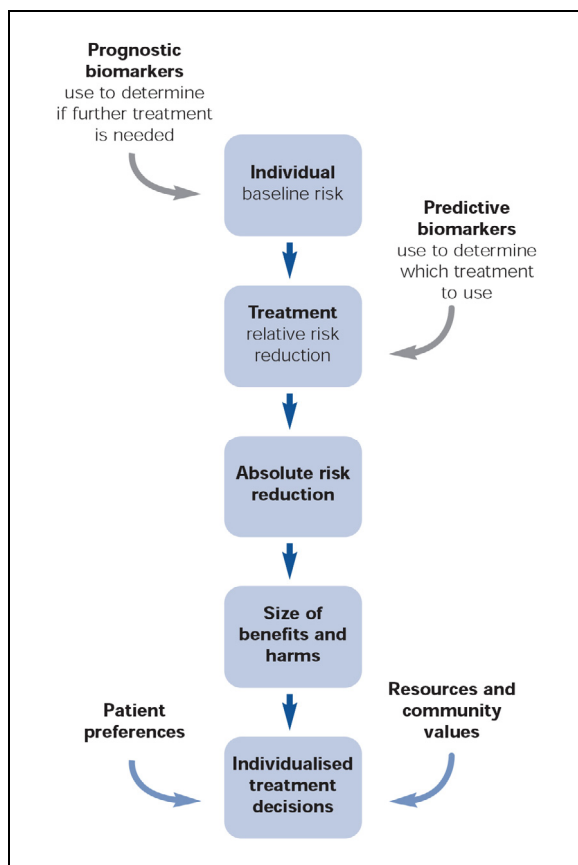


Figure 12 - Role of predictive and prognostic markers to guide individualized treatment decisions. (Lord S. et al., *targeted and individualized therapies 2008*)

The role of predictive/prognostic biomarkers is to guide the clinicians to plan more effective treatments (Fig.12), taking into account the tumour histology and molecular profile.

There is evidence that malignant progression is affected by different cellular signalling pathways converging on several key biological regulators considered potential therapeutic

targets. The identification of these candidate targets is mandatory for improving the survival of STS patients.

To date few studies have proposed prognostic biomarkers for STS, including C-X-C chemokine receptor 4 (CXCR4) and insulin growth factor 1 receptor (IGF1R) for synovial sarcoma [45], NG2 chondroitin sulfate proteoglycan [46,47] and urokinase plasminogen activator system (uPAs) [48] in large series of high grade STS, BCL2 family apoptosis regulator (MCL1) and mitogen-activator protein kinase kinase 4 (MAP2K4) in Rhabdomyosarcoma [49].

Alternative therapy targeting signalling pathways are being currently developed and many clinical trials are ongoing for planning more individualized and less toxic therapies [50].

1.2.1 - IGFBP7

The insulin-like growth factor (IGF) system is one of the most extensively studied target systems in sarcomas [51]. IGF-I receptor (IGF1R) and its substrate, insulin receptor substrate 1 (IRS1) are kinase-activated proteins in IGF axis that play a role in cell proliferation and drug resistance [52]. IGF1R has been previously found highly activated in STS primary and paired bone metastases [53]. IGF1R β and its substrate IRS1 phosphorylated at Serina 612 were uniformly expressed across high-grade STS samples with a variable intracellular localization independently from patient clinical course [54]. IGF signalling is modulated by IGF binding proteins (IGFBPs) that act as tumour suppressor genes or oncogenes depending on the context. Inhibition of IGF1R led to attenuation of mitogen-activated protein kinase pathways. Recently, it was demonstrated [45] that nuclear IGF1R expression was significantly related to poor survival in synovial sarcoma patients who did not receive adjuvant chemotherapy, differentiating a subgroup of synovial sarcoma patient's candidate to the treatment.

IGFBP7, a cell adhesive glycoprotein of about 30kDa also known as IGFBP7-related Protein (IGFBP-rP1) or tumour-derived adhesion factor/angiomodulin, is a member of the IGFBP superfamily that modulating cell functions through dependent- and independent-IGF mechanism may be a useful prognostic biomarker [55]. IGFBP7 binds insulin with high affinity and may be considered a tumour stroma marker in colon cancer [56]. Recent data recognized IGFBP7 as a tumour antigen in mesenchymal-derived tumours acting in TGF β signalling pathway. In addition, IGFBP7 interacts in vitro with various extracellular matrix proteins to stimulate adhesion and migration/invasion [57,58].

Both increased and decreased expression of IGFBP7 has been reported in different tumours, suggesting a complex role in tumour cells [59].

Although IGFBP7 was also detectable in human body fluids, very few studies examined the relationship between circulating IGFBP levels and tumour stage. A recent study demonstrated that circulating IGFBP7, measured with an easily quantifiable assay, had higher mean levels in STS when compared with controls suggesting that its concentration might be useful to discriminate non tumour from tumour patients independently of clinical follow-up [54].

1.2.2 - miRNA and STS

An additional fields of study in cancer is addressed to the involvement of deregulation of microRNA profiling. MiRNA are small non-coding RNAs which bind the complementary sequences within target RNAs to generally down-regulate gene expression. These small molecules can control many different biological pathways, and interference with miRNA function leading to a number of human diseases, including cancer and other pathologies. MiRNAs biogenesis is characterized by a multistep coordinated process that starts in the nucleus with transcription, usually by RNA polymerase II, to create the long primary miRNA (pri-miRNA) housing a hairpin that contains the mature sequence. The microprocessor composed by Drosha, an RNase III enzyme, and its cofactor DGCR8 (also known as Pasha), cleaves the hairpin, producing the precursor miRNA (pre-miRNA) composed by 60–70 nucleotide.

The exportin 5 transports the precursor hairpin to the cytoplasm where Dicer, another RNase III enzyme, processes the precursor into the 21–24 nucleotide double-stranded RNA. The mature miRNA strand is subsequently incorporated into the RNA-induced silencing complex (RISC, or miRISC) where it binds to a member of the AGO protein family while the other strand is normally degraded. The miRNAs imperfect base pairing guide RISC to specific mRNAs to down-regulate their expression by triggering mRNA destabilization or translational repression [60]. Thus non-coding RNAs of 19–24 nucleotides play a crucial role as post-transcriptional regulators repressing gene expression by recognizing complementary target sites, more often in the 3' untranslated region (UTR) of target mRNAs [61,62]. As such, they may control important physiological processes such as cellular development, differentiation and signalling. Anomalous miRNA expression has been found to be strongly correlated with malignancy and in case of STS a strong association has been reported between miRNA expression, patient age and prognosis. miRNA profile

deregulation affecting downstream signalling pathways activates endpoints that represent potential biomarkers for prognosis and treatment of tumour patients [63,64].

During these years it has emerged that microRNAs (miRNAs) have a crucial role in predicting the disease outcome and the prognosis in various cancer types including sarcoma. Different studies report the presence of circulating miRNAs in patients with STS suggesting a potential role as prognostic factors useful for miRNA-targeted therapy. Taking into account the four STS histotype before described, there are various reports that indicate different deregulated miRNAs.

In Leiomyosarcoma there are more than 70 miRNAs that are differentially expressed compared to normal uterine smooth muscles, including miR-17 and miR-92 as well as miR-1 and miR-133a/b, which are regulators of myogenesis, and are significantly overexpressed. Other studies revealed a role of miRNAs as potential biomarkers for differential diagnosis and demonstrated upregulation of miR-221 and miR-21 in LMS when compared to its benign counterparts (leiomyoma). Furthermore, miR-199b-5p, miR-320a, miR-199a-3p, miR-126 and miR-22 were overexpressed in both LMS and UPS, while miR-483-5p, miR-656, miR-323-3p and -206 were downregulated in LMS.

Concerning fibrosarcoma, miRNA profiling has been limited to the cell line, HT1080. In vitro and in vivo analyses demonstrated that miR-409-3p overexpression inhibited cell tumour growth, vascularization, and metastasis.

In liposarcoma there are different miRNAs that were dysregulated in DDLS and not in normal adipose tissue and ALT/WDL; for example miR-193b helps in distinguishing differentiated vs. dedifferentiated liposarcomas. In general, miR-218-1*, HS_303, miR-9, -891a, and -888 are upregulated while miR-144, -1238, miR-486-3p and -1290 are downregulated compared to normal adipose tissues. Importantly, high miR-26a-2 expression levels significantly correlated with poor patient survival in both types of liposarcoma.

Guled et al. discovered 38 human miRNAs significantly differentially expressed in UPS compared to control samples. In detail, miR-126, -223, -451, and -1274b were significantly upregulated while miR-100, -886-3p, -1260, -1274a, and -1274b were downregulated [65-67].

1.2.3 - miR-152

miR-152 belongs to a 3 miRNA family including miR-148a, miR-148b and miR-152. Notably, in humans, the miR-152 gene is located on chromosome 17q21.32, within intron 1 of the coatmer protein complex, subunit zeta 2 (COPZ2) gene, and a CpG island is typically

observed around its promoter region. At cytoplasm level, pre-miR-152 is processed to form a miR-152 duplex. Two different mature miR-152 sequences, known as miR-152-5p and miR-152-3p, are excised from opposite arms of the miR-152 duplex. MiR-152-3p is excised from the 3' arm of the hairpin precursor and it has been detected in more species than miR-152-5p. This molecule is expressed in several species in which exhibits identical sequence (with the exception of the extension at its 3' end) suggesting that it is important in certain gene regulatory networks [68]. Probably, miR-152 is evolutionarily conserved and the recent lineage-specific miR-152 may be common to the old ancestral processor. Hundreds of genes have been proposed as candidate targets of miR-152, some of which were confirmed experimentally. DNA methyltransferase 1 (DNMT1), insulin-like growth factor 1 receptor (IGF-1R), insulin receptor substrate 1 (IRS1), E2F transcription factor 3, a disintegrin and metalloproteinase metalloproteinase domain 17 (ADAM17), matrix metalloproteinase 3 (MMP3), Kruppel-like factor 4 (KLF4), fibroblast growth factor 2 (FGF2), wntless-related integration site (Wnt1), cluster of differentiation (CD) 151, transforming growth factor alpha and mesenchymal to epithelial transition (MET) have been identified as targets of miR-152 in a wide array of human malignancies [68,69]. It may have a promoting effect on cancerogenesis acting as oncogene or more often as oncosuppressor gene. It has been reported that miR-152 may be involved in proliferation, invasion and angiogenesis, and its down-regulation has been observed in ovarian, prostate, bladder, endometrial, pancreatic and gastrointestinal cancers [69,70]. In hepatocarcinogenesis miR-152 controls cell cycle, apoptosis and motility acting as a tumour suppressor on TNFRF6B [71]. In contrast, in neuroblastoma cells miR-152 has been found to be over-expressed compared to normal mature neurons. As yet, few data are available on miR-152 in human sarcomas. A recent study indicated that plasma and tumour tissues from osteosarcoma patients may exhibit lower miR-152 expression levels than healthy controls, suggesting that *miR-152* may serve as a biomarker for early tumour detection [69].

1.2.4 - MET, a miR-152 target

Receptor tyrosine kinases (RTKs) are receptors for polypeptide growth factors, cytokines, and hormones. These receptors regulate many intracellular signal transduction pathways involved in multiple normal and pathological biological processes, including cancer initiation, progression, invasiveness, metastasis and resistance to therapy. The Mesenchymal Epithelial Transition (MET) is a receptor tyrosine kinase of 190 kDa expressed on the surface of epithelial and endothelial cells. MET binds hepatocyte growth factor (HGF) and

guides malignant progression by activating signalling pathways that promote cell motility, survival and proliferation. MET expression is up-regulated in STS and it is significantly inversely correlated with miR-152 expression [69,72]. This proto-oncogene is localized on chromosome 7q21-31 and it is expressed by the epithelial cells of many organs (liver, pancreas, prostate, kidney, muscle, and bone marrow), both during embryogenesis and in the adulthood [73]. It presents an extracellular and intracellular regions with different important sites and domains as well as the Carboxy-terminal site necessary for downstream responses. The binding of HGF, the only known ligand, to the MET extracellular domain causes a stable homo-dimerization of the receptor and a subsequent activation of its intracellular domain. Thus, MET can bind multiple substrates and, consequently, activate various signalling pathways directly or not. The subsequent activation of different intracellular signalling like MAPK, PI3K-AKT cascades, STAT and NF- κ B signalling pathways is responsible for driving proliferation, cell survival, migration and invasiveness. Besides, MET activation is also involved in tumour growth, invasion, resistance to therapy, angiogenesis and in the generation and maintenance of cancer stem cells [72].

1.3 - Rho GTPase and RhoGAPs

Rho GTPases form a distinct family of highly conserved GTP-binding proteins that cooperate or antagonize each other to regulate a wide spectrum of cellular functions.[74,75,76,77,78,79,80]. Moreover, Rho GTPases contribute to most steps of cancer initiation and progression, tissue invasion, development of metastases, inflammation, wound repair [76,79,81,82,83] and neovascularisation [84].

The ability of GTPases to regulate a myriad of cellular functions is due to their interaction with multiple effector as well as their regulatory proteins. Rho GTPases act as molecular switches, cycling between an inactive GDP-bound state and an active GTP-bound state [74,76-81]. In the active form, Rho GTPases bind different effector molecules implicated in the activation of downstream signalling pathways and trigger a signalling cascade to direct cellular responses [76].

This cycle is controlled by three classes of regulatory protein [76,81,82,85]:

- 1) guanine nucleotide exchange factors (GEFs) that activate Rho GTPases by catalyzing GDP/GTP exchange,
- 2) GTPase-activating proteins (GAPs) that inhibit Rho GTPases by stimulating GTP hydrolysis [76,77] (Fig.13).

- 3) Guanine nucleotide dissociation inhibitors (GDIs) that regulate the Rho GTPases intracellular localization [81] by sequestering them in the cytoplasm and inhibit their access to downstream targets [76,80].

Moreover, these regulators can act as scaffolds to bring Rho GTPases and other signalling proteins together with their downstream targets [76].

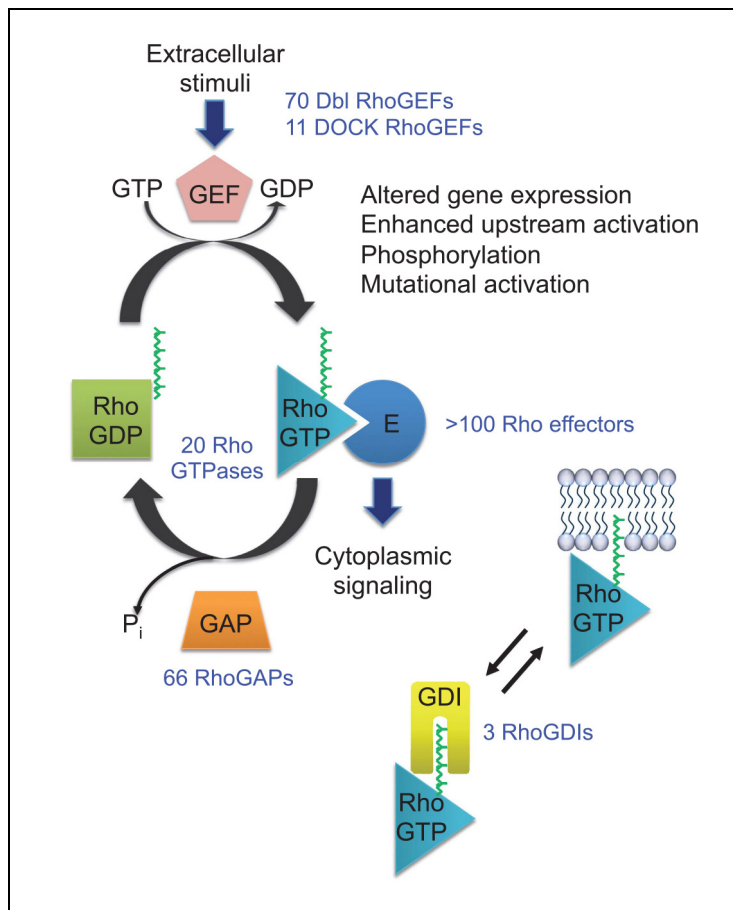


Figure 13 - Regulators of Rho GTPase. (Cook et al. *Oncogene* 2014)

Given the ability of Rho molecules to coordinate different and sometimes opposing cell functions, various human tumours display different Rho GTPases expression and some of them seem to be a tissue-specific expression [81,86,87,88]. The spatiotemporal activation of these members is determined by various GEFs and GAPs [76,80,89] [which, in turn, appear to be downregulated in some tumours and overexpressed in others. Thus, the influence of numerous GEFs and GAPs in part may explain the different, or in some cases opposite, functions of related Rho GTPases in various aspects of cancer progression [76].

1.3.1 - Human RhoGAP domain-containing proteins

RhoGAP domain-containing proteins have been characterized in eukaryotes, ranging from yeast to human, suggesting that these conserved proteins may play important roles in various organisms (Fig.14).

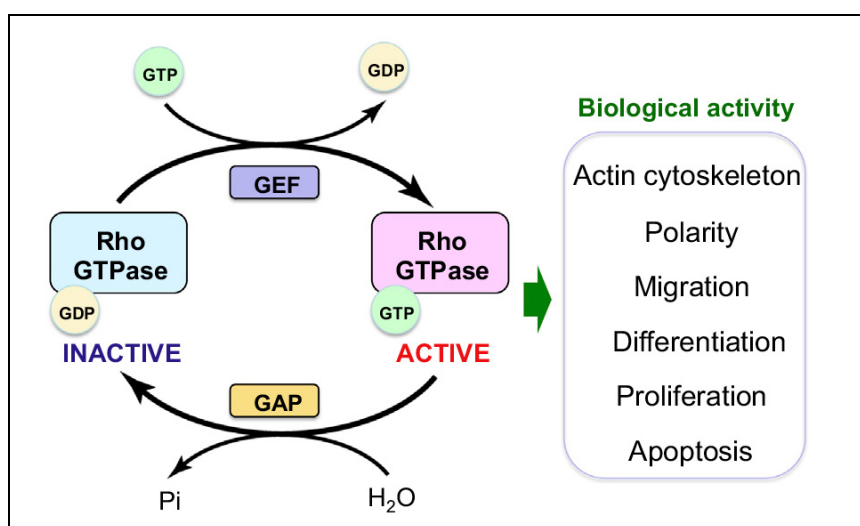


Figure 14 - Regulation of GTP hydrolysis by GAPs. (Yamada A. et al., *Journal of oral Biosciences* 2014)

The RhoGAP regulators are in excess than their targets and there are at least four possible explanations: first, some GAPs, similarly to Rho GTPases, show preferential tissue expression and functions; secondly some of them can specifically act on a single GTPase; thirdly, considering that Rho GTPases are implicated in a large number of biological responses, each GAP may selectively regulate a specific Rho GTPase signalling pathway; fourthly, the GAP domain may serve as a recognition region, so RhoGAPs could act as effectors or scaffold proteins mediating the cross-talk between Rho GTPases and different signalling pathways [81]. A multiple sequence alignment [83] of only RhoGAP domains in human proteins showed high homology of amino acids sequence. This conserved region, also known as BH domain, consists of nine α helices [90] composed by 170 amino acids [83]. Of particular interest, within this domain there is a conserved arginine residue, present in most RhoGAP-containing proteins, which is inserted into the active site of all Rho GTPases [83,90]. The function of this amino acid is to stabilize a conformation needed for hydrolysis. Few RhoGAPs have only a GAP domain, in fact most of them are multidomain molecules [83,91]. It is possible that the presence of additional functional modules is important to integrate signals from a number of signalling pathways [83]. To date, the

functions of most of the domains are not known. Several studies indicated that RhoGAP activities are influenced by a variety of mechanisms, including lipid binding, protein–protein interaction, phosphorylation, proteolytic degradation, subcellular translocation and targeted degradation [81,83,90,91]. The numerous functional domains and other important sites present in GAPs indicate an additional complexity of GTPases activity control.

Specific phosphorylations have a prominent role in the modulation and regulation of many proteins, including GAPs. In fact, tyrosine and serine/threonine phosphorylations influence GAPs enzymatic function or their subcellular localization.

Also lipids seem to have a regulatory role in GTPase-mediated signal transduction. Indeed, phospholipids could regulate GAPs catalytic function or can ‘switch’ the GTPase substrate preference for a GAP.

The cell-type-specific gene expression and the protein degradation represent other potential regulatory mechanisms for controlling GAP activity. Unfortunately these GAP regulatory mechanisms remain rather unclear. Inhibition of RhoGAP activity seems to be sufficient to promote activation of Rho GTPases and, consequently, the start of Rho-mediated biological response. These findings suggest that GAPs might contribute more to the function of GTPases than what it has been predicted by their biochemical activity [91]. The large number and structural complexity of Rho GAP members suggest that it would be important fully understand where, when and how they operate. Considering the ubiquitous nature of most Rho proteins and their involvement in human tumours, GAPs may offer an interesting way to control Rho GTPase activity in cancer [81,90].

XTP1/DEPDC1B is a molecule that belongs to this regulator family. Prosite Scan database (<http://www.expasy.ch/prosite>) revealed the presence of a DEP (Dishevelled, Egl-1, Pleckstrin) domain in its N-terminal region and a RhoGAP (GTPase activating protein) like domain in C-terminal region [92,93]. *XTP1/DEPDC1B* is a peculiar protein because its RhoGAP domain lacks of the catalytic arginine typical of traditional RhoGAPs members [95]. DEPDC1A (DEP domain containing 1A), a high conserved protein similar to *XTP1/DEPDC1B* is also comprised in the RhoGAP family [94].

1.3.2 - *XTP1/DEPDC1B*

XTP1, also known as *DEPDC1B* (DEP domain containing 1B protein) or BRCC3, is a gene mapped to human chromosome 5q12.1 and shows a cDNA sequence similar to *XTP8*.

A recent study reports that *XTP1/DEPDC1B* GAP domain includes the residues 177-400 while the residues 15-106 form the DEP domain that permit the interaction with both

transmembrane and nuclear proteins [95]. There are more predicted post-translational modification sites in the *XTPI/DEPDC1B* ORF such two N-glycosylation sites (aa 18-21 and aa 255-258), ten casein kinase II phosphorylation sites (aa 45-48, 138-141, 202-205, 274-277, 367-370, 401-404, 402-405, 436-439, 466-469, 480-483), two cAMP-dependent phosphorylation points (aa 69-72, 157-160), three PKC phosphorylation residues (aa 68-70, aa 466-468, aa 526-528), and one tyrosine sulfation site (aa 435-449) [92]. *XTPI/DEPDC1B* gene expression is detected only in a few tissues as in the placenta and testis, it is relatively scarce in the heart and small intestine, not detectable in other human normal tissues whereas it is overexpressed in several tumours [96]. The *XTPI/DEPDC1B* open reading frame encodes a putative polypeptide with a molecular mass of 58.3 kDa, but in kidney cells it is detected a band corresponding at a molecular weight of 59-60 kDa [96]. Several studies have reported different subcellular distribution of this protein. In fact, *XTPI/DEPDC1B* shows a predominant location to the membrane in COS-1 cells [92]. In glioma cell lines, treated or not with an alkylating agent, the protein is respectively in the nucleus or in the cytoplasm [97]. In other cell lines it is localized to the plasma membrane that persists during mitosis [94]. The clear function of *XTPI/DEPDC1B* is still uncharacterized, however, in different studies, it seems to promote several biological functions due to the presence of its two domains. Some studies revealed that *XTPI/DEPDC1B* interacts with various signalling molecules, ranging from splicing regulators to transmembrane proteins; all of these interactions could be implicated in the regulation of multiple biological processes. Although *XTPI/DEPDC1B* lacks of conserved residue of arginine an alternative mechanism promotes GTP hydrolysis of Rho GTPases.

The role of *XTPI/DEPDC1B* in glioma cell growth, migration, invasion is under investigation and its downregulation reveals an inefficient DNA repair process [96,97].

Another study [94] showed that *XTPI/DEPDC1B* is a proliferation-associated gene that mediates the interplay between cell-cycle progression and de-adhesion events at the mitotic entry. During the cell cycle, in G2 phase the *XTPI/DEPDC1B* mRNA levels increased and the protein accumulated until mitosis, whereas in M phase the protein is degraded in a proteasome-dependent manner. In different cell types *XTPI/DEPDC1B* modulates adhesion and actin cytoskeleton dynamics in G2 phase, cell adhesion at G2/M transition, while during Zebrafish embryogenesis it is involved in cell proliferation [94] and in G2/M transition. When cells progress into mitosis, the *XTPI/DEPDC1B* expression stimulates de-adhesion, identified as “adhesion-dependent checkpoint”, and cell rounding morphologies (Fig.15) [94,98]. The silencing of *XTPI/DEPDC1B* produces a substantial delay in the transition

from G2 to mitosis, the formation of aberrant actin stress fibers and enlarged and persistent structures (focal adhesions).

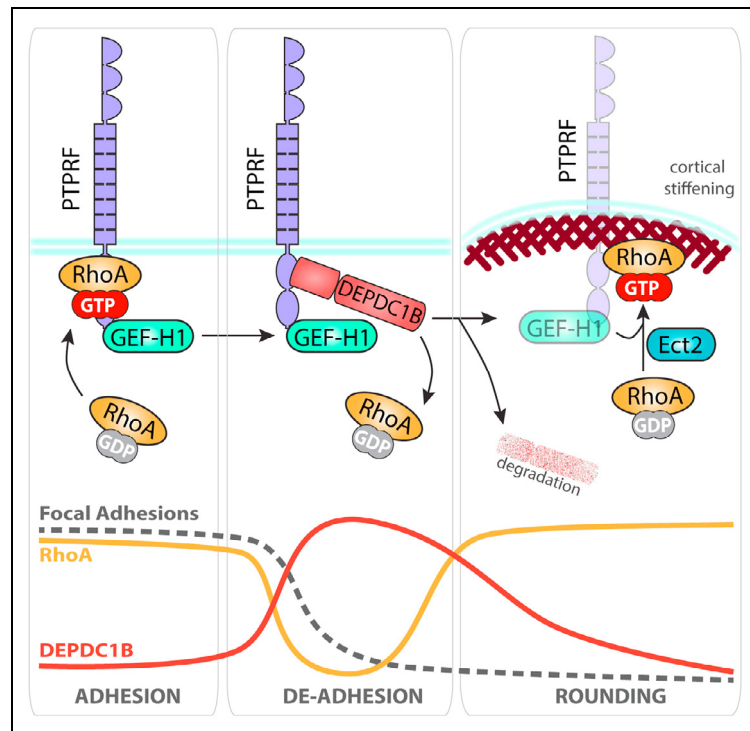


Figure 15 - *XTP1/DEPDC1B*-mediated de-adhesion checkpoint. (Garcia-Mata R. *Developmental Cell* 2014)

An additional role of *XTP1/DEPDC1B* is the promotion of tumour cells migration and invasion through activating Wnt/ β -catenin signalling and cell proliferation [92,93,96]. Moreover, *XTP1/DEPDC1B* might represent a poor prognostic marker for non-small cell lung cancer [93] and nasopharyngeal carcinoma patients [99].

The interaction of *XTP1/DEPDC1B* DEP domain with several molecules implicated in various biological processes such as transcriptional regulation, RNA splicing, cell migration, microtubule assembly, and synapse formation [95], make it a potential biomarker and a possible therapeutic target [100].

1.3.3 - *SDP35 / DEPDC1A*

Genome-wide expression analysis, [101,102,103,104] identified and characterized a *XTP1/DEPDC1B*-like gene, *SDP35/DEPDC1A* or DEPDC1 (DEP domain-containing protein 1A) that is significantly overexpressed in several cancers [104,105,106]. DEPDC1 gene encodes for two isoforms: a 4.6-kb transcript, denoted as DEPDC1 isoform 2 (DEPDC1-V2: GeneBank Accession AB281274), that is abundantly and specifically

expressed in bladder cell lines and a 5.3-kb transcript, DEPDC1 isoform 1 (DEPDC1-V1: GeneBank Accession AB281187), expressed in testis and cancer tissues and cell lines [104]. Although DEPDC1-V1 protein showed expression in testis, none of two variant molecules was observed in normal tissues as heart, liver, kidney and lung [104]. These data are confirmed by another study in which is reported that *SDP35/DEPDC1A* is poorly expressed in the majority of tissues, except in human bone marrow and lymphoid organs while it is highly expressed in human embryonic pluripotent stem cells [107].

Both isoforms showed a nuclear localization and contain the DEP domain in their N-terminal regions. DEPDC1-V1 and DEPDC1-V2 transcriptional variants consisting of 5318 and 4466 nucleotides that encode 811 and 527 amino-acid peptides and consist of 12 and 11 exons respectively. The DEPDC1-V2 variant lacks of exon 8 (852 nucleotides) while the remaining exons are common to the two isoforms, spanning an approximately 23-kb genomic region on the chromosomal band 1p31.2 [104]. The predicted molecular weight of V1 and V2 proteins is respectively 93.1 kDa and 61.5 kDa and it is detected both homo- and hetero-dimerization of the two isoforms [104]. Actually, the biological function of *SDP35/DEPDC1A* is poorly known but several studies show that it is involved in different function and has different roles in various diseases [108,109] It is associated with poor prognosis in bladder cancer [104], glioma, breast cancer, melanoma, lung adenocarcinoma [110], lung cancer [111] and hepatocellular carcinoma [112]. Indeed, it is suggested that in multiple myeloma cells *SDP35/DEPDC1A* promotes cell cycle, blocks the differentiation and induces markers of mature plasma cell suggesting that it may be an indicator of poor prognosis also in this disease [107]. Furthermore, *SDP35/DEPDC1A* seems to be an important gene involved in cancer cells proliferation, migration and invasion as well as in some types of carcinogenesis [102,104,105,106,107,110,113]. Downregulation of *SDP35/DEPDC1A* significantly suppresses bladder cancer cells growth and increases the apoptotic cells, indicating its crucial role in bladder cancer cell growth [104]. Considering the close correlation between carcinogenesis and cell cycle dysregulation, *SDP35/DEPDC1A* may be important in cell cycle progression [113]. *SDP35/DEPDC1A* expression varies during the cell cycle showing high mRNA and protein levels in M-phase cells, whereas its expression significantly decreases in G1 or in S phases. *SDP35/DEPDC1A* knockdown produces a substantial delay in the transition from G2 to mitosis and cell defects for the presence of multiple nuclei structure [113]. Similarly to *XTP1/DEPDC1B* [94], it is required for proper mitotic progress and the simultaneous depletion of both genes produces an additive effect, demonstrating a functional redundancy and a tight cooperative control during the G2/M transition.

In HELA cells, *SDP35/DEPDC1A* protein showed a predominant nuclear localization in S phase, and in prophase while it is localized in the nucleus and redistributed into the cytoplasm under metaphase and anaphase [113].

Finally a clinical study demonstrated that the vaccination with DEPDC1-294 epitope peptide induced a potent immunological response in bladder cancer, correlated with anti-tumour effects and clinical benefits, suggesting a possible role as novel target for the development of new therapeutic strategies [106].

2 - AIM OF THE STUDY

Soft tissue sarcomas (STS) are rare tumours with uncertain histogenesis, diagnosis, prognosis and problems that often cause very vague symptoms which are not immediately recognizable. To date, unfortunately, the biological factors that predict the aggressiveness and the clinical evolution of these tumours are still not very reliable. The basic prognostic factors for STS are size, depth and degree of the lesion, but they are often inefficient because tumours at the same stage and having similar morphology may undergo to a completely different evolution due to intrinsic biological characteristics of each tumour. For these reasons it is important to search for specific and early biomarkers that may be predictive of transformation, malignant progression and response to the therapies.

The rarity of these tumours has resulted in a shortage of human tumour samples useful in order to enhance our understanding of these diseases. The main objective of this research was to identify possible markers for prognostic stratification of patients suffering from high grade STS. This study also could recognize "key" molecules in signalling pathways that may represent potential targets for new therapies. For this reason, we will focus on the identification of biomarkers involved in the STS malignant progression as the oncogene MET, regulated by microRNA-152, growth factors binding protein IGFBP7, involved in the IGF axis and two unique Rho GAPs, *XTP1/DEPDC1B* (DEP domain-containing protein 1B) and *SDP35/DEPDC1A* (DEP domain-containing protein 1A). We will carry out different analyses including immunohistochemistry, RealTime PCR and western blot on a large number of surgical specimens derived from STS patients (leiomyosarcoma, undifferentiated pleomorphic sarcoma, fibrosarcoma and liposarcoma) with complete clinical follow-up (age, gender, therapy, presence of metastasis, time to relapse etc), in order to perform statistical correlations. In addition, in vitro studies will evaluate the impact of most significant molecules on tumour cell behaviour .

Only the combined study of genes, their regulation and expression, as a set of cellular processes, will lead to the recognition of essential pathways and molecules in the malignant progression of sarcomas useful not only for the prognosis but also to the development of new therapeutic strategies.

3 - MATERIALS AND METHODS

3.1 - Phase 1

3.1.1 - Tumour specimens and clinical records

In this study 152 samples (Tab.3) from patients with different histotype of high-grade Soft Tissue Sarcoma (STS), according to the Federation Nationale des Centres de Lutte contre le Cancer grading system (FNCLCC), were taken into account. All patient were diagnosed at Rizzoli Orthopaedic Institute from 1985 to 2011 and the samples were selected from the bank of tissues of the same institute. Selection criteria included tumours deeply localized at the extremities or chest wall, diameter >5 cm, no local relapses at diagnosis and no radio/chemotherapy during follow-up. The diagnosis based on histological, cytogenetic and immunohistochemical criteria [2] was confirmed by independent pathologists. The clinical follow-up was calculated from the date of the original diagnosis to the clinical event, or to the last day of the follow-up period. 5 years was the minimum follow-up for metastasis-free survival.

Patients	Gender	Age	Histotype	Grade	Metastasis site	Outcome
1*	M	64	UPS	II	multiple locations	DOD
2*	M	54	UPS	III	NM	ALIVE
3*	M	63	UPS	III	NM	ALIVE
4*	M	61	UPS	II	lung	DOD
5*	F	73	UPS	III	lung	ALIVE
6*	F	54	UPS	III	lung	DOD
7*	M	64	UPS	III	lung	DOD
8*	M	62	UPS	III	NM	ALIVE
9*	M	38	UPS	III	NM	ALIVE
10 [#]	F	43	UPS	III	NM	ALIVE
11*	F	67	UPS	III	NM	DEAD
12*	F	72	UPS	III	lung	DOD
13*	F	76	UPS	III	lung	DOD
14*	M	38	UPS	III	lung	DOD
15*	M	62	UPS	III	lung	ALIVE
16*	F	66	FS	III	lung	ALIVE
17*	M	71	LMS	III	lung	DOD
18*	M	57	LMS	III	lung	ALIVE
19*	M	63	LMS	III	lung	DOD
20 [#]	F	76	LMS	III	multiple locations	DOD
21*	M	34	LMS	III	lymph nodes	DOD
22*	M	62	LMS	III	lung	DOD
23*	M	66	LMS	III	lung	DOD
24*	M	35	LMS	III	lung	DOD
25*	M	55	LMS	III	lung	DOD
26 [#]	M	78	LMS	II	NM	ALIVE
27*	M	38	LMS	II	NM	ALIVE
28*	F	62	UPS	II	lymph nodes	DOD

Patients	Gender	Age	Histotype	Grade	Metastasis site	Outcome
29*	M	43	LMS	III	NM	ALIVE
30*	M	52	LMS	III	lung	DOD
31*	F	79	LMS	III	NM	DEAD
32*	F	57	LMS	III	lung	DOD
33 [#]	M	76	LMS	III	lymph nodes	DOD
34 [#]	F	66	UPS	III	lung	DOD
35*	F	68	LMS	III	lung	ALIVE
36 [#]	F	74	LMS	III	liver	DOD
37*	F	42	LMS	III	lung	DOD
38*	F	71	LMS	III	lung	DOD
39 [#]	M	49	LS	II	lymph nodes	DOD
40 [#]	M	42	LS	II	NM	ALIVE
41*	M	56	LS	III	NM	ALIVE
42*	M	69	LS	II	lung	DOD
43 [#]	M	47	LS	II	NM	ALIVE
44*	F	73	LS	II	NM	DEAD
45*	F	49	LS	II	NM	ALIVE
46*	F	40	LS	II	NM	ALIVE
47*	M	42	LS	III	NM	ALIVE
48 [#]	F	85	LS	II	NM	DEAD
49*	M	62	LS	III	lung	DOD
50 [#]	F	75	FS	III	multiple locations	DOD
51 [#]	M	54	FS	III	NM	ALIVE
52 [#]	F	29	FS	III	vertebrae	DOD
53 [#]	M	18	UPS	III	vertebrae	DOD
54 [#]	M	76	FS	II	NM	DEAD
55 [#]	F	82	FS	III	lung	ALIVE
56*	M	45	LS	III	femur	DOD
57*	M	46	LS	III	lung	DOD
58 [#]	F	58	LS	II	lung	DOD
59 [#]	M	53	LS	III	lung	DOD
60*	M	44	LS	III	lung	DOD
61*	M	43	LS	III	lung	ALIVE
62*	M	44	LS	III	liver	DOD
63*	M	42	LS	III	lung	ALIVE
64*	M	53	LS	III	osseous	DOD
65*	M	59	LS	III	NM	ALIVE
66*	M	31	LS	III	lung	DOD
67 [#]	M	63	LS	II	NM	ALIVE
68*	M	69	LS	III	lymph nodes	ALIVE
69*	F	32	LS	III	NM	ALIVE
70*	M	41	LS	II	NM	ALIVE
71*	M	42	LS	II	NM	ALIVE
72*	F	66	LS	II	NM	DEAD
73 [#]	M	44	LS	III	lymph nodes	ALIVE
74*	M	78	LS	II	osseous	DOD
75*	M	55	LS	II	NM	ALIVE
76*	M	59	LS	II	NM	ALIVE
77*	M	43	LS	II	lung	ALIVE
78*	F	67	LS	III	lung	DOD
79*	M	35	LS	II	NM	ALIVE
80*	M	29	LS	II	NM	ALIVE
81*	F	36	LS	II	NM	ALIVE
82*	M	39	LS	II	NM	ALIVE
83*	M	31	LS	II	lymph nodes	DOD
84 [#]	M	28	LS	II	NM	ALIVE
85*	M	45	LS	II	osseous	DOD
86*	F	58	LS	II	NM	ALIVE
87	M	50	FS	III	NM	ALIVE

Patients	Gender	Age	Histotype	Grade	Metastasis site	Outcome
88	M	33	UPS	III	NM	ALIVE
89*	M	56	LMS	III	NM	DEAD
90	M	38	FS	III	lung	ALIVE
91*	M	53	LMS	III	vertebrae	ALIVE
92	M	54	FS	III	NM	ALIVE
93	M	50	FS	III	NM	ALIVE
94*	M	15	LMS	III	lung	ALIVE
95	M	15	FS	II	NM	ALIVE
96*	M	31	LMS	III	NA	ALIVE
97	M	65	UPS	III	osseous	DOD
98	M	48	FS	III	NM	ALIVE
99*	M	22	LMS	III	NM	ALIVE
100	M	15	FS	III	NM	ALIVE
101	M	35	FS	III	NM	ALIVE
102	M	21	UPS	III	NM	DOD
103	M	32	FS	III	NM	ALIVE
104	M	72	FS	III	NM	DEAD
105	M	50	FS	III	lung	ALIVE
106*	M	79	LMS	III	osseous	DOD
107	M	58	FS	III	osseous	DOD
108	M	63	UPS	III	NM	ALIVE
109	M	56	FS	III	NM	ALIVE
110*	M	71	LMS	III	NM	ALIVE
111	M	44	FS	III	NM	ALIVE
112	M	17	UPS	III	multiple locations	DOD
113	M	55	LMS	III	multiple locations	ALIVE
114	M	62	LMS	III	osseous	ALIVE
115	M	68	FS	III	NM	ALIVE
116	M	28	FS	III	NM	ALIVE
117	M	48	FS	III	multiple locations	ALIVE
118	M	45	FS	III	lung	ALIVE
119	M	42	UPS	III	NM	ALIVE
120	M	43	UPS	III	lung	DOD
121	M	82	UPS	III	multiple locations	DOD
122	M	64	UPS	III	lung	DOD
123	F	34	UPS	III	lung	DOD
124	M	54	UPS	III	NM	DEAD
125	M	46	UPS	III	NM	ALIVE
126	F	62	UPS	III	lung	DOD
127	F	88	UPS	III	lung	ALIVE
128	M	65	UPS	III	NM	ALIVE
129	M	71	UPS	III	lung	DOD
130	M	52	UPS	III	lung	DOD
131	M	64	UPS	III	lung	ALIVE
132	M	56	UPS	III	NM	ALIVE
133	F	79	UPS	III	NM	DEAD
134	M	55	UPS	III	NM	ALIVE
135	M	61	UPS	III	lung	DOD
136	M	38	UPS	III	lung	DOD
137	M	69	UPS	III	NM	DEAD
138	F	57	UPS	III	NM	ALIVE
139	M	70	UPS	III	NM	DEAD
140	M	71	UPS	III	multiple locations	DOD
141	M	76	UPS	III	NM	ALIVE
142	F	63	FS	III	multiple locations	ALIVE
143	M	50	UPS	III	NM	ALIVE
144	F	54	UPS	III	multiple locations	DOD
145	F	70	UPS	III	multiple locations	DOD
146	M	58	UPS	III	NM	ALIVE

Patients	Gender	Age	Histotype	Grade	Metastasis site	Outcome
147	M	70	UPS	III	lung	DOD
148	F	72	UPS	III	NM	DEAD
149	F	76	UPS	III	multiple locations	DOD
150	M	62	UPS	III	NM	ALIVE
151	F	43	UPS	III	NM	ALIVE
152	F	67	UPS	III	NM	DEAD

Table 3 – Case study. *Patients analyzed with RT-PCR analysis; #Patients without IHC expression UPS = undifferentiated pleomorphic sarcoma; LMS = Leiomyosarcoma; LS = Liposarcoma ; FS = Fibrosarcoma; NM = no metastasis; DOD = Dead of disease; DEAD = Dead for other causes

The clinical cases considered for protein expression consisted of 25 leiomyosarcomas (LMS), 53 undifferentiated pleomorphic sarcomas of the storiform-pleomorphic variant (UPS), 20 fibrosarcomas (FS) and 33 liposarcomas (LS). 99 patients were male and 50 died of disease. 70 patients had metastases from the beginning or during the follow-up period.

Frozen samples of 93 out of 152 primary STS and 22 paired metastatic lesions were available for real-time qPCR (Tab.3). Of the 93 patients 55 developed metastases but of these only 22 lung metastasis specimens were available. 17 non tumour (healthy) tissues were used as a control. Western Blot analyses were performed in the 22 paired primary STS lesions and lung metastases.

For all tumour specimens the percentage of neoplastic cells in reference histological sections was $\geq 90\%$ with no detectable signs of substantial intralesional lymphocyte infiltrations as determined by morphological and immunohistochemical criteria. All samples were managed in accordance with the authorizations issued by the Ethical Committee of Rizzoli Orthopaedic Institute. Informed consent was obtained from all patients.

3.1.2 - Cell lines

The cell lines used in the in vitro experiments for siRNA or miR-152 transfection, proliferation, migration and apoptosis were the uterin leiomyosarcoma SKLMS1 (ATCC HTB88™), fibrosarcoma HT1080 (ATCC CCL121™) liposarcoma SW872 (ATCC HTB92™) and the hMSC (ATCC CRL-1486™). Cells were obtained from the American Type Culture Collection (ATCC, Manassas, VA, USA) and were already available in the Laboratory of Experimental Oncology Institute Rizzoli. The cells were grown in a humidified incubator-Iscove Modified Dulbecco's Medium (IMDM) supplemented with 10% fetal bovine serum (FBS) in the presence of 100 U/ml penicillin and 100 µg/ml streptomycin (Invitrogen-Life Technology, Paisley, UK) and L-glutamine (2 mM), at a temperature of 37 °C and 5% CO₂.

3.1.3 - Primary cell cultures

Primary STS cells were obtained from 8 surgically removed metastatic lesions according to standard procedures for isolation of tumour cells from neoplastic formations. These cells were made available by COMT directed by Prof. Roberto Perris and were cultured in DMEM supplemented with 2mM glutamine, 5% FBS, 5% newborn calf serum (NCS), 10 mM non-essential amino acids and antibiotics (100 U/ml penicillin and 100 µg/ml streptomycin) at 37°C and 5% CO₂

3.1.4 - RNA extraction

Total RNA was extracted from 86 primary tumours, 22 paired metastatic lesions and 17 healthy control frozen tissue samples using Trizol reagent (Invitrogen, Carlsbad, CA, USA), a monophasic solution of phenol and guanidine isothiocyanate which can irreversibly inhibit ribonuclease and lyse the cells. To avoid RNA degradation samples were kept on ice and in complete sterility. Thorough cell lysis was obtained with a rotor-stator type homogenizer (Polytron). Samples were centrifuged at 10000 rpm for 2-3min at 4°C in order to separate the insoluble material from the solution. 200µl of cold chloroform were added to the solution. The alkyl halide allows to differentiate the solution in three phases: an aqueous top that contains the RNA, an interphase in which DNA is localized and a lower organic phase of higher density containing lipids and proteins.

The obtained solution was incubated on ice for 15 min and centrifuged for 15 min at 4°C at 12000 rpm. The aqueous phase containing the RNA was recovered taking care not to contaminate it from the genomic DNA present on the tube walls. An equal volume of isopropanol was added to precipitate the nucleic acid of interest. Samples were incubated on ice for 15 min and centrifuged at 13000 rpm for 15 min at 4°C. The pellet thus obtained was recovered and washed with cold 75% ethanol to eliminate the salts. Samples were centrifuged at 12000 rpm at 4°C for 5 minutes, the ethanol removed and the pellet allowed to dry under a hood for a few minutes.

The RNA was resuspended in 30µl of 1X *RNAsecure reagent* (Ambion, Inc, Austin TX). The RNA concentration was determined using the UV-visible spectrophotometer Nanodrop (ND-1000). Purity and quality were checked by a denatured gel electrophoresis. The RNA samples thus obtained were kept at -80 ° C and used for subsequent Affymetrix and Real Time PCR analyses. The RNA extraction method from cellular was the same used for the tissue samples.

3.1.5 - Reverse transcription and Real Time PCR of miR-152

To analyse miR-152 expression, the RNA samples previously obtained (paragraph 3.1.4) were reverse transcribed to complementary DNA strand (cDNA) using the *TaqMan MicroRNA Reverse Transcription Kit*. Reaction was conducted in a total volume of 15 μ l containing 5 μ l of RNA and the following components:

- 100 mM dNTPs 0.15 μ l
- Multiscribe™ Reverse Transcriptase, 50U/ μ l 1 μ l
- 10X Reverse Transcription Buffer 1.50 μ l
- RNase Inhibitor, 20U/ μ l 0.19 μ l
- Nuclease-free water 4.16 μ l
- 5X Random Primer 3 μ l

The reverse transcription reaction was carried out in the thermal cycler 2400 Applied and the following conditions were used:

- 30 minutes at 16°C
- 30 minutes at 42°C
- 5 minutes at 85°C
- ∞ a 4°C

The samples thus obtained were amplified by real-time PCR using the TaqMan microRNA assay (Applied Biosystems, Foster City, CA, USA) specific for the miRNA of interest (miRNA Assay n. 000475 for miR-152). The reaction was carried out in duplicate for each cDNA sample and were used 1.33 μ l of the RT product. The following master mix was added for a total volume of 20 μ l:

- TaqMan MicroRNA Assay (20X) 1 μ l
- TaqMan 2X Universal PCR Master Mix, No AmpErase UNG^a 10 μ l
- Nuclease-free water 7.7 μ l

Each sample was amplified for the miRNA of interest and a reference housekeeping gene RNU44 (assay n. 001094), RNA constitutively expressed in all cell types.

The reaction was carried out using the ABI PRISM 7900 HT instrument (Applied Biosystems, Foster City, CA, USA) with the following conditions:

- 10 min at 95 ° C, enzyme activation phase
 - 5 sec at 95 ° C denaturation step
 - 1 min at 60 ° C, annealing and synthesis phases
- 40 reaction cycles.

3.1.6 - Reverse transcription and Real Time PCR of XTP1/DEPDC1B, SDP35/DEPDC1A, MET

RNA of all samples was reverse transcribed into complementary DNA strand (cDNA) using the High capacity cDNA archive kit (Applied Biosystems, Foster City, CA); subsequently the samples were amplified by real-time PCR to validate expression of MET and the two RhoGAPs genes. Reactions were carried out in a total volume of 100 μ l using 4 μ l of RNA (100ng / μ L) and the following components.

- RNase-free water 68 μ l
- 10X Reverse Transcription buffer 10 μ l
- 25X dNTPs 4 μ l
- 10X random primers 10 μ l
- Multiscribe Reverse Transcriptase 50U/ μ l 4 μ l

The reverse transcription reaction was carried out in thermocycler Applied 2400 properly using following conditions:

- 10min at 25° C
- 120min at 37° C
- ∞ at 4° C.

For each gene, the amplification reaction was carried out in duplicate, in a total volume of 25 μ l. The reaction mixture contained:

- 1,25 μ l of Target Assay 20X or Endogenous Control Assays Mix 20X;
- 25ng of cDNA diluted in 11,25 μ l of Rnase free water (Qqiagen, Valencia, CA);
- 12,5 μ l of TaqMan Universal Master Mix 2X (Ampli Taq Gold DNA polymerase, AmpErase UNG, deoxynucleotide triphosphate, passive reference fluorophore, optimized PCR buffer) (Applied Biosystems, Foster City, CA, USA).

The reaction took place under the following conditions:

- Phase of activation of the enzyme UNG (Uracil-N-glycosylase): 2 minutes at 50° C
- Denaturation step: 10 minutes at 95° C
- Annealing and synthesis step: 1 minute at 60° C

45 reaction cycles.

The assays used are shown in table 4 , all products are provided by Applied Biosystems:

Gene	ASSAY ID
<i>XTPI/DEPDC1B</i>	Hs00293551_m1
<i>SDP35/DEPDC1A</i>	Hs00854841_g1
<i>GAPDH</i>	Hs99999905_m1
<i>MET</i>	Hs01565584_m1
<i>ACTB</i>	Hs99999903_m1

Table 4 – Assays used for Real Time PCR

The target genes expression was quantified using the comparative method of $2^{-\Delta\Delta CT}$ [114] and normalized to a reference gene specifically (Glyceraldehyde-3-Phosphate Dehydrogenase (GAPDH) (TaqMan Expression Assays-Applied Biosystems, Foster City, CA, USA) for *XTPI/DEPDC1B* and *SDP35/DEPDC1A* and Actin (ACTB) for MET (TaqMan Expression Assays-Applied Biosystems, Foster City, CA, USA), and relative to a calibrator sample (pool of healthy cells). This protocol was also employed to evaluate the transcriptional levels of *SDP35/DEPDC1A* and *MET* gene in cell pellets.

3.1.7 - Immunohistochemistry (IHC) on TMA

Representative samples of the tumour lesions were collected and placed in paraffin block using the TMA Master tool (3DHistech Ltd, , Budapest, Hungary). The block included 2 or 3 samples of each patient, each TMA about 70 \ 80 sections. The TMA used "cores" of tissue fixed in formalin and embedded in paraffin, from 152 cases of patients with STS (Tab.3), 22 paired lung metastases. Kidney and prostate were used as control.

The sections of TMA were deparaffinized, rehydrated and immunostained with specific antibodies (Tab.5).

Antibody	Dilution	Company
rabbit polyclonal anti- <i>XTPI/DEPDC1B</i>	1:500	Novus Biologicals, Littleton CO, USA
rabbit polyclonal anti- <i>SDP35/DEPDC1A</i>	1:1000	Novus Biologicals, Littleton CO, USA
goat polyclonal anti-IGFBP7	5 µg/ml	R&D Systems, Abingdon, UK
rabbit polyclonal anti-MET	1:300	Santa Cruz Biotechnology, Santa Cruz, CA, USA
mAb 2200D12 (<i>SDP35/DEPDC1A</i>)	1:2	
mAb 2191H11 (<i>XTPI/DEPDC1B</i>)	1:10	

Tab 5 – Antibody and dilution used for Immunohistochemistry analysis

After washing with PBS 1X buffer the sections were incubated for 30 minutes with biotinylated secondary antibody (Dako k0679 kit). After appropriate washes, the sections were incubated with a solution to allow the enzyme immunoassay reaction detection and covered with a solution containing the substrate buffer and the chromogen DAB (3,3'-diaminobenzidine) or the chromogen alkaline phosphatase necessary for the colorimetric reaction.

Subsequently, the sections were counterstained with hematoxylin, dehydrated and the coverslips were mounted by means of non-aqueous mounting.

The level of immunoreactivity was assessed by assigning a score determined by the sum of the intensity immunostaining (score 0 = no expression; 1=weak expression; 2=moderate expression; 3=strong expression) and positive cell-percentage score (negative; 1=10-49%; 2=>50%). Cut-off levels of the sum of scores were applied 0 for negative, 1-3 for weakly positive, and 4-5 for moderate to strong positivity in more than 50% of tumour cells which is considered protein up-regulation. Normal prostate and kidney tissue sections were used respectively as positive and negative controls.

3.1.8 - Protein extraction and Western blot

According to standard procedures, protein extracts were prepared by mincing and homogenizing fresh samples in extraction buffer (50 mmol/L Tris-hydrochloride at pH 8, 150 mmol/L sodium chloride, 1 mmol/L DTT, 50 mmol/L sodium fluoride, 0.5% sodium deoxycholate, 0.1% SDS, 1% Nonidet P-40, 0.1 mmol/L PhenylMethaneSulfonylFluoride) and specific protease inhibitors (protease inhibitor Mix, 80-6501-42, Amersham Biosciences).

The protein concentration was determined by method of Bradford and absorbance obtained using a spectrophotometer at the wavelength of 595nm. Protein extracts (50 g) were analyzed by means of 8 % SDS–polyacrylamide gel electrophoresis, and the samples were run using a voltage of 70 V at the stage of stacking and 100V in the running stage. After electrophoresis, the separated proteins were transferred onto nitrocellulose membranes (voltage 100V, 1 hour at 4°C). Subsequently the membranes were immersed in a blocking solution 5% non-fat dry milk in TBST 1X and incubated with the respective primary antibodies: anti-SDP35/DEPDC1A (Novus Biologicals) diluted 1:5000 and anti-XTPI/DEPDC1B (Biorbyt, Cambridge, UK) diluted 1:250. Primary antibodies were diluted in 5% milk in TBST 1X. The membranes were incubated over night at + 4°C. Secondary antibody (Anti-Rabbit IgG, GE Healthcare, Amersham, diluted 1: 1000 in 5% milk in TBST

1X for both primary antibodies. The signal was visualized by using the Immobilon Western Chemiluminiscent HRP substrate (Millipore, Billerica, MA, USA) and quantified by densitometric analysis (GS-800 imaging densitometer and Quantity One software; Bio-Rad, Hercules, CA, USA). A rabbit anti-actin polyclonal antiserum (Sigma Chemical Co., St. Louis, MO, USA) was used as a loading control.

When using tumour cells proteins from SKLMS1, HT1080, SW872wt and SW872 *SDP35/DEPDC1A* siRNA-mediated knockdown, the pellets were extracted using 100µl of a suitable extraction buffer (Lysis Buffer) containing the protease inhibitors mix (GE Healthcare, 1: 100) and incubated for 30 minutes under stirring and, occasionally, pipetting gently with a syringe. Subsequently, the samples were centrifuged (4°C for 5 minutes at 12000 rpm) to recover the supernatant containing the protein extract. The Lysis Buffer used includes: NaCl 250 mM, Tris-HCl (pH 7.5), 25 mM, EDTA (pH 8) and 5 mM, Nonidet P40 (NP40) 0.1%. The proteins were then dosed and Western blot analysis was carried out as described above.

3.1.9 - Statistical analysis

All data regarding mRNA expression levels obtained from RealTime technique were evaluated as median within 25th and 75th percentile because of their non-Gaussian distribution. Non-parametric Kruskal-Wallis and Mann-Whitney U tests were used to compare the gene expression data in non-paired samples; while non-parametric The Wilcoxon and Friedman non-parametric statistical tests were used to establish the differences in gene expression levels in paired surgical specimens.

Chi-square (χ^2) test with Fischer's exact p value was used to correlate protein expression with clinical parameters of the population.

The probability of metastasis-free survival (MFS) was calculated using the Kaplan-Meier analysis and statistical difference between survival curves was obtained by the Log-Rank test. Multivariate analysis was assessed by Cox's analysis: Hazard ratios and their 95% confidence intervals (95% CIs) were calculated for Cox's univariate and multivariate regression analyses to define the risk of developing metastases. All statistical analyzes were performed with SPSS software (SPSS Inc., Chicago, IL). For all statistical analyzes the values of $p \leq 0.05$ were considered statistically significant.

3.1.10 - Monoclonal antibody (mAb)

The mAbs were produced and supplied by COMT headed by Prof. Roberto Perris and were generated in rabbits by immunization with synthetic peptides corresponding to amino acid sequences selected within the most divergent regions of the two proteins and outside of the conserved DEP and GAP domains. The antibody used were 2191H11 (*XTPI/DEPDC1B*) and 2200D12 (*SDP35/DEPDC1A*).

3.2 - Phase 2: *In vitro* studies

3.2.1 - Cell count

To verify cell viability 200,000 cells were seeded in 6-well plates. The cell suspension was carried out during the normal process of cell detachment from flask, which involves several steps including: the removal of medium, the addition of 4-5 ml of 1 X PBS to wash cell monolayer, the addition of 1 ml of trypsin-EDTA, which acts at an optimal temperature of 37 ° C and finally the addition of 4 ml of IMDM 10% FBS to inactivate the trypsin. The suspension obtained was inserted into a 15 ml tube and centrifuged at 1000 rpm for 5 minutes at room temperature to allow the removal of the supernatant and the pellet obtained was resuspended in a known volume of IMDM.

The number of adherent, viable cells was assessed microscopically using an improved Neubauer haemocytometer and proliferation was assessed as the percentage of cells that excluded 0.2% trypan blue.

Living cells were counted and the number of cell/ml calculated by multiplying the average number of cells for 10,000, chamber conversion factor, and then for the volume of the flask, 5ml.

3.2.2 - Transfection of *miR-152* precursor molecules

For each transfection, SKLMS1 cells were seeded at a density of 2.5x 10⁵ cells/well in 6-well plates with IMDM culture medium supplemented with 10% FBS to reach a 70% cell confluency. The transfections were performed using Lipofectamine 2000 (Invitrogen, Carlsbad, CA, USA). In each well 50 nM miR-152 precursor (cod. PM12269; Ambion Inc, Austin, TX, USA) or negative control miRNA precursor (scramble) (cod. AM17110; Ambion) molecules were transfected using IMDM culture medium devoid of FBS and

antibiotics. Finally the cells were incubated at 37°C with 5% CO₂ and the transfection efficiencies were monitored after 12h, 24h and 48h by flow cytometry (FACS Calibur, BD, San Jose, CA, USA) using CyTM3 and FAMTM dye-labeled Pre-miR Negative Controls (cod. AM17120; Ambion) and RT-PCR (paragraph 3.1.5) according to the TaqMan MicroRNA Assay Protocol (Applied Biosystems; miR-152 assay no. 000475).

3.2.3 - SDP35/DEPDC1A siRNA transfection

SDP35/DEPDC1A knockdown was performed using the silencing kit (Santa Cruz biotechnology DEPDC1 siRNA(h)) containing a pool of 3 target-specific. In a six well culture plate 2x10⁵ SW872 cells were seeded in 2ml of antibiotic-free IMDM growth medium supplemented with 10% of FBS. The cells were incubated at 37°C in a CO₂ incubator overnight to reach a 70% cell confluency. For each transfection two solutions were prepared: A and B. At first, 60nM of siRNA were diluted into 100µl of siRNA transfection medium (solution A). For the second solution, 8µl of siRNA transfection reagent were added to 100µl of siRNA transfection medium(solution B). The solution A was directly diluted in the solution B and mixed gently by pipetting up and down. This mixture was incubated for 45 minutes at room temperature. The cells were washed once with 2ml of siRNA transfection medium, and to the solution A + solution B were added 800µl of siRNA transfection medium. The cells were thus incubated for 5-7 hours in incubator at 37°C with 5% of CO₂. At the end of incubation and after checking the efficiency of transfection by reading the Fluorescein Conjugated Control siRNA with flow cytometry (FACS Calibur, BD Biosciences, San Jose, CA, USA). 1 ml of normal growth IMDM medium was added in each well and the cells were incubated for 18h. The medium was aspirated and the cells were assayed for the experiments 24h, 48h and 72h after the addition of fresh. To verify knockdown efficiency, RNA was extracted from the pellets obtained 24 48 and 72 hours after transfection (paragraphs 3.1.4 and 3.2.7). They were reverse transcribed into cDNA and amplified with Real-Time PCR as previously described (paragraph 3.1.6)

3.2.4 - Annexin test to determine apoptotic cells

Apoptotic and necrotic cells were analysed by means of the "Annexin-V-FLUOS" kit (MBL Medical and Biological Laboratories International, Woburn, MA, USA) The trypsin-cell-medium suspension (2 ml) was centrifuged at 1000 rpm for 5 minutes so as to obtain a visible pellet at the bottom of the tube. The pellet was resuspended and the cell count was carried out at 24, 48, 72 hours after transfection or seeding. A total of 300,000-500,000 cells were centrifuged at 3000 rpm for 5 minutes; the pellet obtained was resuspended in 85 µl of

Binding Buffer to which 10µl of Annexin-V-FITC and 5µl of propidium iodide were added. The cell suspension obtained was resuspended and incubated at room temperature for 15 minutes in the dark. Finally 400µl of Binding Buffer were added and the samples analyzed by flow cytometry (FACSCalibur, BD Biosciences, San Jose, CA, USA). The amount of live cells (Annexin- / PI), apoptotic (Annexin + / PI) and necrotic (Annexin + / PI +) was determined using the CellQuest software (BD Biosciences, San Jose, CA, USA). Data were presented as mean percentage ±SE from three independent experiments.

3.2.5 - Wound Healing Assay

Migration assay was performed on human SKLMS1, HT1080 and SW872 cells under normal growth conditions and in SW872 after 48h of siRNA transfection. Cells were cultured in a confluent layer, then a sterile 10µl pipette tip was used to make a wound across a cell culture monolayer. To investigate cell migration the plate was photographed at different time points after wounding (0,3,6,12,18h) and the area of wound was measured by ImageJ v.1.45r software (<http://rsbweb.nih.gov/ij/>). The experiment was repeated three times.

3.2.6 - Cell immunolabelling

The cells were seeded on glass slides, let adhere and incubated (37 ° C, 5% CO₂) in the culture medium. Slides were subsequently fixed in a solution of acetone 70% - 30% methanol and they were subjected to immunocytochemistry using the Dako LSAB + kit System-AP following the kit instructions, (see paragraph 3.1.7). The primary antibodies used were the rabbit polyclonal anti-DEPDC1B (anti-XTP1) and the anti-DEPDC1A (anti-SDP35) (Novus Biologicals,), diluted 1:500 and 1:1000 respectively and the mAb 2191H11 (XTP1) and 2200D12 (SDP35/DEPDC1A). To display the antigen reaction with the primary antibody a detection system based on diaminobenzidine (DAB) or on alkaline phosphatase was used. In both cases the nuclei were labelled with hematoxylin.

3.2.7 - Cell pellets for Real time PCR and Western blot

The cells were detached from the plates with the usual procedure which: the removal of the culture medium, 2 washes with 2 ml of PBS, the addition of 500µl of trypsin and finally the addition of 1.5 ml of IMDM medium to inactivate the action of the trypsin. The cells were collected from the suspension by centrifugation (10 minutes at 1500 rpm or 7 minutes at

1700 rpm) and the pellets thus formed were washed with 1 ml of PBS, centrifuged again at 3000 rpm for 5 minutes. The supernatant was removed and pellet frozen at -80 ° C.

4 - RESULTS

4.1 - Tumour samples and analysis of patients

4.1.1 - Population study

The clinical records included 152 patients afflicted with high grade STS (Tab.3) according to the Federation Nationale des Centres de Lutte contre le Cancer grading system (FNCLCC).

Selection criteria included tumours deeply localized at the extremities or chest wall, diameter >5 cm, no local relapses at diagnosis, no post-operative radio/chemotherapy. The diagnosis based on histological, cytogenetic and immunohistochemical criteria [2] was confirmed by independent pathologists. 29 were leiomyosarcomas (LMS), 56 undifferentiated pleomorphic sarcomas of the storiform-pleomorphic variant (UPS), 25 fibrosarcomas (FS) and 42 liposarcomas (LS). 111 were males and 41 females; the age ranged from 15 to 88 years with a median age of 55.5 years. Localization of the primary tumour resulted in 15 cases at the trunk level and 137 in the extremities.

82 of these 152 patients developed metastasis during follow-up, accurately, 38 of them presented metastasis at diagnosis or into the first three months of follow up.

Average metastasis-free survival (MFS) estimated according to Kaplan Meier method was 142.5 months (95%CI = 110.79-174.39) with a median of 38 months (95%CI =0.00-94.83). Gender, tumour size, site and chemotherapeutic treatment did not significantly correlate with metastatic condition. Cox's univariate analysis showed an increased risk of metastasis associated with age (HR=1.02 , 95% CI= 1.005-1.030, p=0.008) and lack of radiotherapy (HR=0.366, 95%CI=0.229-0.586,p<0.0005).

By Kaplan Meier survival analysis, the patients under 60 years (n=89) had a higher probability of MFS (log rank =9.30, p=0.002) compared to those with older age. Moreover even those who were given radiotherapy (n=77) had a higher probability of MFS (log rank=19.21, p<0.0005) compared with those who had been subjected to different treatment or even no therapy (Fig.16).

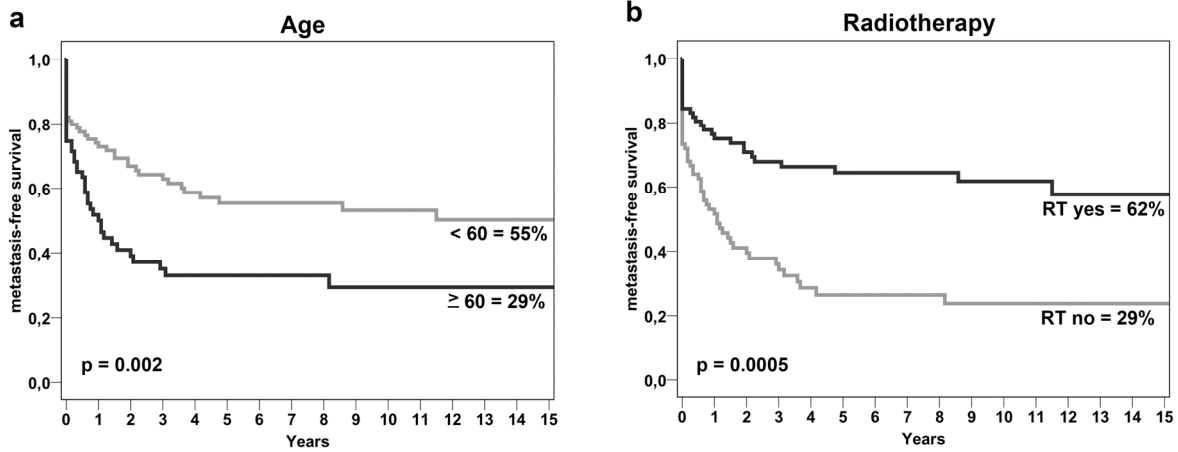


Figure 16 - Metastasis free survival. Curves respectively of patients under or over the age of 60 (a) and of patient treated or not with radiotherapy (b)

Concerning histotypes, it was shown that patients with liposarcoma had a higher probability of disease-free survival compared to other types of tumours, especially LMS and FS demonstrating worse prognosis (log rank = 11.68, $p = 0.009$), indeed, 5-years MFS is 64% for LS, 43% for UPS, 39% for FS and 32% for LMS (Fig.17). No significant correlation between survival, type of surgery, chemotherapy administration, gender and location of the tumour was observed in terms of disease-free survival.

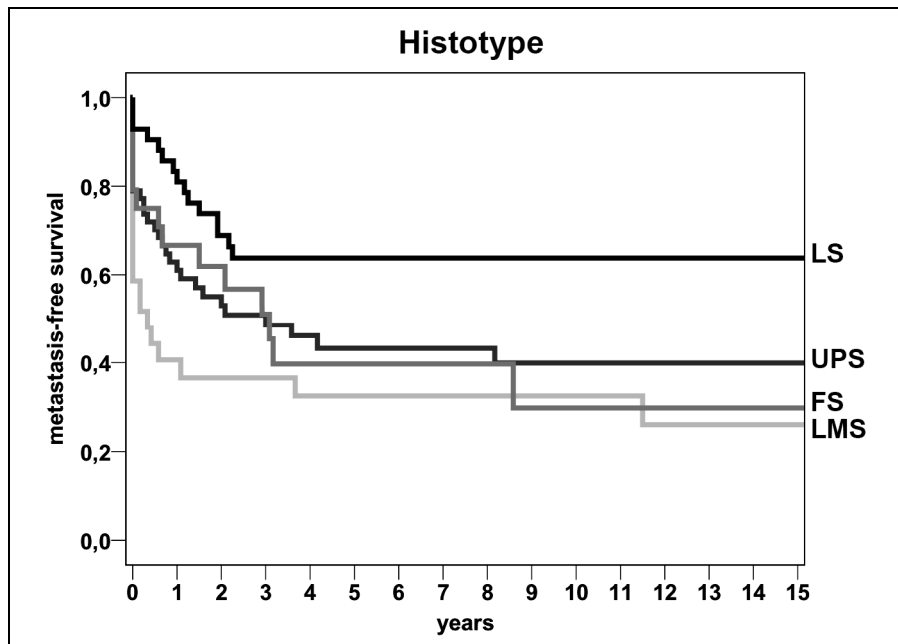


Figure 17 - Metastasis free survival according to tumour histotype

4.1.2 - Identification of MET as a putative STS-related miR-152 target and miR-152 role cell behaviour

The gene expression analysis of miR-152 in 59 out of 152 primary high-grade STS tumour samples (27 LMS and 32 UPS) indicated a significant lower expression of miR-152 when compared to normal tissue (Mann Whitney test, $p = 0.028$). In order to subsequently investigate the putative role of miR-152 in LMS cell behaviour, we transfected its pre-miRNA precursor into SKLMS1 cells and we found that ectopic miR-152 expression induced a decrease of the mRNA levels of its putative target, MET. The reduction was of 16.7% at 24h after transfection and 11.1% at 48h after transfection, respectively, shifting back to control values at 72h after transfection.

By using a Neubauer cell counting chamber assay, we found that after ectopic miR-152 expression SKLMS1 cells exhibited a significant decrease in proliferation compared to non-transfected cells up to 48h (27% at 24h; $p = 0.05$ and 41% at 48h; $p = 0.007$) and to a lesser extent at 72h (18.7%). Concomitantly, a gradual increase in apoptosis was seen compared to non-transfected cells up to 48h (11.6% at 24h; $p = 0.08$ and 39.6% at 48h; $p = 0.03$), while at 72h the apoptotic cell percentage shifted back to control values (Fig.18).

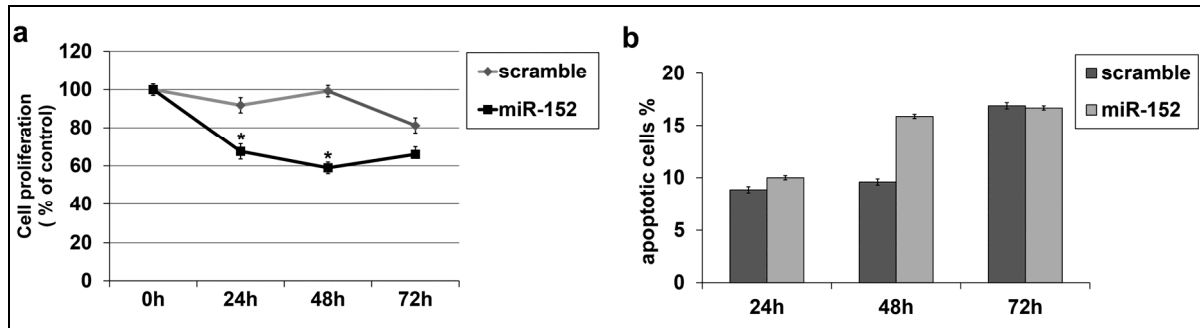


Figure 18 – Proliferation (a) and apoptosis (b) in SKLMS1 (Leiomyosarcoma) cells with miR-152 ectopic expression

Using IHC on TMA sections, we found that the MET protein was predominantly expressed in the cytoplasm of the STS tumour cells, with overexpression corresponding to a uniform (> 50% positive cells) and moderate to strong immunoreactivity (score = 4-5) in 79% of the metastatic and 25% of the non-metastatic patients ($\chi^2 = 11.5$; $p = 0.001$) (Fig.19). In the corresponding normal tissues MET was found to be focally and weakly expressed (score = 2).

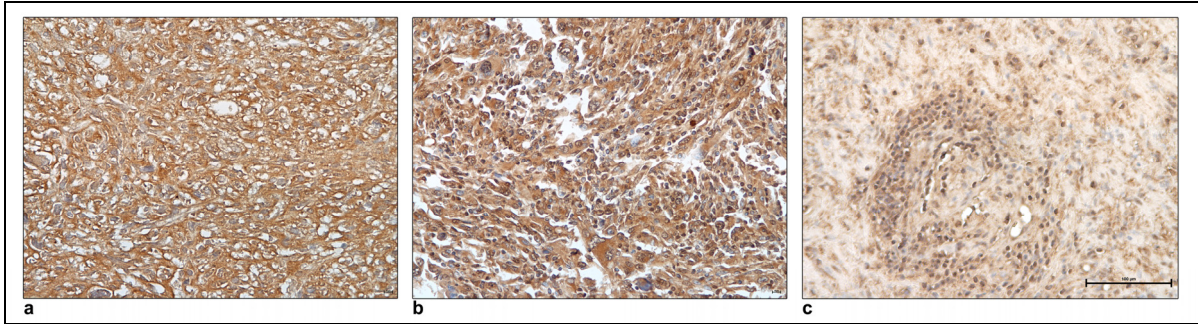


Figure 19 - MET protein expression. A representative immunostaining of MET in primary leiomyosarcoma (LMS) (left), undifferentiated pleomorphic sarcoma (UPS) and in prostate used as normal control (right)

4.1.3 - Immunohistochemical analysis on TMA of other potential biomarkers associated with STS metastatic progression

The clinical impact validation of IGFBP7, *XTP1/DEPDC1B* and *SDP35/DEPDC1A* was carried out by means of immunohistochemical analysis on TMA, comprising a population of 152 patients (Tab.3) with primary STS with different histopathological and clinical features. 28 samples were not evaluable for immunostaining (7 for IGFBP7 and 21 for RhoGAPs) and thus excluded from the study.

In detail, 81% of metastatic STS presented a moderate to strong IGFBP7 staining in more than 25% of tumour cells, with both cytoplasmic and nuclear distribution (Fig.20).

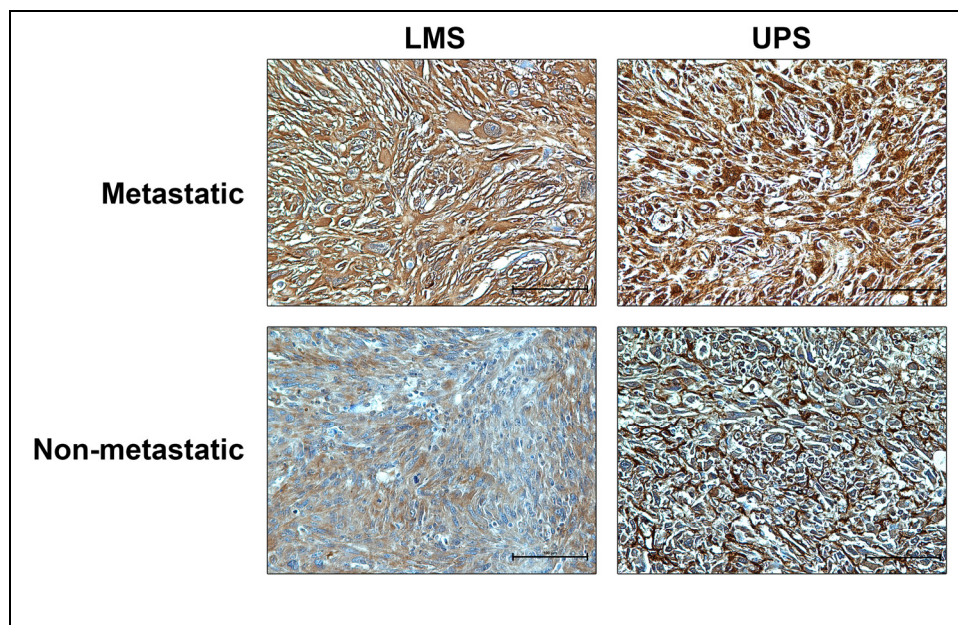


Figure 20 - IGFBP7 protein expression. A representative immunostaining of IGFBP7 in leiomyosarcoma (LMS) and undifferentiated pleomorphic sarcoma (UPS) (*Benassi M.S. et al. Am J Cancer Res 2015*).

The staining was more intense and uniform in 82.7 % patients with metastasis at presentation or within the first 4 months. In 76% of disease-free samples staining intensity ranged from negative to moderate in less than 25% of tumour cells with cytoplasmic and/or nuclear intracellular distribution. Based on cytoplasmic IGFBP7 staining intensity score (range 1-5), univariate Cox's analysis demonstrated that the risk of metastasis increased by 78.4% (95%CI=1.32-2.41; p<0.0005), in correlation to the staining intensity score. Accordingly, Mann-Whitney analysis revealed a statistically significant higher IGFBP7 staining levels in metastatic compared to non-metastatic samples (p= 0.01). No significantly different expression intensity was seen according to histological subtypes.

Then, the expression of both Rho GAPs has been studied in a total of 131 (Tab.6) available samples of which 78 (59%) and 51 (40%) presented an overexpression for *SDP35/DEPDC1A* and *XTP1/DEPDC1B* (score 4-5) respectively, with moderate to strong immunoreactivity in more than 50% of tumour cells. 37 cases showed a moderate/strong staining intensity for both enzymes.

	IHC RhoGAPs(131)
Gender	<i>No.</i>
Male	99
Female	32
Median age (yr - range)	55
Site	<i>No.</i>
Upper Limbs	11
Lower Limbs	107
Trunk	13
Total median follow up (months)	43
Metastasis median time (months)	24
Histology	<i>No.</i>
UPS	53
LMS	25
LS	33
FS	20
Outcome	<i>No.</i>
Alive	59
Dead of Disease	50
Metastasis	70
Local relapses	22
Adjuvant Treatments	<i>No.</i>
Chemotherapy	21
Radiotherapy	68

Table 6 - Case study for RhoGAP Immunohistochemistry analysis

XTP1/DEPDC1B was diffusely distributed throughout the cytoplasm, whereas *SDP35/DEPDC1A* displayed a predominant nuclear localization, although focal cytoplasmic immunostaining was also observed. A negative or minimal protein expression was seen in healthy tissues (kidney) except for *SDP35/DEPDC1A* that was detected in human prostate used as positive control tissue for immunolabelling. (Fig.21).

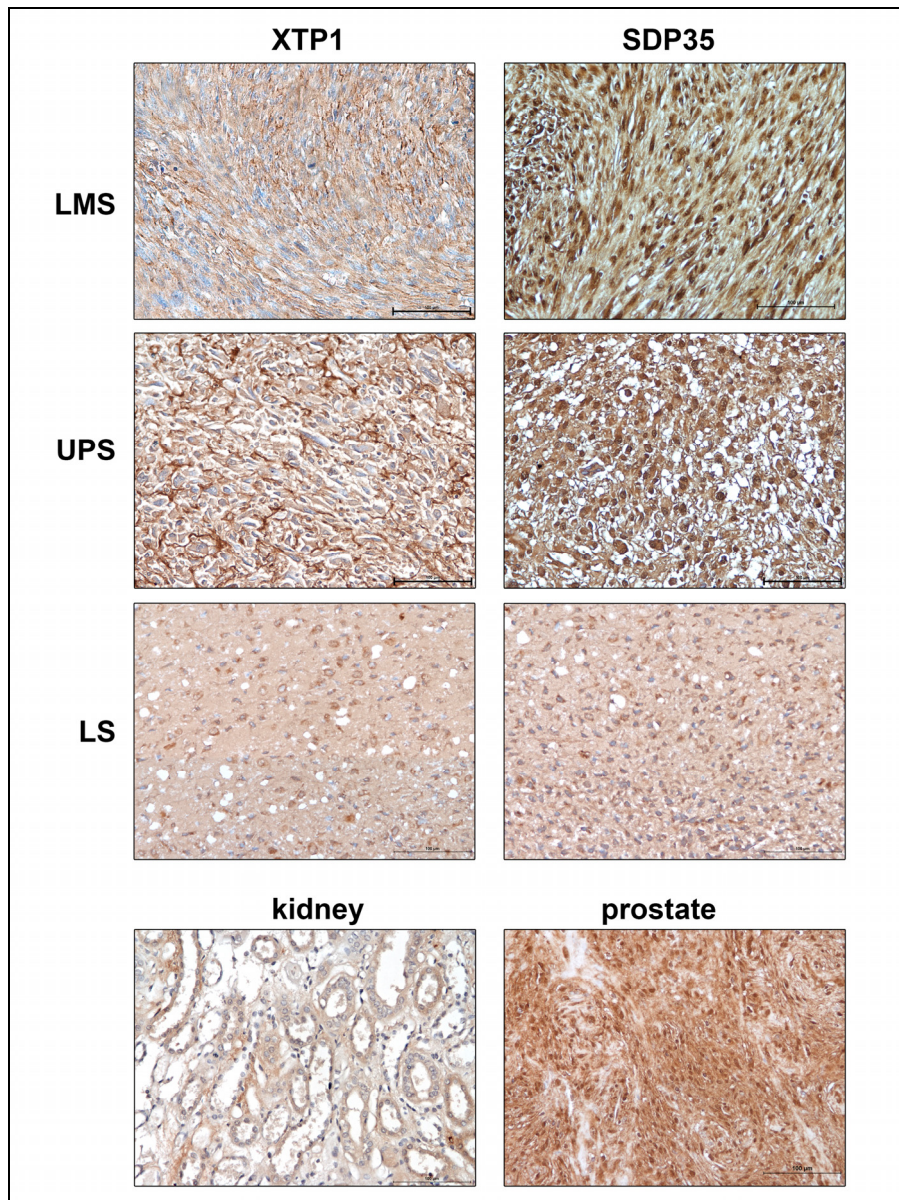


Figure 21 - *XTP1/DEPDC1B* and *SDP35/DEPDC1A* protein expression. A representative immunostaining of *XTP1/DEPDC1B* and *SDP35/DEPDC1A* in primary leiomyosarcoma (LMS), undifferentiated pleomorphic sarcoma (UPS) liposarcoma(LS) and in healthy tissues.

In all 22 paired metastases examined, *XTP1/DEPDC1B* and *SDP35/DEPDC1A* were uniformly expressed in tumour cells with variable staining intensity that ranged from moderate to strong according to the adopted arbitrary scoring (scores 4-5). (Fig.22).

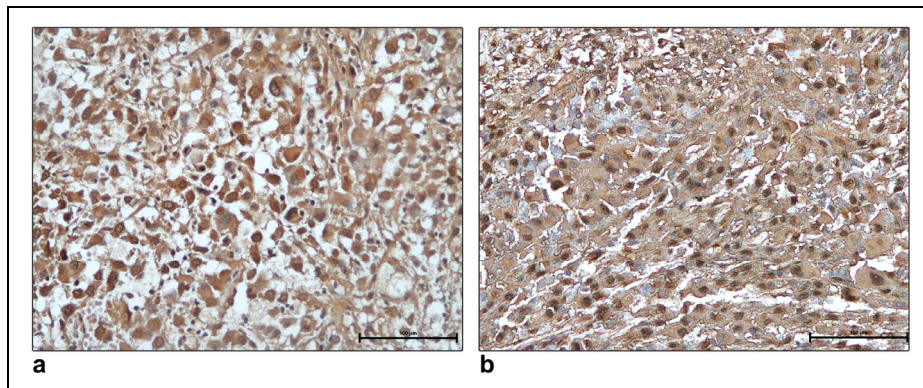


Figure 22 - A representative immunostaining of *XTP1/DEPDC1B* (a) and *SDP35/DEPDC1A* (b) in metastatic lesions.

The distribution of *XTP1/DEPDC1B* and *SDP35/DEPDC1A* protein immunostaining across tumour histotypes revealed no significant differences for *XTP1/DEPDC1B* (Fisher Chi-square $p>0.05$), while *SDP35/DEPDC1A* was more frequently over-expressed (score 4-5) in LMS, UPS and FS than in LS, the latter also presenting the best prognosis (Fisher Chi-square=9.189; $p= 0.027$).

Considering the clinical course of patients and their primary lesion, metastatic patients ($n=70$) showed a higher overexpression of both RhoGAPs compared to the non-metastatic ($n=61$). In detail, 72% of patients who relapsed showed a significant overexpression of *SDP35/DEPDC1A*, whereas it was overexpressed only in 45% of metastasis-free patients (Fisher Chi-square=10,105; $p=0.001$). Precisely, 43.4% of metastatic patients revealed an overexpression of *XTP1/DEPDC1B* compared to 33.8% of non-metastatic patients (not statistically significant, $p>0.05$). Kaplan Meier analysis based on immunoreactivity pointed out that upregulation of *SDP35/DEPDC1A* significantly decreased MFS probability (log rank=12.108, $p=0.001$) (Fig.23a) while no significant differences were seen for *XTP1/DEPDC1B* ($p>0.05$) (Fig.23b).

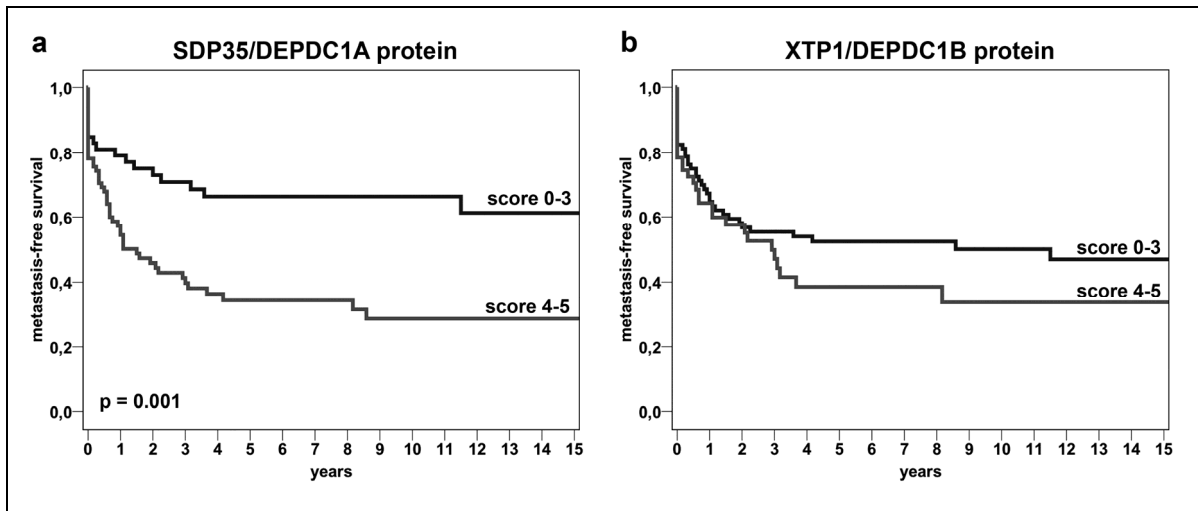


Figure 23 - Metastasis free survival in relation to immunoreactivity for *SDP35/DEPDC1A* (a) and for *XTP1/DEPDC1B* (b). Scores were applied as 0-3 for negative/weakly positive, and 4-5 for moderately to strongly positive.

4.1.4 - *XTP1/DEPDC1B* and *SDP35/DEPDC1A* gene expression in human STS specimens

To analyze the expression levels of genes *XTP1/DEPDC1B* and *SDP35/DEPDC1A*, we selected 86 of the 152 STS primary tumour specimens (Tab.7), 22 of the associated lung metastases samples and 17 paired normal tissues that were used as controls; then we have compared the values obtained.

	RT-PCR (86)
Gender	<i>No.</i>
Male	57
Female	29
Median age (yr - range)	55.5
Site	<i>No.</i>
Upper Limbs	5
Lower Limbs	77
Trunk	4
Total median follow up (months)	47
Metastasis median time (months)	18
Histology	<i>No.</i>
UPS	18
LMS	20
LS	42
FS	6

	RT-PCR (86)
Outcome	No.
Alive	36
Dead of Disease	41
Metastasis	52
Local relapses	16
Adjuvant Treatments	No.
Chemotherapy	17
Radiotherapy	54

Table 7 - Case study for RhoGAPs Real Time PCR analysis

The Real-Time PCR analysis of genes coding for both RhoGAPs showed a different expression of the median values of mRNAs in the different types of tissue. For both genes, in 17 patients the expression mean values were significantly higher in primary and metastatic lesions than in paired healthy tissues. *XTP1/DEPDC1B* values were 173.5 in primary and 3595 in paired metastases versus 0.20 in paired normal tissue (Friedman, $p=0.028$; $p<0.0005$ respectively), while *SDP35/DEPDC1A* ranged from 195.5 and 1354 versus 0.38 (Friedman, $p=0.025$; $p<0.0005$ respectively) (Fig. 24).

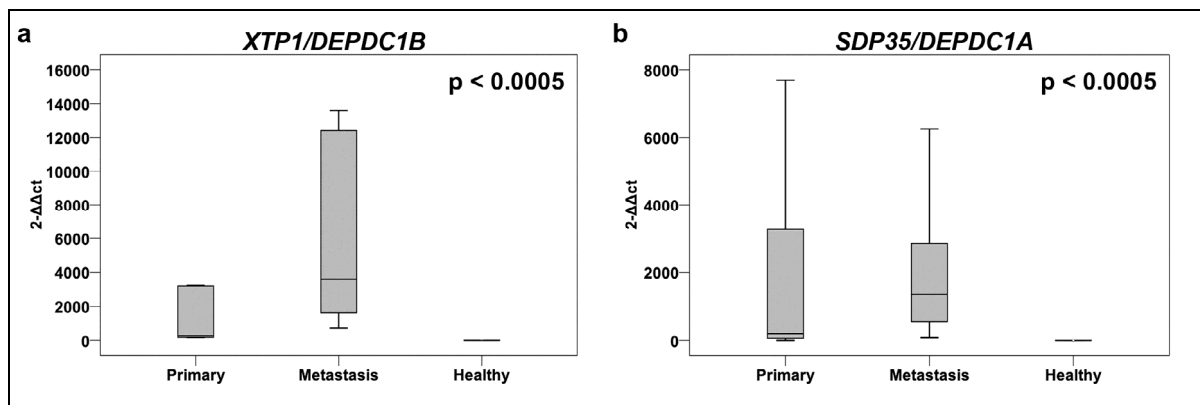


Figure 24 - Friedman test. *XTP1/DEPDC1B* (a) and *SDP35/DEPDC1A* (b) gene expression analysis in primary STS, paired metastases and healthy tissue.

In 22 patients Wilcoxon test for paired data was performed by comparing the gene expression values obtained in 22 primary tumours and in paired metastatic lesions obtained from the same patients. The statistical analysis revealed, for both genes, that the metastatic samples exhibited consistently higher mRNA levels compared to primary lesions (299 and 3595, $p=0.02$ for *XTP1/DEPDC1B*; and 366 and 1354, $p=0.05$ for *SDP35/DEPDC1A*) (Fig.25).

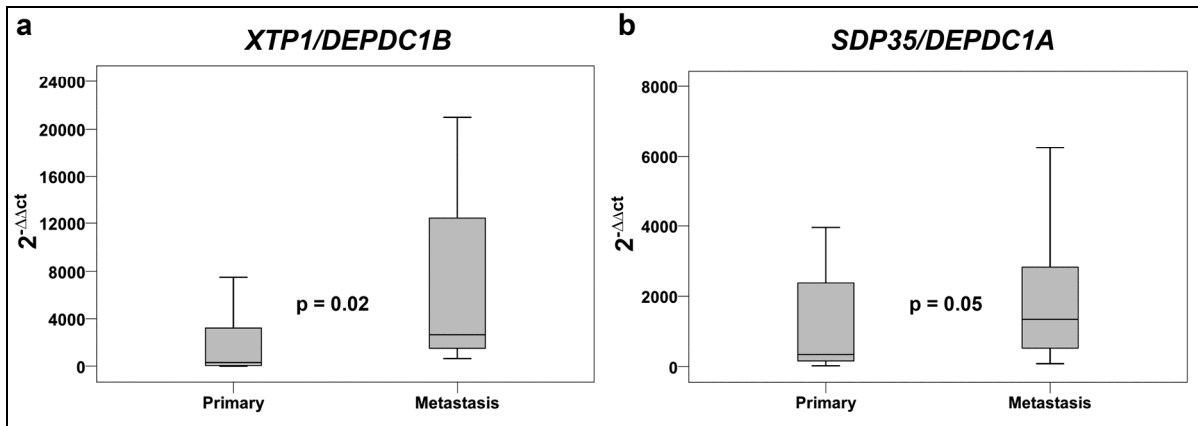


Figure 25 - Wilcoxon test. *XTP1/DEPDC1B* (a) and *SDP35/DEPDC1A* (b) gene expression analysis in primary STS and paired metastases

Taking into account, the expression levels of *SDP35/DEPDC1A* and *XTP1/DEPDC1B* in different histological types of primary tumours, Kruskal-Wallis test did not show statistical differences ($p=0.20$), but LMS and FS primary lesions had higher mRNA median values of *SDP35/DEPDC1A* (843.0 and 232.5 respectively), than LS and UPS (respectively 164.5 and 130) while FS had higher $2^{-\Delta\Delta CT}$ levels of *XTP1/DEPDC1B* (1121) than LMS (215.5), LS (205) and UPS (51.5).

When the patients were divided according to clinical follow-up, median values of *XTP1/DEPDC1B* and *SDP35/DEPDC1A* were significantly higher in samples from metastatic patients when compared to non-metastatic group (respectively 258.0 vs 66.0 for *XTP1/DEPDC1B*; Mann Whitney $p=0.03$; and 621.5 vs 59.5 for *SDP35/DEPDC1A*; Mann Whitney $p=0.01$) (Fig.26).

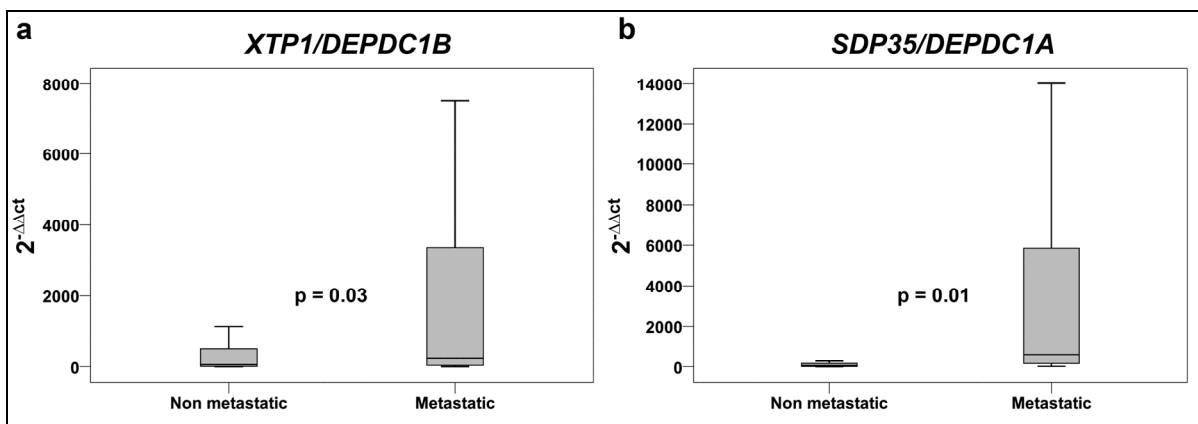


Figure 26 - Mann-Whitney analysis. Comparison of *XTP1/DEPDC1B* (a) and *SDP35/DEPDC1A* (b) mRNA median values between metastatic and non-metastatic patients.

Accordingly, when the cut-off of *XTP1/DEPDC1B* and *SDP35/DEPDC1A* was set respectively at 173 and 195 ($2^{-\Delta\Delta ct}$) corresponding to median values detected in STS primary tumours, we found that patients with mRNA levels over the cut-off had a significantly higher probability to develop metastasis than patients with lower values (Kaplan-Meier: log-rank = 16.48; $p < 0.0005$ for *SDP35/DEPDC1A*; log-rank = 6.45; $p = 0.01$ for *XTP1/DEPDC1B*) (Fig.27 a,b);

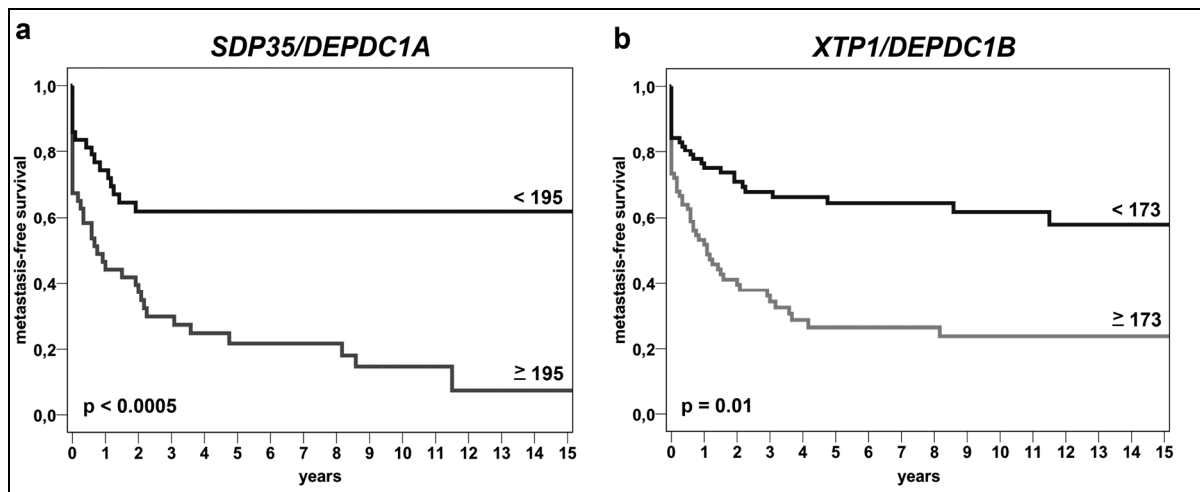


Figure 27 - Kaplan Meier analysis. Metastasis free survival in relation to *SDP35/DEPDC1A* (a) and *XTP1/DEPDC1B* (b) mRNA cut-off levels.

Considering the significant parameters emerged by univariate analysis, we proceeded to perform a multivariate analysis according to the Cox's regression model that further confirmed that the risk of developing metastases significantly increased with age (HR=1.029, CI95%=1.002-1.056; $p=0.032$), with higher *SDP35/DEPDC1A* mRNA expression levels (HR= 3.126, CI95%=1.518-6.44, $p=0.002$) and without radiotherapeutic treatment (HR=0.483, CI95%=0.259-0.901, $p=0.02$).

4.1.5 - Western blot analysis

Western blot analysis was carried out to evaluate the presence of *SDP35/DEPDC1A* (61kDa) and *XTP1/DEPDC1B* (62kDa) proteins in 44 fresh frozen tissue samples of four different STS histologic types (22 primary tumours and 22 associated lung metastases) previously subjected to immunohistochemistry and Real-Time PCR studies. Densitometric analysis was performed with special software "Quantity One" (Bio-Rad) and it showed and confirmed, for

SDP35/DEPDC1A protein, the increased expression in metastases compared to primary lesions (Fig.28).

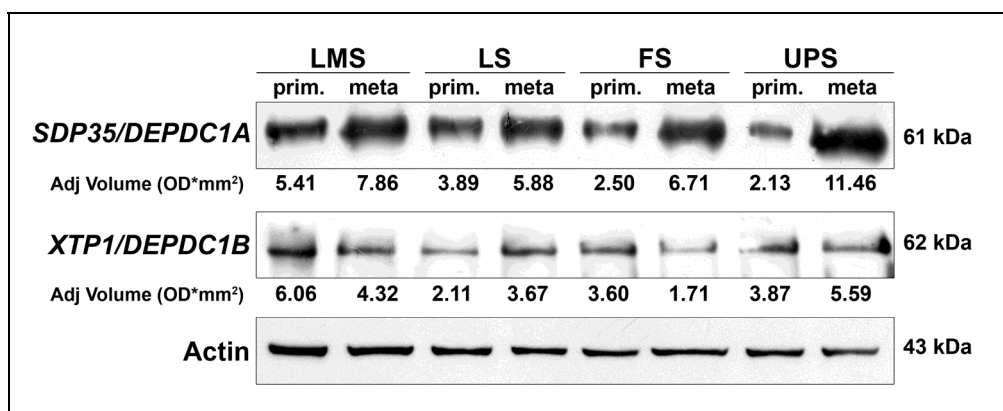


Figure 28 - Western Blot analysis. Expression of *SDP35/DEPDC1A* and *XTP1/DEPDC1B* proteins in primary and metastasis lesions. (Actin used as control).

4.1.6 - mAbs against both RhoGAPs in STS lesions

Next we evaluated the quality of a panel of mAbs raised by immunizing mice with recombinant His-tagged full-length *XTP1/DEPDC1B* and *SDP35/DEPDC1A* proteins. These antibodies have been produced in the interdepartmental Centre for Molecular and Translational Oncology (COMT) managed by Prof. Roberto Perris.

Initially, we performed the immunolabelling study of 65 primary tissue sections, 22 lung metastasis and 17 non-cancer tissues all previously analyzed by the same technique with the use of commercial antibodies. In 42 of 65 tumours, both *XTP1/DEPDC1B* and *SDP35/DEPDC1A* were detected, in 11 only *SDP35/DEPDC1A* was expressed with a strong and uniform intensity and distribution and in 3 cases only *XTP1/DEPDC1B* was detected. Minimal or no detectable levels of the molecules were observed in the healthy tissues. In 22 lung metastases that paired with primary lesions of the same individuals, expression of both RhoGAP proteins was considerably higher than in the latter lesions. These data confirmed the good function of the monoclonal antibodies produced in the COMT (Fig.29).

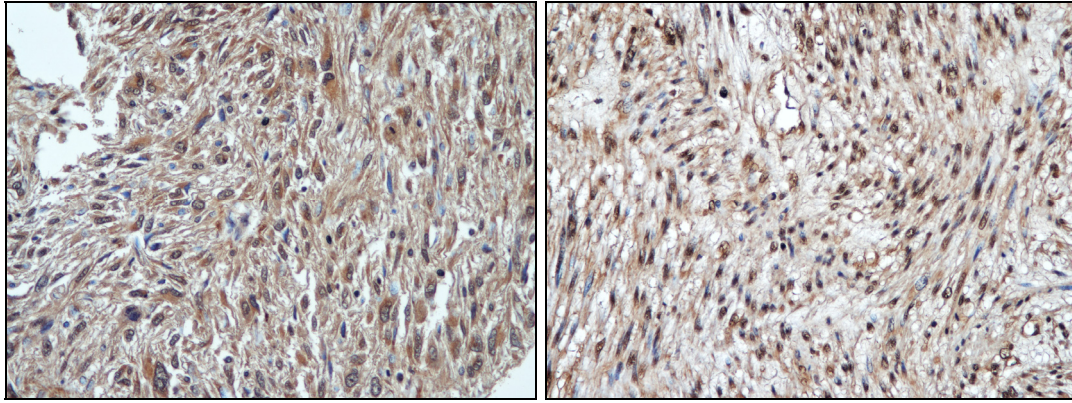


Figure 29 - A representative immunostaining performed with monoclonal antibodies against *XTPI/DEPDC1B* in primary undifferentiated pleomorphic sarcoma (left) or against *SDP35/DEPDC1A* in leiomyosarcoma (right).

4.2 - *in vitro* studies

4.2.1 - mRNA and protein levels of RhoGAPs in STS primary cell cultures

The expression of *XTPI/DEPDC1B* and *SDP35/DEPDC1A* was determined in a panel of cells isolated from STS metastatic lesions and compared the gene expression patterns with those detected in healthy reference cells (hMSC).

XTPI/DEPDC1B and *SDP35/DEPDC1A* mRNA levels was higher when compared to healthy mesenchymal cells considered as control.

In primary cultures of cells derived from lung nodules of 8 metastatic patients we observed two distinct cell subsets assuming entirely different shapes and displaying a highly divergent growth behaviour: one subset manifested a spindle-shaped elongated morphology (SP cells) and grew in a conventional anchorage-dependent manner; the other exhibited a round, light-refracting shape (RS cells) and grew poorly attached to the substrate, or fully suspended in the culture medium (Fig.30).

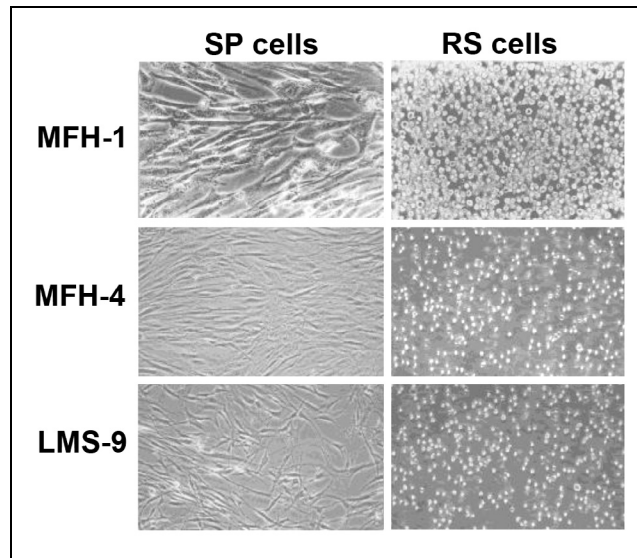


Figure 30 - Spindle and Round shaped cells subgroups in primary culture. MFH=UPS (Undifferentiated pleomorphic sarcoma); LMS (leiomyosarcoma)

Analysing the transcriptional levels by means Real-Time PCR, it was found that although some variations in the relative expression levels of *XTP1/DEPDC1B* and *SDP35/DEPDC1A* were detectable in these cells, the RS subset consistently expressed higher levels of the transcripts. In fact, this subset expressed on average 92- (*XTP1/DEPDC1B*) and 33- (*SDP35/DEPDC1A*) fold (37.5-413.3 and 1.5-170.4 folds, respectively) higher mRNA levels of the two GAPs (Fig. 31).

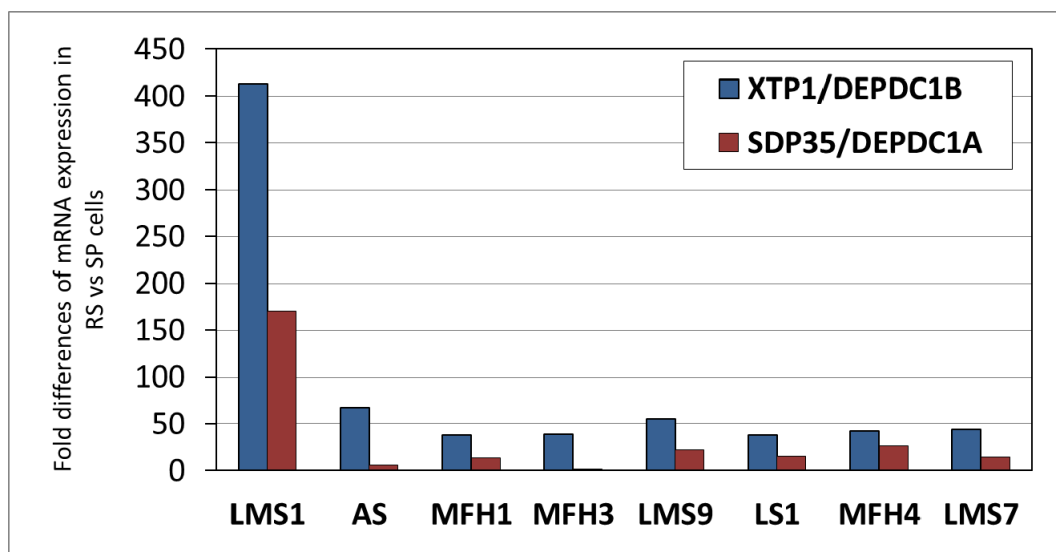


Figure 31 – *XTP1/DEPDC1B* and *SDP35/DEPDC1A* gene expression in Spindle and Round shaped cells subgroups in primary culture.

Parallel immunochemical analyses with specific mAbs confirmed that *XTP1/DEPDC1B* and *SDP35/DEPDC1A* protein levels were different in the two subsets. The analyses also demonstrated that *XTP1/DEPDC1B* was diffusely expressed in the cytoplasm and nucleus, whereas *SDP35/DEPDC1A* displayed a more frequent nuclear localization (Fig.32). In most cases, the higher transcriptional rates seen in the RS versus SP subset corresponded to a higher protein translational rate.

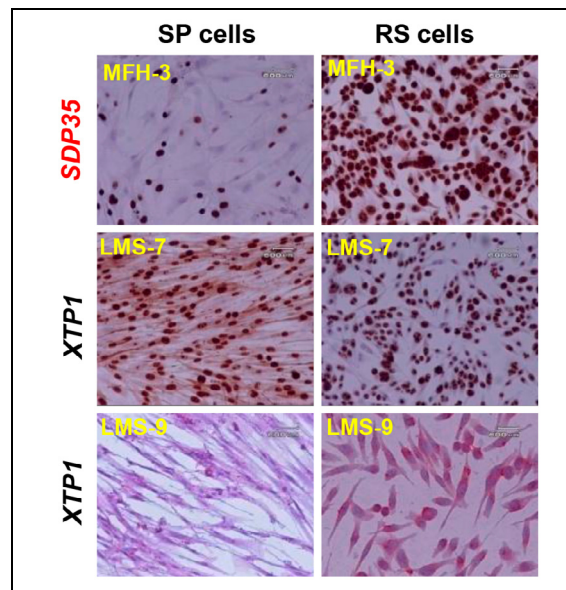


Figure 32 - *XTP1/DEPDC1B* and *SDP35/DEPDC1A* protein expression in Round and Spindle shaped subset cells. MFH=UPS (Undifferentiated pleomorphic sarcoma); LMS (leiomyosarcoma)

4.2.2 - *XTP1/DEPDC1B* and *SDP35/DEPDC1A* expression in STS cell lines

Taken together, our results and those that emerged from earlier studies conducted in the laboratory of prof. Roberto Perris do infer an important role of *XTP1/DEPDC1B* and, in particular, *SDP35/DEPDC1A* in regulating the metastatic process of STS cells. With the aim to assess the influence of these molecules on STS cell growth and migration, we performed a preliminary in vitro study on cells lines representative of three histological STS subtypes, SKLMS1 (leiomyosarcoma), SW872 (liposarcoma) and HT1080 (fibrosarcoma).

4.2.3 - Western blot analysis of protein expression

As determined by densitometric analyses of the blotted bands, all cells displayed positive expression of both *XTP1/DEPDC1B* and *SDP35/DEPDC1A*. Higher expression of

SDP35/DEPDC1A were detected in SW872 while no significant differences between the cells taken into account were seen for *XTP1/DEPDC1B* (Fig. 33).

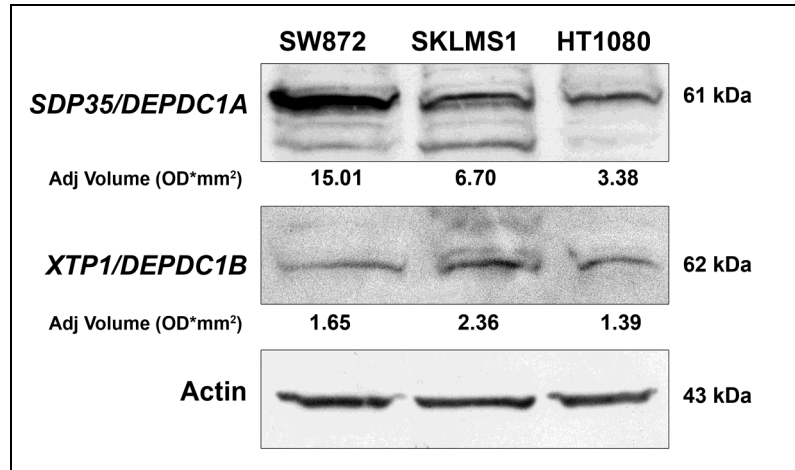


Figure 33 – Western blot analysis. Expression of *SDP35/DEPDC1A* and *XTP1/DEPDC1B* proteins in SW872 (liposarcoma), SKLMS1 (leiomyosarcoma) and HT1080 (fibrosarcoma) cells (Actin used as control).

4.2.4 - *XTP1/DEPDC1B* and *SDP35/DEPDC1A* mRNA in STS cell lines

For these analyses we used a pool of human lymphocytes as a calibrator: the analyses indicated an increased gene expression of *XTP1/DEPDC1B* and *SDP35/DEPDC1A*.

SW872 and SKLMS1 were found to express higher mRNA levels (respectively 3350 and 11,6 for *XTP1/DEPDC1B*; 1217,7 and 10,41 for *SDP35/DEPDC1A*) when compared to HT1080 (fibrosarcoma) (0,0625 for *XTP1/DEPDC1B* and 13.7 for *SDP35/DEPDC1A*) (Fig. 34).

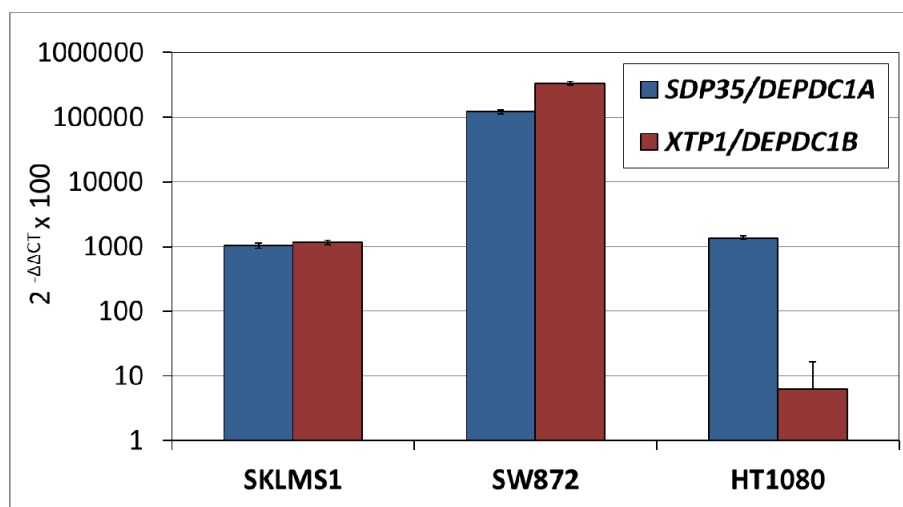


Figure 34 – *XTP1/DEPDC1B* and *SDP35/DEPDC1A* gene expression. The mRNA values are reported graphically as 2^{-ΔΔCT} x 100 and reported the log scale graph

4.2.5 - Analysis of cell proliferation, migration and apoptotic rate in basal condition

Next we performed proliferation, migration and apoptosis tests under basal conditions in order to determine if the cell lines taken into account displayed different aggressive behaviour. SW872 and SKLMS1 cells showed a higher migration (Fig.35) and proliferation (Fig.36) rate when compared to HT1080 cells while no differences in apoptotic rates was seen among STS cell lines.

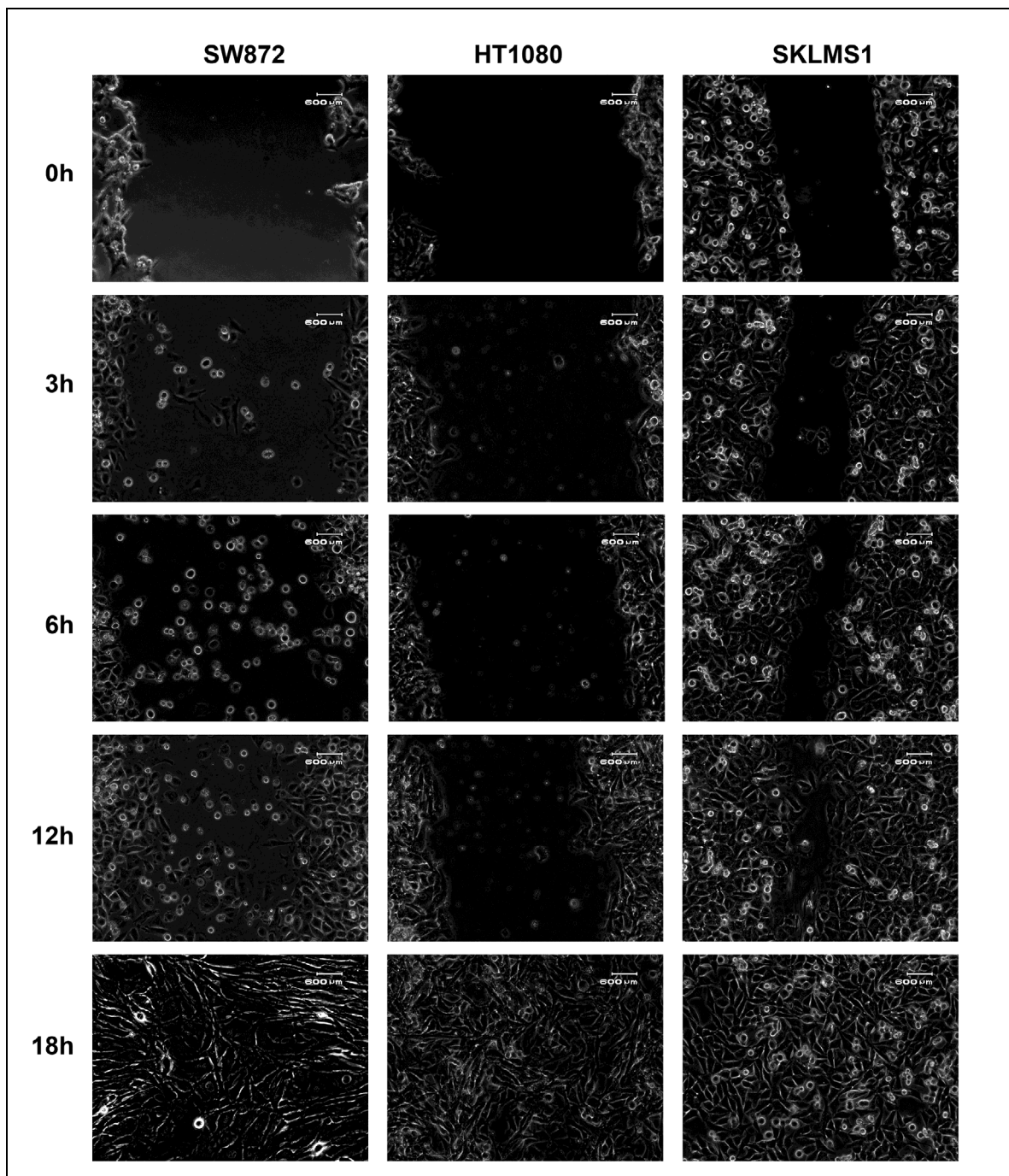


Figure 35 - Migration of STS cells in basal condition as determined by wound healing assay. HT1080= fibrosarcoma; SKLMS1= leiomyosarcoma; SW872= liposarcoma

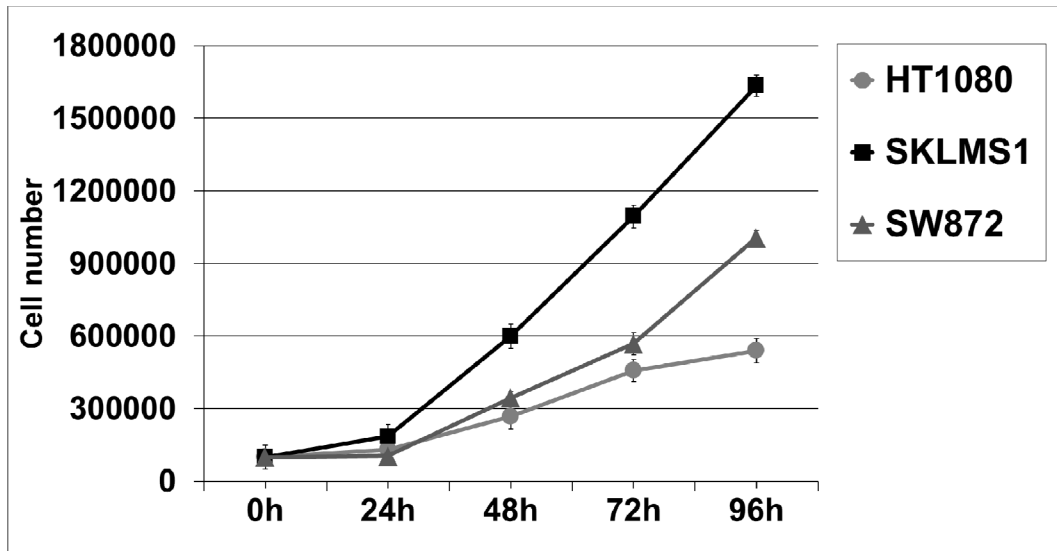


Figure 36 - Proliferation rate of different STS cells in basal condition. HT1080= fibrosarcoma; SKLMS1= leiomyosarcoma; SW872= liposarcoma

4.2.6 - Knockdown of *SDP35/DEPDC1A* in SW872 cell line

Since the SW872 displayed the highest levels of *SDP35/DEPDC1A* expression, we chose these cells to knockdown the gene and analyze the effects on *SDP35/DEPDC1A* transcript. siRNA transfection presented the highest transfection efficiency at 72h at concentration of 60nM (Fig.37).

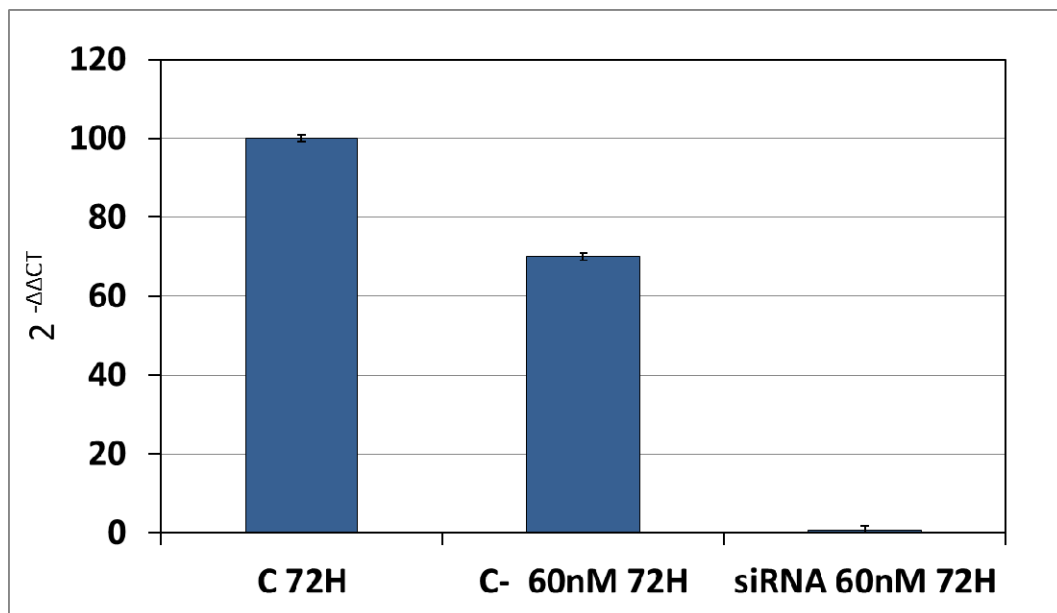


Figure 37 – *SDP35/DEPDC1A* siRNA transfection efficiency at 72 hours in SW872 cells

A strong reduction of *SDP35/DEPDC1A* mRNA expression was seen after 48h (80 %) and 72h (93%) compared to reference control and concomitantly cells proliferation rate was reduced (20% of control at 72h) (Fig.38).

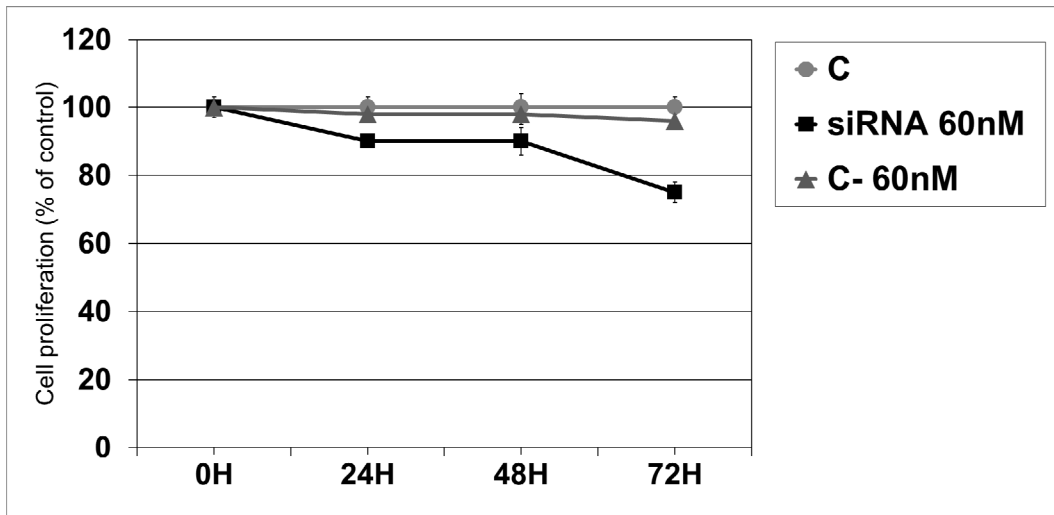


Figure 38 – Proliferation rate of *SDP35/DEPDC1A*- knocked-down SW872 cells

The wound healing assay showed that the cell motility also was influenced by the silencing with the closure of cut area reduced by 50% compared to the control within the first 6 hrs of movement (Fig. 39). No effect on apoptosis was seen at any time (19.46% and 20.54% of apoptotic cells in controls; 16.04% in transfected cells).

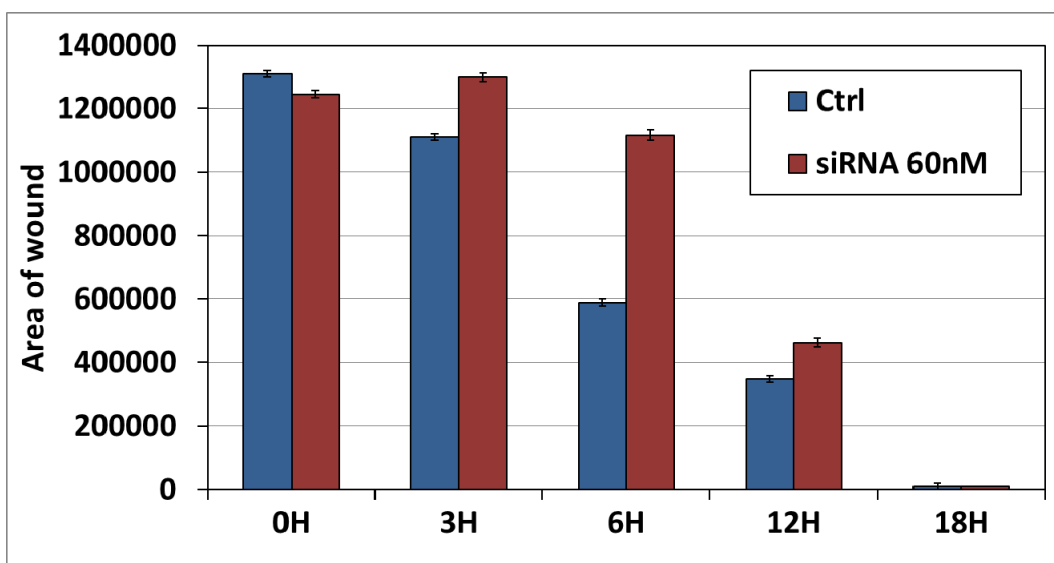


Figure 39 – Wound Healing Assay. The area of wound was measured for all the fields of each well using Image J.

5 - DISCUSSION

During the first year among several cancer related miRNA previously identified in the Experimental Oncology Lab of the Rizzoli Institute, we found that miR-152 was significantly down-regulated in a series of high grade STS also showing that ectopic miR-152 expression may reduce STS growth through down-regulation of its target MET, identified by in silico target gene analysis[69]. It has been reported that miR-152 may be involved in proliferation, invasion and angiogenesis [115], but few data are available in human sarcoma. MET is a receptor tyrosine kinase that binds hepatocyte growth factor (HGF) and guides malignant progression by activating signalling pathways that promote cell motility, survival and proliferation [116]. Interestingly, we found that MET expression levels were significantly higher in patients who developed metastasis during follow-up than in those that did not. These data, in conjunction with a strong and uniform MET expression in the majority of metastatic patients, underscore the clinical relevance of MET in sarcoma development and prognosis [69]. With the aim to find additional prognostic molecules that may be useful for new and more effective therapeutic strategies we also analysed the insulin-like growth factor (IGF) system focusing the study on IGF1R substrate, IGFBP7 protein, that play a role in cell proliferation and drug resistance.

IGFBP7 protein expression was significantly higher and more homogeneous in metastatic than in non-metastatic tumours. Accordingly, metastatic risk significantly increased in correlation to the staining intensity score (1-5) and indicated IGFBP7 tissue overexpression as a poor prognostic biomarker, also confirming the role of radiotherapy treatment in preventing metastatic progression. In accordance with previous studies that found IGFBP7 associated with poor prognosis [55], IGFBP7 tissue expression appears to have a predominant prognostic role in high-grade STS independently from histological subtype [54].

Finally, we address our interest on the results of a previous differential mRNA expression study [113] where we identified the unique RhoGAP family member *XTP1/DEPDC1B* as one of the transcripts differentially expressed by STS cells when compared to their putative healthy cell counterpart. Subsequent independent investigations have implicated that *XTP1/DEPDC1B* is involved in neoplastic transformation by controlling cancer cell migration and invasion [93]. Moreover, it may also act as a cell-cycle regulator [92,94,98] by inhibiting RhoA/Rho-Associate Protein Kinase activity during G2/M transition. [94].

In the human genome *XTP1/DEPDC1B* has a homologue known as *SDP35/DEPDC1A*, which has been reported to be up-regulated in bladder cancer [102,104] and its enhanced

expression may discriminate malignant from non-malignant forms of breast carcinoma [105]. *SDP35/DEPDC1A*, encodes two isoforms whose expression is regulated during the cell cycle and their silencing causes a mitotic phenotype similar to that of *XTP1/DEPDC1B* knockdown. Of great importance, the simultaneous depletion of both genes had strong and additive effects, demonstrating a functional redundancy and tight cooperative control during the G2/M transition [94].

Publicly accessible global gene mappings infer that *XTP1/DEPDC1B* and *SDP35/DEPDC1A* are poorly transcribed in most healthy human tissues, but are selectively up-regulated in certain tumour types. These observations are largely confirmed by the present data generated on a series of specimens from STS patients, providing novel hints about the importance of these molecules in cancer formation and/or progression. Indeed, our findings corroborate the low frequency of *XTP1/DEPDC1B* - *SDP35/DEPDC1A* mRNA and protein expression in healthy tissues, revealing a significantly higher expression of both in STS lesions. Thus, neoplastic up-regulation of *SDP35/DEPDC1A* and *XTP1/DEPDC1B* does not seem to be restricted to epithelial tumours, but may occur also in tumours of mesenchymal origin. Although no statistical differences were seen among histological subtypes, higher mRNA median values were seen in fibrosarcomas and leiomyosarcomas, tumours that also presented with a worse prognosis.

When median mRNA levels were assessed, we observed that individuals with *XTP1/DEPDC1B* and *SDP35/DEPDC1A* expression above median values had a significantly higher probability of a metastatic event than patients falling below this cut-off. Following multivariate analysis, *SDP35/DEPDC1A* up-regulation, age over 60 and no radiation therapy were considered independent prognostic factors for metastatic development. Accordingly, Kaplan Meier analysis consolidated a high prognostic value of the abundant expression of *SDP35/DEPDC1A* also at the protein level.

Expression of the RhoGAP proteins in STS lesions showed that *XTP1/DEPDC1B* was predominantly immunostained in cytoplasm while *SDP35/DEPDC1A* displayed a predominant nuclear, and occasionally cytoplasmic, localization suggesting that it may undergo cytoplasmic-nuclear shuttling. It has been shown that the levels of *XTP1/DEPDC1B* and *SDP35/DEPDC1A* proteins oscillate during the cell-cycle. *SDP35/DEPDC1A* is highly expressed during mitotic phase, distributed in nucleus during prophase, and within the cytoplasm during metaphase and anaphase [113]. *XTP1/DEPDC1B* protein augments during the G2 phase [94] and its activity seems to be concentrated within the cytoplasm

corroborating our ongoing findings that may highlight a direct effect of the RhoGAP on actin cytoskeletal dynamics.

When compared to the corresponding primary tumours, the production of both RhoGAP proteins was observed to be enhanced in the 22 paired metastatic lesions, suggesting that up-regulation of the molecules could be associated with the expansion of the original tumour to form distant secondary lesions. Interestingly, this data was confirmed by Western blot analysis which showed, in particular for *SDP35/DEPDC1A*, higher expression in metastatic samples than those of primary lesions. The same result was also revealed at transcriptional level. It remains to be established whether such enhanced expression of RhoGAPs in primary lesions may be instrumental for dissemination of pro-metastatic cells, or whether it accompanies up-regulation of molecules in the ultimate metastatic lesions. At date it is known that Wnt/ β -catenin pathway plays a pivotal role in supporting tumour metastasis. Yi Yang et al. [93] found that overexpression of *XTP1/DEPDC1B* increased transactivity and enhancement of nuclear accumulation of β -catenin in non-small cell lung cancer cell lines, suggesting that *XTP1/DEPDC1B* may activate Wnt/ β -catenin signalling. Considering these data, *XTP1/DEPDC1B* and perhaps also *SDP35/DEPDC1A* might be involved in this pathway and this could be the means by which they may promote tumour progression. Our preliminary in vitro studies show that primary cells isolated from STS metastatic lesions as well as cell lines representative of STS histological types maintained in culture a high expression of the two RhoGAPs. On the contrary, no or minimal mRNA and protein expression was seen in normal cells, confirming previous results. Cancer metastasis is a process of dissemination of tumour cells from a primary tumour mass to a different site through blood vessels and lymphatic vessels. To invade tissues and vessels, cells must acquire the ability to migrate, thus many tumour cells show changes in their plasticity via morphological and phenotypical conversions during cancer progression [117,118]. Acquiring a rounded morphology may facilitate this phenomenon and in fact, round cell sarcomas are among the most aggressive soft tissue tumours [119]. Moreover, numerous highly malignant cancer types are characterized by a high intra-lesional content of rounded, highly proliferating cells, but the biological significance and underlying mechanisms of this diagnostic trait are still partly unknown. In this context, of considerable importance is our result obtained by analyzing the two cell subgroups observed in eight primary cultures isolated from metastatic lesions. These analyses indicate a consistently higher mRNA and protein levels expression of both molecules in the Round Shape subset, suggesting their involvement in promoting cell shape changes. Further in vitro studies showed that SKLMS1

and SW872 cells, which constitutively express higher levels of *XTP1/DEPDC1B* and *SDP35/DEPDC1A*, displayed higher migration and proliferation rates than HT1080 cells which were characterized by lower expression levels. Upon siRNA-mediated knockdown of *SDP35/DEPDC1A*, cell displayed a slight reduction of cell proliferation accompanied by a transitory slowdown of cell motility. Also these data suggest a possible role of this molecule in STS progression.

In conclusion, our results confirm the low frequency of *XTP1/DEPDC1B* and *SDP35/DEPDC1A* expression in healthy tissues and reveal a marked expression of the GAPs in lesions of patients affected by different STS histological subtypes highly correlated to metastatic progression. Infact, the patients who developed metastasis during follow-up had significantly higher mRNA and protein levels than metastasis-free patients and the production of these molecules was strongly enhanced in metastatic lesions. In addition, multivariate analysis indicated *SDP35/DEPDC1A* as a prognostic independent risk factor. Additional in vitro studies need to better explain the involvement of these molecules in tumour progression and define their possible role as candidate targets for more selective and personalized therapies

6 - BIBLIOGRAPHY

- [1] Honoré C., Mééus P., Stoeckle E., et al. **Soft tissue sarcoma in France in 2015: Epidemiology, classification and organization of clinical care.** *Visc Surg* 2015; 152:223-30.
- [2] Fletcher C.D.M., Bridge J.A., Hogendoorn C.W., et al. **World Health Organization. WHO classification of tumours of soft tissue and bone.** IARC Press: Lyon 2013.
- [3] Goldblum J., Weiss S.W., Folpe A.L. **Enzinger and Weiss's Soft Tissue Tumors.** 6th ed. Saunders 2016.
- [4] Jagannathan J.P., Tirumani S.H., Ramaiya N.H. **Imaging in Soft Tissue Sarcomas: Current Updates.** *Surg Oncol Clin N Am* 2016; 25:645-75.
- [5] Coindre J.M. **Molecular biology of soft-tissue sarcomas.** *Bull Cancer* 2010; 97:1337–1345.
- [6] Maretty-Nielsen K. **Prognostic factors in soft tissue sarcoma.** *Danish Medical Journal* 2014; 61:B4957.
- [7] Coindre J.M. **Grading of soft tissue sarcomas: review and update.** *Arch Pathol Lab Med* 2006; 130:1448-53.
- [8] Nuzhat Husain & Nidhi Verma Indian. **Current Concepts in Pathology of Soft Tissue Sarcoma.** *J Surg Oncol* 2011; 2:302–308
- [9] Ben Salha I., Zaldi S., Noujaim J., et al. **Rare aggressive behaviour of MDM-2 amplified retroperitoneal dedifferentiated liposarcoma with brain, lung and subcutaneous metastases.** *Rare Tumors* 2016; 8:6282.
- [10] Picci P., Manfrini M., Fabbri N., et al. **Atlas of Musculoskeletal Tumors and tumorlike lesions.** Springer 2014
- [11] Tran D., Kundan V., Ward K., et al. **Functional Genomics Analysis Reveals a MYC Signature Associated with a Poor Clinical Prognosis in Liposarcomas.** *Am J Pathol.* 2015; 185:717-28.
- [12] Li C., Shen Y., Ren Y., et al. **Oncogene mutation profiling reveals poor prognosis associated with FGFR1/3 mutation in liposarcoma.** *Human Pathology* 2016; 55:143–150.
- [13] Boland J. M., Folpe A. L. **The impact of advances in molecular genetics on the classification and diagnosis of liposarcoma.** *Diagnostic Histopathology* 2011; 17:348-354.
- [14] Singer S., Antonescu C.R., Riedel E., et al. **Histologic subtype and margin of resection predict pattern of recurrence and survival for retroperitoneal liposarcoma.** *Ann Surg* 2003; 238:358-70
- [15] Nascimento A.G. **Dedifferentiated liposarcoma.** *Semin Diagn Pathol* 2001, 18:263-6
- [16] Coindre, J.M., Pedeutour, F., Aurias, A. **Well-differentiated liposarcomas.** *Virchows Arch* 2010; 456:167-79.
- [17] Bahrami A., Folpe A. **Adult-type Fibrosarcoma: a reevaluation of 163 putative cases diagnosed at a single institution over a 48-years period.** *Am J.Surg Pathol* 2010; 34:1504-1513.

- [18] Gibbs J., Henderson-Jackson E., Bui M.M. **Bone and Soft Tissue Pathology Diagnostic and Prognostic Implications.** Surg Clin North Am 2016; 96:915-962.
- [19] Guillou L., Aurias A. **Soft tissue sarcomas with complex genomic profiles.** Virchows Arch 2010; 456:201-217.
- [20] de Graaff M.A., de Jong D., Briaire-de Bruijn I.H., et al. **A translocation t(6;14) in two cases of leiomyosarcoma: Molecular cytogenetic and array-based comparative genomic hybridization characterization.** Cancer Genet 2015; 208:537-544.
- [21] Campanacci M. **Bone and Soft Tissue Tumors.** 2th ed. Piccin Nuova Libreria Editore Padova, 1999.
- [22] Goldblum J.R. **An approach to pleomorphic sarcomas: can we subclassify, and does it matter?.** Mod Pathol. 2014;27:S39-S46.
- [23] Matushansky I., Charytonowicz E., et al. **MFH classification: differentiating undifferentiated pleomorphic sarcoma in the 21st century.** Expert Rev Anticancer Ther 2009; 9:1135-44.
- [24] Cipriani N.A., Kurzawa P., Ahmad R.A., et al. **Prognostic value of myogenic differentiation in undifferentiated pleomorphic sarcomas of soft tissue.** Hum Pathol. 2014; 45:1504-8.
- [25] Matushansky I., Hernando E., Socci N.D., et al. **Derivation of sarcomas from mesenchymal stem cells via inactivation of the Wnt pathway.** J Clin Invest. 2007; 117: 3248-57
- [26] Oniscu A., Salter D. **Pathology of soft tissue tumors. Surgery (Oxford)** 2016; 34:436-439
- [27] Neuville A., Chibon F., Coindre J.M. **Grading of soft tissue sarcomas: from histological to molecular assessment.** Pathology 2014;46:113-20.
- [28] Russell W.O., Cohen J., Enzinger F., et al. **A clinical and pathological staging system for soft tissue sarcomas.** Cancer 1977; 40:1562-70.
- [29] Meister P. **Histological grading of soft tissue sarcomas: stratification of G2-sarcomas in low-or high-grade malignant tumors.** Pathologe 2005; 26:146-8.
- [30] Coindre J.M., Chibon F. **Grading sarcomas: histologic and molecular approaches.** Diagnostic Histopathology 2011; 17:8:325-32.
- [31] Jones N.B., Iwenofu H., Scharschmidt T., et al. **Prognostic factors and staging for soft tissue sarcomas: an update.** Surg Oncol Clin N Am 2012; 21:187-200.
- [32] Umar Jawad M., Scully S.P. **Enneking Classification: Benign and Malignant Tumors of the Musculoskeletal System.** Clin Orthop Relat Res 2010; 468:2000-02.
- [33] Kotilingam D., Lev D.C., Lazar A.J., et al. **Staging soft tissue sarcoma: evolution and change.** CA Cancer J Clin. 2006; 56:282-91.
- [34] Wunder J.S., Healey J.H., Davis A.M., et al. **A comparison of staging systems for localized extremity soft tissue sarcoma.** Cancer 2000; 88:2721-30.
- [35] Wolf R.E., Enneking W.F. **The staging and surgery of musculoskeletal neoplasms.** Orthop Clin North Am. 1996; 27:473-81.

- [36] Saddegh M.K., Lindholm J., Lundberg A., et al. **Staging of soft-tissue sarcomas. Prognostic analysis of clinical and pathological features.** J Bone Joint Surg Br. 1992; 74:495-500.
- [37] Enneking W.F., Spanier S.S., Goodman M.A. **A system for the surgical staging of musculoskeletal sarcoma.** 1980; Clin Orthop Relat Res. 2003; 415:4-18.
- [38] Deyrup A.T., Weiss S.W. **Grading of soft tissue sarcomas: the challenge of providing precise information in an imprecise world.** Histopathology 2006; 48:42-50.
- [39] Parmiani G., **Gli antigeni tumorali e la risposta immune cellulomediata contro i tumori: dagli studi sperimentali alle possibili applicazioni terapeutiche nell'uomo.** Edizioni Minerva Medica 1987.
- [40] Bonadonna G., Robustelli della Cuna G., **Manuale di Oncologia Medica.** 3^{ed} Masson Italia Editori 1987.
- [41] Metha S., Shelling A., Muthukaruppan A., et al. **Predictive and prognostic molecular markers for cancer medicine.** Ther Adv Med Oncol. 2010; 2:125-148.
- [42] Diana D., Lalitha R.M. **Tumor markers - A bird's eye view.** Journal of Oral and Maxillofacial Surgery, Medicine, and Pathology 2016; 28:475-480.
- [43] Kulasingam V., Diamandis E.P. **Strategies for discovering novel cancers biomarkers trough utilization of emerging technologies.** Nat Clin Pract Oncol 2008;5:588-99
- [44] Lord S., Chee Lee, R. J. Simes. **Role of predictive and prognostic markers in cancer.** Targeted and individualised therapies 2008; 32.
- [45] Palmerini E., Benassi M.S., Quattrini I., et al. **Prognostic and predictive role of CXCR4, IGF-1R and Ezrin expression in localized synovial sarcoma: is chemotaxis important to tumor response?.** Orphanet J Rare Dis.2015; 23;10:6. doi: 10.1186/s13023-014-0222-5.
- [46] Cattaruzza S., Nicolosi P.A., Braghetta P., et al. **NG2/CSPG4-collagen type VI interplays putatively involved in the microenvironmental control of tumour engraftment and local expansion.** J Mol Cell Biol. 2013; 5:176-93.
- [47] Benassi M.S., Pazzaglia L., Chiechi A., et al. **NG2 expression predicts the metastasis formation in soft-tissue sarcoma patients.** J Orthop Res. 2009; 27:135-40.
- [48] Benassi M.S., Ponticelli F., Azzoni E., et al. **Altered expression of urokinase-type plasminogen activator and plasminogen activator inhibitor in high-risk soft tissue sarcomas.** Histol Histopathol. 2007; 22:1017-24.
- [49] Pazzaglia L., Chiechi A., Conti A., et al. **Genetic and molecular alterations in rhabdomyosarcoma: mRNA overexpression of MCL1 and MAP2K4 genes.** Histol Histopathol. 2009; 24:61-7.
- [50] Palmerini E., Paioli A., Ferrari S. **Emerging therapeutic targets for synovial sarcoma.** Expert Rev Anticancer Ther. 2014; 14:791-806.
- [51] Rikhof B., de Jong S., Suurmeijer A.J., et al. **The insulin-like growth factor system and sarcomas.** J Pathol 2009; 217:469-482.
- [52] Reuveni H., Flashner-Abramson E., Steiner L., et al. **Therapeutic destruction of insulin receptor substrates for cancer treatment.** Cancer Res 2013; 73:4383-94.

- [53] Conti A., Espina V., Chiechi A., et al. **Mapping protein signal pathway interaction in sarcoma bone metastasis: linkage between rank, metalloproteinases turnover and growth factor signalling pathways.** Clin Exp Metastasis 2014; 31:15-24.
- [54] Benassi M.S., Pazzaglia L., Novello C., et al. **Tissue and serum IGFBP7 protein as biomarker in high-grade soft tissue sarcoma.** Am J Cancer Res 2015; 5:3446-54.
- [55] Baxter R.C. **IGF binding proteins in cancer: mechanistic and clinical insight.** Nat Rev Cancer 2014; 14: 329-341
- [56] Rupp C., Scherzer M., Rudisch A., et al. **IGFBP7, a novel tumor stroma marker, with growth-promoting effects in colon cancer through a paracrine tumor-stroma interaction.** Oncogene 2015; 34:815-25.
- [57] Kishibe J., Yamada S., Okada Y., et al. **Structural requirements of heparan sulfate for the binding to the tumor-derived adhesion factor/angiomodulin that induces cord-like structures to ECV-304 human carcinoma cells.** J Biol Chem 2000; 275: 15321-9
- [58] Pen A., Moreno M.J., Durocher Y., et al. **Glioblastoma secreted factors induce IGFBP-7 and angiogenesis by modulating Smad-2-dependent TGF-beta signalling.** Oncogene 2008; 27: 6834-44
- [59] Wang Z., Liang Z., Liu J., et al. **Expression and clinical significance of IGF-1, IGFBP-3, and IGFBP-7 in serum and lung cancer tissues from patients with non-small cell lung cancer.** Onco Targets Ther 2013; 6:1437-44.
- [60] Finnegan E.F., Pasquinelli A.E. **MicroRNA biogenesis: Regulating the Regulators.** Crit Rev Biochem Mol Biol. 2013; 48:51–68.
- [61] Melo S.A., Esteller M. **Dysregulation of microRNAs in cancer: playing with fire.** FEBS Lett. 2011; 585:2087-99.
- [62] Garzon R., Fabbri M., Cimmino A., et al. **MicroRNA expression and function in cancer.** Trends Mol Med 2006;12:580-7.
- [63] Novello C., Pazzaglia L., Cingolani C., et al. **miRNA expression profile in human osteosarcoma: role of miR-1 and miR-133b in proliferation and cell cycle control.** Int J Oncol. 2013; 42:667-75.
- [64] Mosakhani N., Pazzaglia L., Benassi M.S., et al. **MicroRNA expression profiles in metastatic and non-metastatic giant cell tumor of bone.** Histol Histopathol. 2013; 28:671-8.
- [65] Varshney J., Subramanian S. **MicroRNAs as potential target in human bone and soft tissue sarcoma therapeutics.** Front Mol Biosci. 2015; 2:31 doi: 10.3389/fmolb.2015.00031.
- [66] Guled M., Pazzaglia L., Borze I., et al. **Differentiating soft tissue leiomyosarcoma and undifferentiated pleomorphic sarcoma: A miRNA analysis.** Genes Chromosomes Cancer. 2014; 53:693-702.
- [67] Fujiwara T., Kunisada T., Takeda K., et al. **MicroRNAs in Soft Tissue Sarcomas: Overview of the Accumulating Evidence and Importance as Novel Biomarkers.** BioMed Res International 2014; 2014:592868 doi: 10.1155/2014/592868.
- [68] Liu X., Li J., Qin F., et al. **miR-152 as a tumor suppressor microRNA: Target recognition and regulation in cancer.** Oncol Lett. 2016; 11:3911-16.

- [69] Pazzaglia L., Novello C., Conti A., et al. **miR-152 down-regulation is associated with MET up-regulation in leiomyosarcoma and undifferentiated pleomorphic sarcoma.** *Cell Oncol (Dordr)*. 2017;40:77-88.
- [70] Azizi M., Teimoori-Toolabi L., Arzanani M.K., et al, **MicroRNA-148b and microRNA-152 reactivate tumor suppressor genes through suppression of DNA methyltransferase-1 gene in pancreatic cancer cell lines.** *Cancer Biol. Ther.* 2014; 15:419-27.
- [71] Dang Y.W., Zeng J., He R.Q., et al. **Effects of miR-152 on cell growth inhibition, motility suppression and apoptosis induction in hepatocellular carcinoma cells.** *Asian Pac J Cancer Prev.* 2014; 15:4969-76.
- [72] Garajová I., Giovannetti E., Biasco G., et al. **c-Met as a Target for Personalized Therapy.** *Transl Oncogenomics*.2015;7(Suppl 1):13-31.
- [73] Organ S.L., Tsao M.S. **An overview of the c-MET signalling pathway.** *Ther Adv Med Oncol.* 2011;3:S7-S19.
- [74] Karlsson R., Pedersen E.D., Wang Z., et al. **Rho GTPase function in tumorigenesis.** *Biochim Biophys Acta* 2009; 1796:91-8.
- [75] Otsu K., Harada H. **Rho GTPases in ameloblast differentiation.** *Japanese Dental Science Review* 2016; 52:32-40.
- [76] Vega F.M., Ridley A.J. **Rho GTPases in cancer cell biology.** *FEBS Lett* 2008; 582:2093–101.
- [77] Duman J.G., Multherkar S., Tu Y.K., et al. **Mechanisms for spatiotemporal regulation of Rho-GTPase signalling at synapses.** *neurosci Lett.* 2015; 601:4-10.
- [78] Tolias KF, Duman JG, Um K. Control of synapse development and plasticity by Rho GTPase regulatory proteins. *Prog Neurobiol* 2011; 94:133-48
- [79] Riching K.M., Keely P.J. **Rho family GTPases: Making it to the third dimension.** *Int J Biochem Cell Biol* 2015; 59:111–5.
- [80] Guilluy C., Garcia-Mata R. Burrridge K. **Rho protein crosstalk: another social network?** *Trends Cell Biol* 2011; 21:718-26.
- [81] Tcherkezian J., Lamarche-Vane N. **Current knowledge of the large RhoGAP family of proteins.** *Biol. Cell* 2007; 99:67-86.
- [82] Benitaha S.A., Valerón P.F., van Aelstb L., et al. **Rho GTPases in human cancer: an unresolved link to upstream and downstream transcriptional regulation.** *Biochim Biophys Acta* 2004; 1705:121–32.
- [83] Peck J., Douglas G., Wub C.H., et al. **Human RhoGAP domain-containing proteins: structure, function and evolutionary relationships.** *FEBS Lett* 2002; 528:27-34.
- [84] Merajver, S.D., Usmani, S.Z. **Multifaceted role of Rho proteins in angiogenesis.** *J. Mammary Gland Biol. Neoplasia* 2005; 10:291–8.
- [85] Rao P.V., Pattabiraman P.P., Kopczynski C. **Role of the Rho GTPase/Rho kinase signalling pathway in pathogenesis and treatment of glaucoma: Bench to bedside research.** *Exp Eye Res* 2016; doi: 10.1016/j.exer.2016.08.023.
- [86] Sahai E., Marshall C.J., **RHO-GTPases and cancer.** *Nat. Rev., Cancer* 2002;2:133-42.

- [87] Benitah S.A., Espina C., Valerón P.F., et al. **Rho GTPases in human carcinogenesis: a tale of excess.** *Rev. Oncol.* 2003; 5:70-8.
- [88] Gomez del Pulgar T., Benitah S.A., Valerón P.F., et al. **Rho GTPase expression in tumorigenesis: evidence for a significant link.** *Bioessays.* 2005;27:602-13.
- [89] Bos J.L., Rehmann H., Wittinghofer A. **GEFs and GAPs: critical elements in the control of small G proteins.** *Cell* 2007; 129:865-77
- [90] Moon S.Y., Zheng Y. **Rho GTPase-activating proteins in cell regulation.** *Trends Cell Biol* 2003; 13:13-22.
- [91] Bernardis A., Settleman J. **GAP control: regulating the regulators of small GTPases.** *Trends Cell Biol* 2004; 14:377-85.
- [92] Boudreau H.E., Broustas C.G., Gokhale P.C., et al. **Expression of BRCC3, a novel cell cycle regulated molecule, is associated with increased phospho-ERK and cell proliferation.** *Int J Mol Med* 2007; 19:29-39.
- [93] Yang Y., Liu L., Cai J., et al. **DEPDC1B enhances migration and invasion of non-small cell lung cancer cells via activating Wnt/b-catenin signalling.** *Biochem Biophys Res Commun* 2014; 450:899–905.
- [94] Marchesi S., Montani F., Deflorian G., et al. **DEPDC1B Coordinates De-adhesion Events and Cell-Cycle Progression at Mitosis.** *Dev Cell* 2014; 31:420-33.
- [95] Wu D., Zhu X., Jimenez-Cowell K., et al. **Identification of the GTPase-activating protein DEP domain containing 1B (DEPDC1B) as a transcriptional target of Pitx2.** *Exp Cell Res* 2015; 333:80-92.
- [96] Su Y.F., Liang C.Y., Huang C.Y., et al. **A putative novel protein, DEPDC1B, is overexpressed in oral cancer patients, and enhanced anchorage-independent growth in oral cancer cells that is mediated by Rac1 and ERK.** *J Biomed Sci* 2014, doi: 10.1186/s12929-014-0067-1.
- [97] Chai K.M., Wang C.Y., Liaw H.J., et al. **Downregulation of BRCA1-BRCA2-containing complex subunit 3 sensitizes glioma cells to temozolomide.** *Oncotarget*, 2014; 5:10901-15.
- [98] Garcia-Mata R. **Arrested Detachment: A DEPDC1B-Mediated De-adhesion Mitotic Checkpoint.** *Dev Cell* 2014; 31:387-9.
- [99] Tu Z., Xu B., Qu C., et al. **BRCC3 acts as a prognostic marker in nasopharyngeal carcinoma patients treated with radiotherapy and mediates radiation resistance in vitro.** *Radiat Oncol.* 2015; doi: 10.1186/s13014-015-0427-3.
- [100] Ahuja P., Singh K. **In Silico Approach for SAR Analysis of the Predicted Model of DEPDC1B: A Novel Target for Oral Cancer.** *Adv Bioinformatics* 2016; doi: 10.1155/2016/3136024.
- [101] Park J.H., Lin M.L., Nishidate T., et al. **PDZ-binding kinase / T-LAK cell-originated protein kinase, a putative cancer/testis antigen with an oncogenic activity in breast cancer.** *Cancer Res* 2006; 66:9186-95.
- [102] Harada Y., Kanehira M., Fujisawa Y., et al. **Cell-Permeable Peptide DEPDC1-ZNF224 Interferes with Transcriptional Repression and Oncogenicity in Bladder Cancer Cells.** *Cancer Res* 2010; 70:5829-39.
- [103] Petricoin E.F. 3rd., Hackett J.L., Lesko L.J., et al. **Medical applications of microarray technologies: a regulatory science perspective.** *Nat Genet* 2002; 32:474-9.

- [104] Kanehira M., Harada Y., Takata R., et al. **Involvement of upregulation of DEPDC1 (DEP domain containing 1) in bladder carcinogenesis.** *Oncogene* 2007; 26:6448-55.
- [105] Kretschmer C., Sterner-Kock A., Siedentopf F., et al. **Identification of early molecular markers for breast cancer.** *Molecular Cancer* 2011; doi: 10.1186/1476-4598-10-15.
- [106] Obara W., Ohsawa R., Kanehira M., et al. **Cancer peptide vaccine therapy developed from oncoantigens identified through genome-wide expression profile analysis for bladder cancer.** *Jpn J Clin Oncol* 2012; 42:591-600.
- [107] Kassambara A., Schoenhals M., Moreaux J., et al. **Inhibition of DEPDC1A, a bad prognostic marker in multiple myeloma, delays growth and induces mature plasma cell markers in malignant plasma cells.** *PLoS One* 2013; doi: 10.1371/journal.pone.0062752.
- [108] Ponting C.P., Bork P. **Pleckstrin's repeat performance: a novel domain in G-protein signalling?** *Trends Biochem Sci* 1996; 21:245-6.
- [109] Martemyanov K.A., Lishko P.V., Calero N., et al. **The DEP domain determines subcellular targeting of the GTPase activating protein RGS9 in vivo.** *J Neurosci* 2003; 23:10175-81.
- [110] Okayama H., Kohno T., Ishii Y., et al. **Identification of Genes Upregulated in ALK-Positive and EGFR / KRAS / ALK-Negative Lung Adenocarcinomas.** *Cancer Res*; 2012; 72:100-11.
- [111] Yan Y., Jiang Y., Jiang M., et al. **Protocadherin 10 inhibits cell proliferation and induces apoptosis via regulation of DEP domain containing 1 in endometrial endometrioid carcinoma.** *Exp Mol Pathol.* 2016;100:344-52.
- [112] Yuan S.G., Liao W.J., Yiang J.J., et al. **DEP domain containing 1 is a novel diagnostic marker and prognostic predictor for hepatocellular carcinoma.** *Asian Pac J Cancer Prev.* 2014;15:10917-22.
- [113] Mi Y., Zhang C., Bu Y., et al. **DEPDC1 is a novel cell cycle related gene that regulates mitotic progression.** *BMB Rep.* 2015; 48:413-8.
- [114] Winter J., Junk C.K., Shackel I., et al. **Development and validation of real-time quantitative reverse transcriptase-polymerase chain reaction for monitoring gene expression in cardiac myocytes in vitro.** *Anal Biochem* 1999; 270:41-49
- [115] Trusolino L., Berotti A., Comoglio P.M. **MET signalling: principles and functions in development, organ regeneration and cancer.** *Nat. Rev. Mol. Cell. Biol.* 2010; 11:834-48.
- [116] Lahat G., Zhang P., Zhu Q.S., et al, **The expression of c-Met pathway components in unclassified pleomorphic sarcoma/malignant fibrous histiocytoma (UPS/MFH): a tissue microarray study.** *Histopathology* 2011; 59:556-61.
- [117] Geiger T.R., Peeper D.S. **Metastasis mechanisms.** *Biochim Biophys Acta* 2009;1796: 293–308.
- [118] Guan X. **Cancer metastases: challenges and opportunities.** *Acta Pharm Sin B* 2015; 5:402–18.
- [119] Marino-Enriquez A., Fletcher C.D. **Round cell sarcomas – biologically important refinements in subclassification.** *Int J Biochem Cell Biol* 2014; 53:493–504.

7 - PUBLICATIONS

Quattrini I, **Pollino S**, Pazzaglia L, Conti A, Novello C, Ferrari C, Pignotti E, Picci P, Benassi MS “**Prognostic role of Nuclear Factor/IB and bone remodeling proteins in metastatic Giant Cell Tumor of bone: a retrospective study**”. *J of Orthop Res* 2015;33:1205-11

Novello C, Pazzaglia L, Conti A, Quattrini I, **Pollino S**, Perego P, Picci P, Benassi MS “**p53-Dependent Activation of microRNA-34a in Response to Etoposide-Induced DNA Damage in Osteosarcoma Cell Lines Not Impaired by Dominant Negative p53 Expression**” *PLoS One* 2014, 9:e114757

Benassi M.S, Pazzaglia L, Novello C, Quattrini I, **Pollino S**, Magagnoli G, Picci P, Conti A “**Tissue and serum IGFBP7 protein as biomarker in high-grade soft tissue sarcoma**” *Am J Cancer Res* 2015;5:3446-3454.

Savi M, Bocchi L, Sala R, Frati C, Lagrasta C, Madeddu D, Falco A, **Pollino S**, Bresciani L, Miragoli M, Zaniboni M, Quaini F, Del Rio D, Stilli D. “**Parenchymal and Stromal Cells Contribute to Pro-Inflammatory Myocardial Environment at Early Stages of Diabetes: Protective Role of Resveratrol.**” *Nutrients*. 2016 Nov 16;8 pii: E729

Pazzaglia L, Novello C, Conti A, **Pollino S**, Picci P, Benassi MS. “**miR-152 down-regulation is associated with MET up-regulation in leiomyosarcoma and undifferentiated pleomorphic sarcoma**”. *Cell Oncol (Dordr)* 2017; 40:77-88

Pollino S, Benassi MS, Pazzaglia L, Conti A, Bertani N, Picci P, Perris R. “**Prognostic role of XTP1/DEPDC1B and SDP35/DEPDC1A in Soft- tissue sarcomas**” (under revision)

8 - ACKNOWLEDGMENTS

There are so many people that have contributed in a way or another to this big achievement of my life. I would like to thank them all because I certainly could have not done any of this alone.

I would like to express my thank to Prof. Roberto Perris for supervising in these past three years.

I wish to express my gratitude to Dr. Maria Serena Benassi for being always there for me throughout my Ph.D adventure, not only by providing practical assistance and scientific advice, but also for helping me emotionally, guiding me to the end of this long path with affection and compassion.

I would like to express my special appreciation and thanks to Dr. Piero Picci, director of the Experimental Oncology Laboratory, for believing in me and for giving me the opportunity to be a doctoral candidate in his department.

I also wish to thank:

Prof. Donatella Stilli and Prof. Emilio Macchi for their enormous availability

Drs Laura and Giovanna for the great support, their valuable advice and for baring with me every single day.

Chiara, Amalia and especially Irene for being wonderful colleagues and good friends.

Alba, Cristina G., Cristina F, Manuela, Daniela and Elena for their vital work "behind the scenes".

Dr. Nicoletta, Dr. Monia, Dr. Leonardo, Dr. Francesca, Dr Stefano, Maria Elena and Mattia for their help

and finally, all my lab mates at Rizzoli for all the special moments spent together troubleshooting with experiments or simply having fun.

I could have not done anything without the love and support of my family. They always encouraged me and believed in me. So I wish to dedicate this thesis and all the work behind it to my mom, my dad, and my two wonderful sisters Elisa and Anna Chiara.

Special thank also to my partner Fabrizio, for his love, his tenderness, and for being there always, no matter what.

I want to thank Katia for her words of encouragement when I most needed them

Many thanks to all my friends for always being there for me, no matter how far they lived from me

Last but not least, a special thanks to my grandparents that I am sure will be always with me.

I also want to thank myself for never giving up.

